Published by
NIGERIAN SOCIETY OF PHYSICAL SCIENCES
Available online @ https://journal.nsps.org.ng/index.php/jnsps

J. Nig. Soc. Phys. Sci. 8 (2026) 3376

Journal of the Nigerian Society of Physical Sciences

Mathematical modelling and optimal-control strategies of schistosomiasis–typhoid fever co-infection: using the demographic setting of Makurdi, Benue State, Nigeria

Kazeem A. Tijani, Chinwendu E. Madubueze*, Reuben I. Gweryina, Terhemen Aboiyar

Department of Mathematics, Joseph Sarwuan Tarka University, formerly Federal University of Agriculture, Makurdi, Benue State, Nigeria

Abstract

Co-infection of schistosomiasis and typhoid fever presents a significant public-health challenge and complicates clinical management. Both diseases are prevalent and endemic in African regions, particularly Nigeria, but their co-dynamics remain insufficiently studied. This study developed a deterministic mathematical model to examine the co-dynamics of schistosomiasis and typhoid fever in Makurdi, Benue State, Nigeria. The basic reproduction number (R_0) for the sub-models and the full co-infection model was calculated to assess the stability of the disease-free equilibrium and to conduct bifurcation analysis. The endemic equilibrium was derived. Global sensitivity analysis was conducted, and an optimal-control model was formulated with five time-dependent controls: prevention of schistosomiasis, prevention of typhoid fever, screening and treatment for schistosomiasis, screening and treatment for typhoid fever, and screening and treatment for co-infections. The model was analysed using the Pontryagin maximum principle and the forward–backward sweep method. Numerical simulations included single, pairwise, and combined interventions. The results indicate that prevention strategies for both diseases are more effective than treatment alone. The study recommends implementing concurrent control interventions for both diseases to achieve optimal co-infection management.

DOI: 10.46481/jnsps.2026.3376

Keywords: Co-infection, Mathematical model, Schistosomiasis–typhoid fever, Optimal control

Article History:
Received: 26 March 2026
Received in revised form: 13 May 2026
Accepted for publication: 26 May 2026
Available online: 22 June 2026

Communicated by: B. J. Falaye

1. Introduction

Schistosomiasis, also referred to as bilharzia, is among the most prevalent neglected tropical diseases (NTDs) in tropical and subtropical regions, particularly in Africa, Asia, and parts of South America [1]. The disease is caused by parasitic trematodes of the genus *Schistosoma* and is transmitted through contact with freshwater contaminated by cercariae released from infected snail hosts [2]. Despite extensive global control efforts, schistosomiasis remains a significant public health and socio-economic challenge, ranking second only to malaria in its impact among parasitic diseases [3]. The World Health Organisation (WHO) estimates that more than 240 million people are infected, with over 700 million at risk worldwide, primarily in communities without access to safe water, sanitation, and healthcare services [4].

The disease manifests in acute and chronic forms, with symptoms ranging from abdominal pain, blood in urine or stool, and anaemia to long-term complications such as liver fibrosis, bladder carcinoma, and portal hypertension. Despite the

*Corresponding author: Tel. No.: +234-8039-523-389.
Email address: ce.madubueze@gmail.com (Chinwendu E. Madubueze)

Table 1: State variables of the model.

State variable	Epidemiological interpretation	Unit
$S_h(t)$	Susceptible human population at time, t	Human population
$I_{sc}(t)$	Schistosomiasis only infected population at time, t	Human population
$I_t(t)$	Typhoid fever only infected and infectious population at time, t	Human population
$I_{tsc}(t)$	Co-infected and infectious human population at time, t	Human population
$R_{sc}(t)$	Schistosomiasis only recovered human population at time, t	Human population
$R_t(t)$	Typhoid fever only recovered human population at time, t	Human population
$R_{tsc}(t)$	Co-infected recovered human population at time, t	Human population
$S_s(t)$	Susceptible snail population at time, t	Snail population
$I_s(t)$	Infected and infectious snail population at time, t	Snail population
$B_t(t)$	Bacteria concentration at time, t	Bacteria concentration

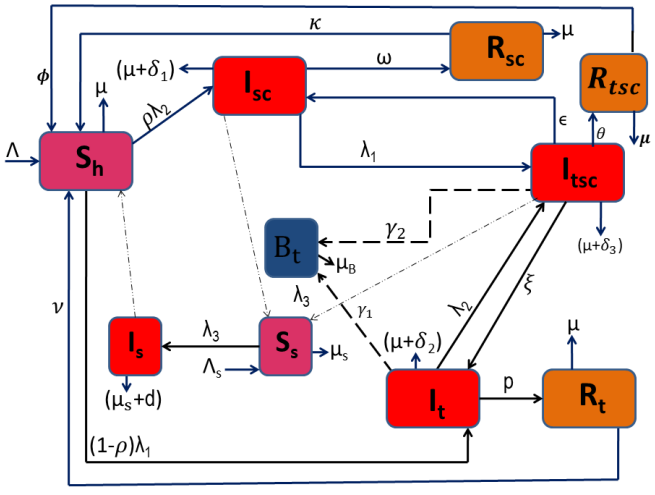

Figure 1: Systematic Diagram of typhoid fever and schistosomiasis co-infection mechanisms.

widespread use of praziquantel as a chemotherapeutic intervention, re-infection remains common due to persistent environmental contamination, heterogeneity in snail populations, and the lack of sustainable sanitation infrastructure [3, 5].

Schistosomiasis transmission involves a complex life cycle in which humans and other mammals serve as definitive hosts, while freshwater snails function as intermediate hosts [2]. Infected individuals contaminate water sources with parasite eggs through urine or faeces; these eggs hatch into miracidia that infect snails. The snails subsequently release cercariae, which penetrate human skin upon contact. Chronic infection frequently leads to anaemia, liver and kidney damage, bladder pathology, and reduced productivity [2]. The persistence of schistosomiasis is primarily attributed to environmental contamination, heterogeneity in snail populations, and recurrent re-infection, all of which undermine chemotherapy-based control efforts [1].

Typhoid fever remains a major public health concern in many developing nations, particularly in sub-Saharan Africa and parts of Asia, where inadequate sanitation, poor waste management, and contaminated water sources facilitate its persistence [6]. The disease is a systemic bacterial infection caused primarily by *Salmonella enterica* serovar Typhi, transmitted through the faecal-oral route via ingestion of contaminated food or water. Despite advances in antibiotic therapy and vaccination, typhoid continues to cause significant morbidity and mortality, with millions of cases reported annually, especially in low- and middle-income countries [7]. Globally, more than 21 million new cases and over half a million deaths occur annually, with the highest burden in sub-Saharan Africa and South Asia [6]. Clinical symptoms such as high fever, headache, fatigue, and gastrointestinal distress often overlap with malaria and other febrile illnesses, leading to misdiagnosis and inappropriate treatment. Diagnostic challenges, particularly reliance on the Widal test, have resulted in false positives and excessive antibiotic use, contributing to multidrug-resistant *Salmonella Typhi* [8].

The exact prevalence varies by region; co-infection with Schistosoma mansoni and Salmonella species is often observed in sub-Saharan Africa [4]. Co-infection with Schistosoma and

Table 2: Description and parameter values of the model.

Parameter	Description	Unit	Value per week	Source
Λ	Human recruitment rate	$\frac{\text{Human population}}{\text{time}}$	175	Calculated
Λ_s	Recruitment rate snail population	$\frac{\text{Non-mammals population}}{\text{time}}$	10	Calculated
β_2	Typhoid fever effective transmission rate from environment-to-human population	time^{-1}	3.6×10^{-8}	Assumed
β_1	Typhoid fever effective transmission rate from human-to-human population	time^{-1}	7.14×10^{-7}	[9]
β_3	Schistosomiasis effective transmission rate from infected snail-to-human population through shedding of cercariae in freshwater	time^{-1}	5.8×10^{-7}	[10]
β_4	Schistosomiasis effective transmission rate from infected human-to-snail population through shedding of miracidia in freshwater	time^{-1}	8.79×10^{-5}	[10]
δ_1	Disease induced death rate for Schistosomiasis infected and infectious human population	time^{-1}	0.00056	[11]
δ_2	Disease induced death rate for Typhoid fever symptomatic infected human population	time^{-1}	0.000286	[12]
δ_3	Disease induced death rate for Co-infected human population	time^{-1}	0.000846	Estimated
K	Carrying capacity for Bacteria	$\frac{\text{Bacteria}}{\text{concentration}}$	71428.57	[13]
d	Disease induced death rate for infected snail population	time^{-1}	0.0209	[14]
μ	Natural human death rate	time^{-1}	0.000343	[15]
μ_s	Natural death rate for snail population	time^{-1}	0.00192	[16]
μ_B	Bacteria decay rate	time^{-1}	0.0049	[17]
γ_1, γ_2	Bacteria shedding rates from I_t, and I_{tsc}, respectively into bacteria concentration B_t	$\frac{\text{Bacteria concentration}}{\text{human population} \times \text{time}}$	0.1, 0.1	[9]
ω	Recovery rate due to screening and treatment for schistosomiasis only infected humans	time^{-1}	0.00033	[5]
p	Recovery rate due to screening and treatment for typhoid fever only infected humans	time^{-1}	0.0143	[18]
θ	Recovery rate due to screening and treatment for co-infected humans	time^{-1}	0.0176	Estimated
ρ	Proportion of population that move from S_h to I_{sc}	Nil	0.45	Assumed
ϕ	progression rate from R_{tsc} to S_h due to loss of immunity	time^{-1}	0.1	Assumed
κ	progression rate from R_{sc} to S_h due to loss of immunity	time^{-1}	0.00186	[10]
ν	progression rate from R_t to S_h due to loss of immunity	time^{-1}	0.00013	[19]
ξ	progression rate from I_{tsc} to I_t due to screening and treatment of schistosomiasis	time^{-1}	0.0033	[5]
ϵ	progression rate from I_{tsc} to I_{sc} due to screening and treatment of typhoid fever	time^{-1}	0.0143	[18]

Salmonella poses a significant public health concern and complicates clinical management [20]. More than 20 Salmonella species of human and animal origin are believed to be associated with schistosome infections [21].

Benue State in the North Central geopolitical zone of Nigeria is predominantly agrarian, hydrologically endowed by the Benue River and its tributaries, and prone to water-related diseases [22]. It is established that major parts of the state, including Makurdi, face significant challenges in accessing safe water, with risks of microbial contamination, poor sanitation, and limited awareness of open defecation hazards, among others [22].

Maxwell *et al.* [23] carried out research on water-related diseases in Benue state, Nigeria, to analyse the trend and spatial dimension of the diseases in the state. Their findings showed that water related diseases were recorded in all the 23 local governments of the states in order of magnitude of cases in the following order; malaria, diarrhea, dysentery, filariasis, onchocerciasis, schistosomiasis, typhoid fever and cholera and they further recommended for intensified, public education on personal hygiene, provision of improved water supply in communities-among others, for effective control of water-related disease in

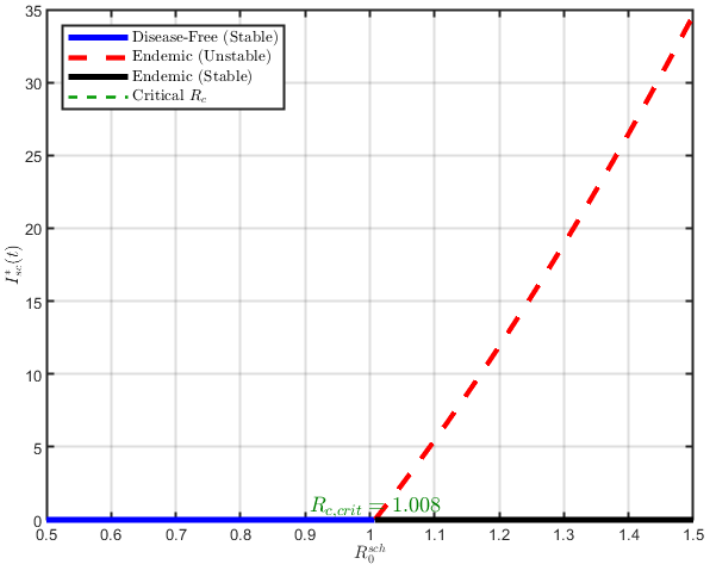

Figure 2: Plot of forward bifurcation of the schistosomiasis Sub-Model.

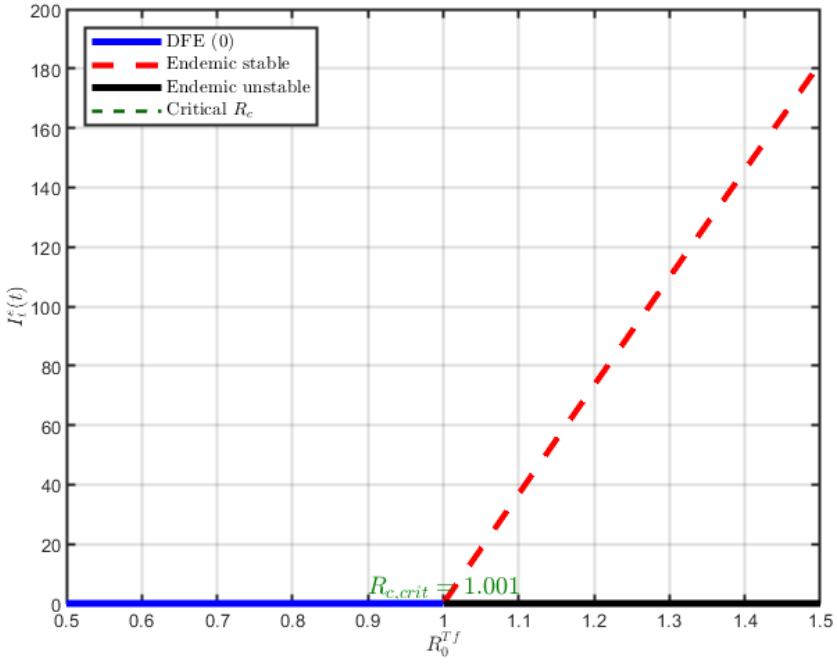

Figure 3: Plot of forward bifurcation of the Typhoid Fever Sub-Model.

the state. Refs. [24–26] also established the prevalence of schistosomiasis and typhoid fever in the state. Meanwhile, Yandev *et al.* [26] conducted a detailed study on the prevalence of typhoid fever and schistosomiasis co-infection in the state and the need for appropriate actions to combat these diseases. Hence, this study will employ mathematical modelling and optimal control theory to examine the dynamics of schistosomiasis-typhoid fever co-infection, using Makurdi's demographic data for analysis and to provide appropriate control measures.

The mathematical modelling of infectious diseases is a vital means for examining and investigating the spread of contagious diseases. It is an essential tool for understanding and assisting in formulating control interventions to predict appropriate control measures Refs. [27, 28]. Optimal control is an aspect of mathematics that specialises in providing suitable techniques for managing or controlling dynamical systems Refs. [29]. Sev-

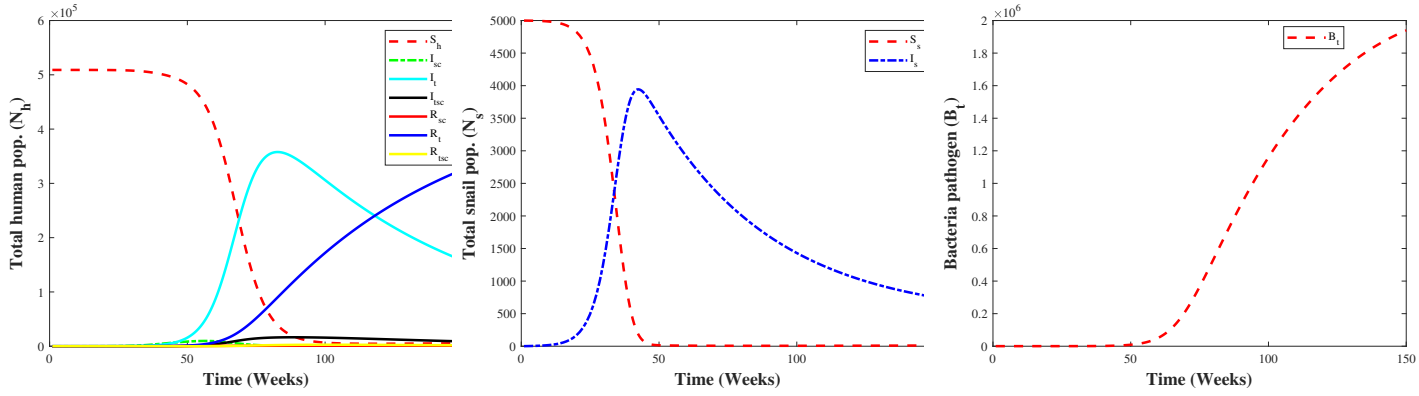

(a) (b) (c)

Figure 4: Plots of (a) the human populations ($S_h, I_{sc}, I_t, I_{tsc}, R_{sc}, R_t, R_{tsc}$), (b) the snail populations (S_s, I_s), and (c) the bacteria pathogen population.

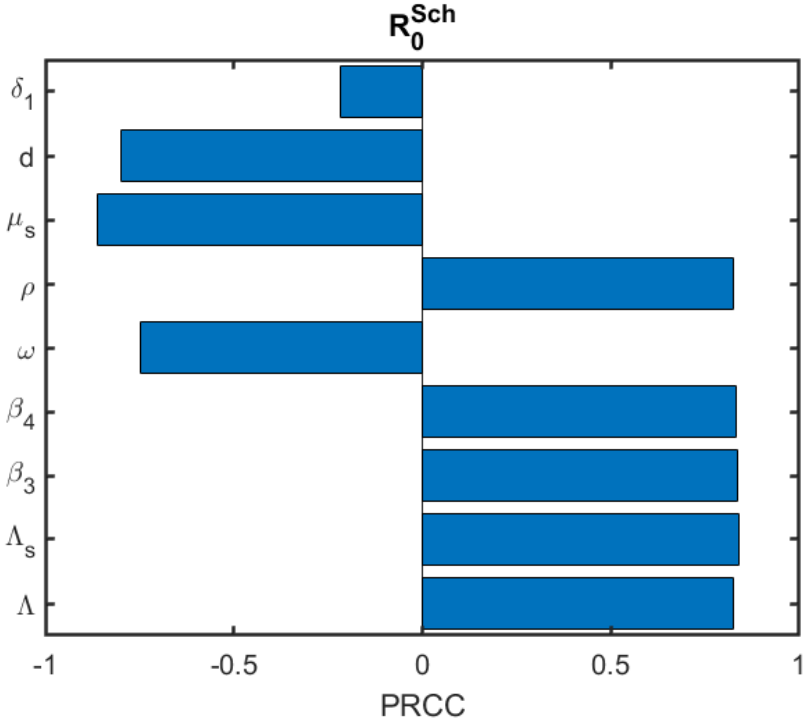

Figure 5: PRCCC results showing sensitivity indices of the schistosomiasis sub-model parameters on reproduction number, R_0^{Sch}.

eral authors have studied the dynamics of schistosomiasis and typhoid disease as single models, respectively. For instance, Refs. [29–33], have developed mathematical models of schistosomiasis only-over the years while, Refs. [9, 34–39] worked on mathematical model of typhoid fever only-over the years. Also, detailed mathematical analyses of the co-infection models between schistosomiasis and HIV/AIDS, schistosomiasis and malaria, schistosomiasis and lymphatic filariasis, and schistosomiasis and tuberculosis were conducted by Refs. [40–43]. In this same light, Refs. [17, 44–46] studied co-infection typhoid fever with cholera, malaria, COVID-19 and hepatitis A, respectively, while Refs. [9, 10, 47] carried out optimal control analysis in their studies. However, despite the prevalence and endemicity of co-infection between schistosomiasis and typhoid fever in African regions, it remains insufficiently explored [4], and to the best of our knowledge, no author has used mathematical modelling to investigate the dynamics of this co-infection.

Many African countries experience co-infections involving S. mansoni and Salmonella, both of which are waterborne pathogens [4]. However, a review of the literature shows that the prevalence and geographic distribution of this co-infection in endemic African regions remain insufficiently explored [4]. Several researchers in the biological and clinical sciences, such as Refs. [4, 20, 26, 48, 49], have investigated the co-infection

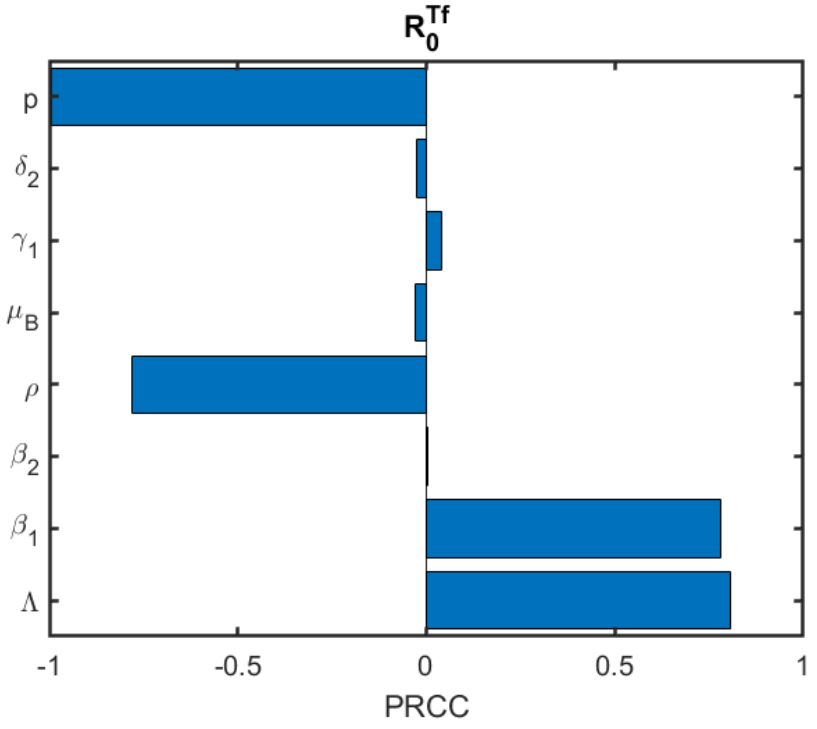

Figure 6: PRCCC results showing sensitivity indices of the typhoid fever sub-model parameters on reproduction number, R_0^{Tf}.

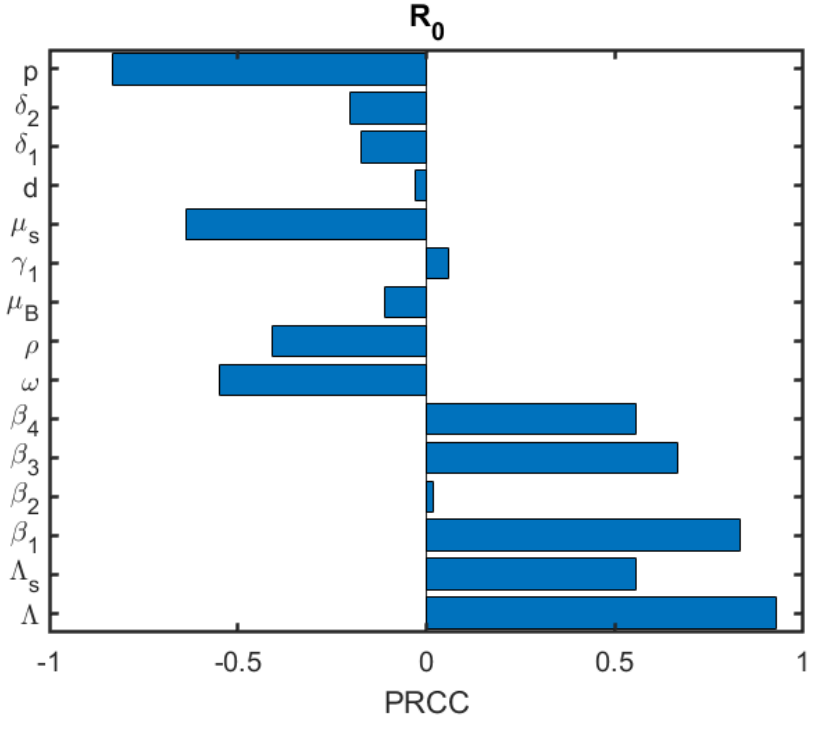

Figure 7: PRCCC results showing sensitivity indices of the co-infection model parameters on reproduction number, R_0^{Sch-Tf}.

of schistosomiasis and typhoid fever, with valuable findings. However, to the best of our knowledge, no study to date has applied mathematical modelling to analyse the transmission dynamics of co-infection with these two diseases. Therefore, this study aims to employ a mathematical modelling approach to examine the co-infection dynamics of schistosomiasis and typhoid fever, and to identify possible solutions for the eradication of the diseases in society, using the demographic setting

of Makurdi, Benue State, Nigeria. Hence, in this study, we develop a co-infection model that captures the combined dynamics of schistosomiasis and typhoid with ten (10) compartments, $S_h(t)$, $I_{sc}(t)$, $I_t(t)$, $I_{tsc}(t)$, $R_{sc}(t)$, $R_t(t)$, $R_{tsc}(t)$, $S_s(t)$, $I_s(t)$, $B_t(t)$, to investigate the transmission dynamics of the schistosomiasis-typhoid fever co-infection with a view of minimising this burden in the population by providing optimum control interventions.

The rest of the paper is arranged as follows: the model formulation is presented in Section 2, while the mathematical/qualitative analysis of the model is carried out in Section 3. Numerical simulations comprising baseline plots and varying impact of parameters, and sensitivity analysis using Latin Hypercube Sampling (LHS) with Partial Rank Correlation Coefficient (PRCC) method to identify the most influential parameters, were conducted in Section 4. In Section 5, based on the sensitivity results in Section 4, we applied optimal control theory using Pontryagin's Maximum Principle with a forward-backwards scheme to determine the most effective strategies to control the co-infection dynamics. Also, numerical simulations of optimal control strategies are conducted to identify the most viable intervention and to inform the study's findings. Finally, Section 6 of the paper contains the conclusion and recommendations.

2. Model description and formulation

In line with the epidemiology of schistosomiasis and typhoid fever co-infection among human population, the human population is sub-divided into susceptible human population, $S_h(t)$, these are individuals that are yet to be infected but are prone to the two diseases, Schistosomiasis-only Infected and infectious human population, $I_{sc}(t)$, these are people that are infected with only schistosomiasis and are capable of releasing schistosoma eggs into the freshwater and hatch into miracidia to infect snails (they can be symptomatic or asymptomatic), Typhoid-only infected human population, $I_t(t)$, these individuals are infected with typhoid fever only and are infectious and can shed the bacteria into the environment (they can be symptomatic or asymptomatic), Co-infected and infectious human population, $I_{tsc}(t)$, these are individuals who are infected with both diseases, Schistosomiasis only recovered human population, $R_{sc}(t)$, these humans that have recovered from schistosomiasis due to screening and treatment, Typhoid fever only recovered human population, $R_t(t)$, these humans who have recovered from typhoid fever due to screening and treatment, Co-infected recovered human population, $R_{tsc}(t)$, these are individuals who have concurrently recovered due to screening and treatment. The total human population at any time, t, is given as:

$$N(t) = S_h(t) + I_{sc}(t) + I_t(t) + I_{tsc}(t) + R_{sc}(t) + R_t(t) + R_{tsc}(t).$$

Also, the snail population is divided into two classes, namely, the susceptible snail population, $S_s(t)$, who are free of schistosomiasis but risk infection through miracidia from infected humans in the environment, and the infected snail population, I_s, who shed cercariae into fresh water and infect humans [1]. The total snail population is given by $N_s = S_s + I_s$. The $B_t(t)$ denotes the bacteria concentration in the environment, shed by the infected individuals in $I_t(t)$, and $I_{tsc}(t)$, respectively.

The susceptible population increases due to the recruitment rate, Λ. Individuals in this category also increase as a result of individuals joining from co-infected recovered class, $R_{tsc}(t)$, schistosomiasis only recovered class, $R_{sc}(t)$, and typhoid fever only recovered class, $R_t(t)$, due to loss of immunity at the rates, ϕ, κ and ν, respectively. This class reduces due to interaction with typhoid fever-infected individuals or schistosomiasis-infected individuals of proportions $(1-\rho)$ and ρ at the rates λ_1 and λ_2, respectively. It is also declining due to the natural death rate, μ. This yields

$$\frac{dS_h}{dt} = \Lambda + \phi R_{tsc} + \kappa R_{sc} + \nu R_t - \rho\lambda_2 S_h - (1-\rho)\lambda_1 S_h - \mu S_h,$$

where $\lambda_1 = \left[\beta_1(I_t + I_{tsc}) + \frac{\beta_2 B_t}{K+B_t}\right]$, with β_1 as the typhoid fever effective transmission rate from human-to-human, β_2 is the typhoid fever effective transmission rate from environment-to-human and K is the carrying capacity. Also, $\lambda_2 = \beta_3 I_s$ with β_3 as the schistosomiasis effective transmission rate from snail-to-human through shedding of cercariae in the freshwater.

The schistosomiasis-only infected population increases due to the proportion ρ of susceptible individuals being infected at a rate, λ_2, and people who progress from the co-infected class as a result of screening and treatment for typhoid fever only at a rate, ϵ. This class reduces due to infection of its individuals with typhoid fever at a rate λ_1, as well as due to the natural death rate μ and the disease-related death rate δ_1. It is also declining at a rate ω due to screening and treatment. This dynamics gives:

$$\frac{dI_{sc}}{dt} = \rho\lambda_2 S_h + \epsilon I_{tsc} - \lambda_1 I_{sc} - (\mu + \delta_1 + \omega) I_{sc}.$$

The typhoid fever-only infected population increases at a rate λ_1 due to the proportion $(1-\rho)$ of susceptible individuals contracting typhoid fever, and at a rate ξ due to people entering from the co-infected class through screening and treatment for schistosomiasis. This class reduces at a rate λ_2 when infected with schistosomiasis, and then progresses to the co-infected class. The class also declines due to screening and treatment at a rate, p, as well as due to natural death and disease-induced death rates, μ and δ_2, respectively. This illustration yields:

$$\frac{dI_t}{dt} = (1-\rho)\lambda_1 S_h + \xi I_{tsc} - \lambda_2 I_t - (\mu + \delta_2 + p) I_t.$$

The co-infected population increases at the rates, λ_1 and λ_2 from I_{sc} and I_t, respectively. It decreases when people infected with typhoid fever only and schistosomiasis only are being screened and treated at the rates, ϵ and ξ, respectively. It also reduces due to concurrent screening and treatment of co-infected individuals at a rate, θ, together with natural and disease-related death rates, μ and δ_3, respectively. Thus,

$$\frac{dI_{tsc}}{dt} = \lambda_1 I_{sc} + \lambda_2 I_t - (\mu + \delta_3 + \epsilon + \xi + \theta) I_{tsc}.$$

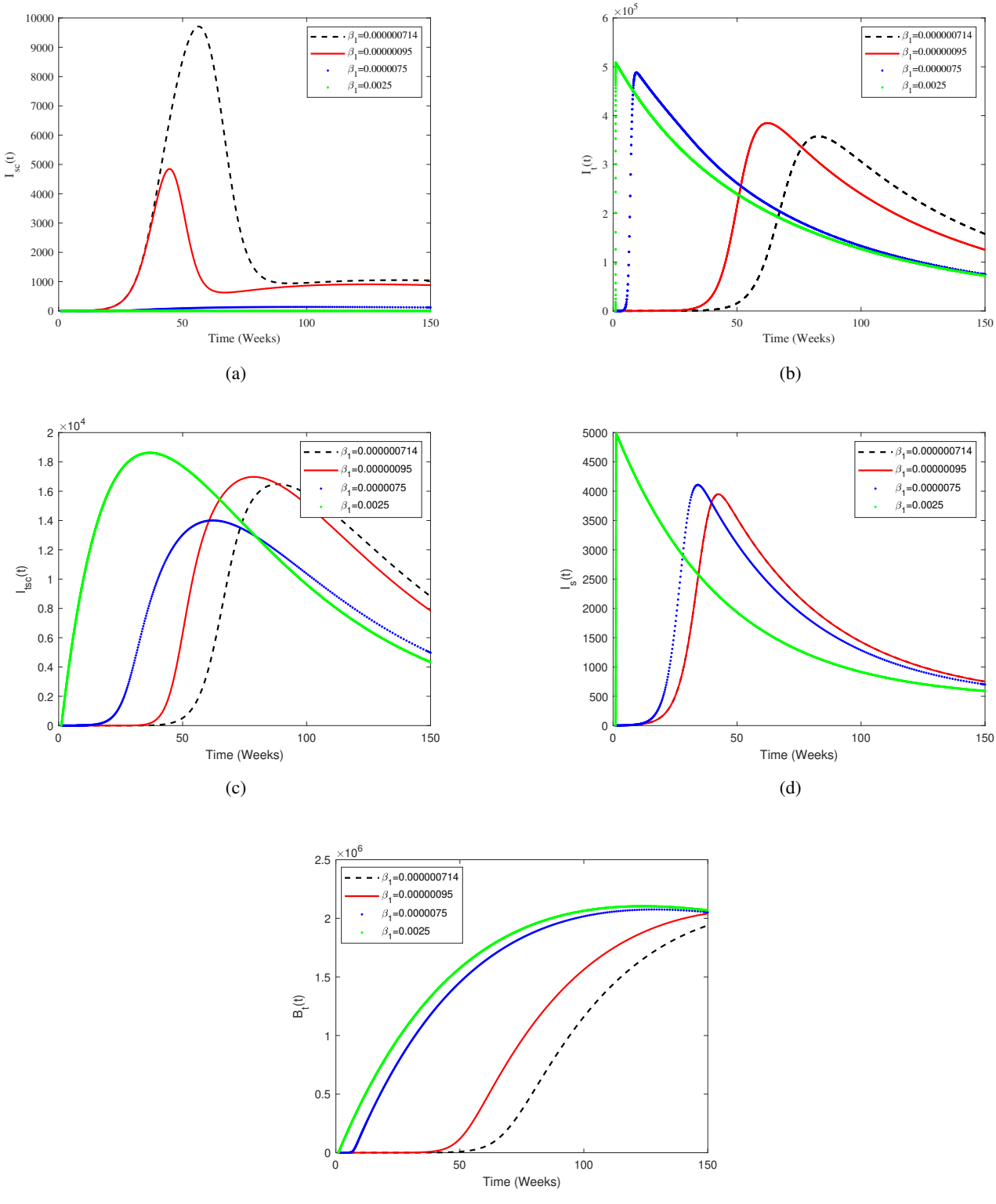

Figure 8: Plots showing the varying impact of typhoid fever effective transmission rate from human-to-human population, β_1: (a) Impact on $I_{sc}(t)$, (b) Impact on $I_t(t)$, (c) Impact on $I_{tsc}(t)$, (d) Impact on $I_s(t)$ and (e) Impact on $B_t(t)$.

The schistosomiasis-only recovered population increases when individuals at I_{sc} are screened and treated at a rate ω. It reduces at rates κ and μ. This is represented as

$$\frac{dR_{sc}}{dt} = \omega I_{sc} - (\kappa + \mu)R_{sc}.$$

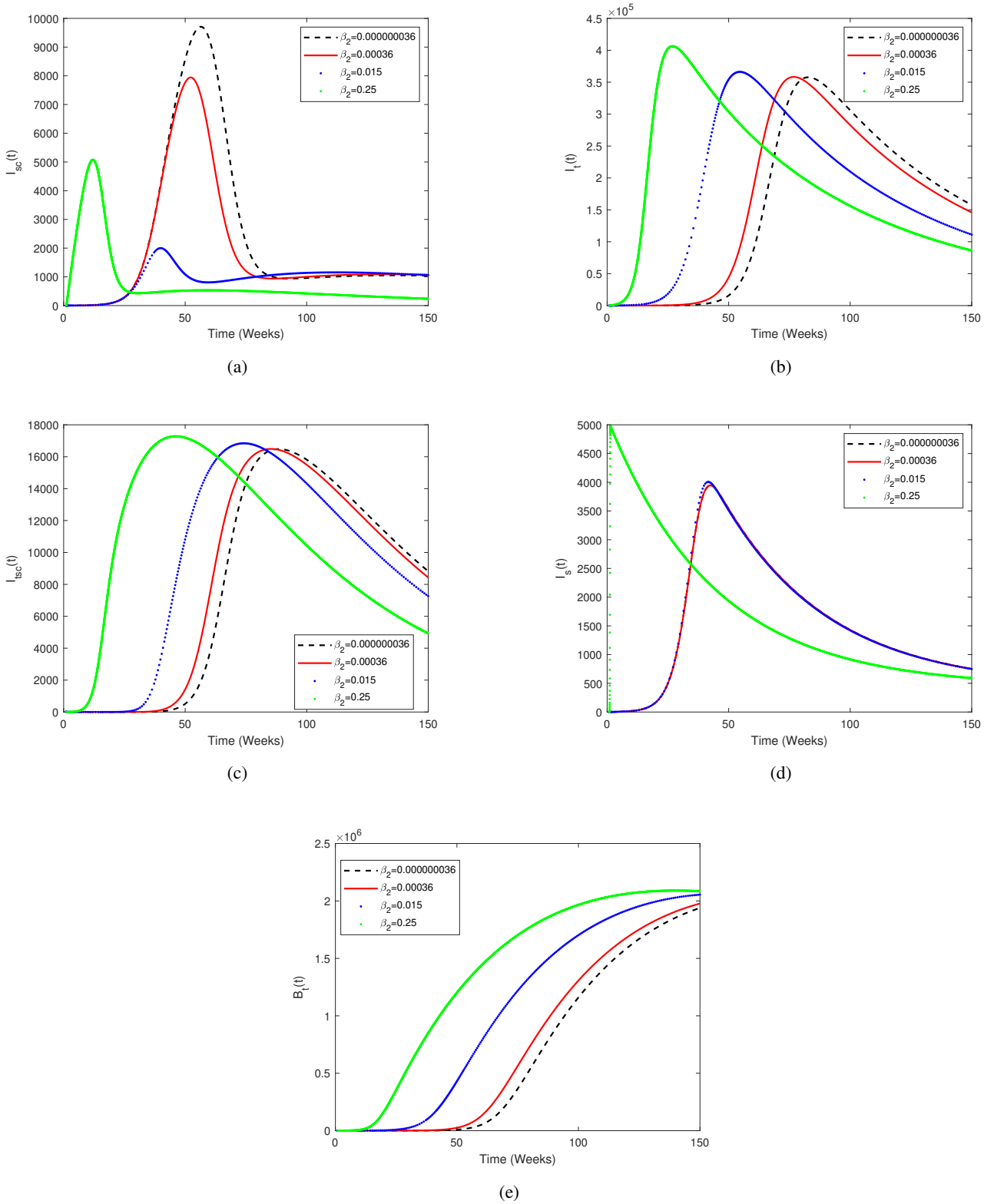

Figure 9: Plots showing the varying impact of typhoid fever effective transmission rate from environment-to-human population, β_2: (a) Impact on $I_{sc}(t)$, (b) Impact on $I_t(t)$, (c) Impact on $I_{tsc}(t)$, (d) Impact on $I_s(t)$ and (e) Impact on $B_t(t)$.

The typhoid fever-only infected class grows due to individuals from the typhoid fever-only infected class entering it at a rate p. The population declines at a rate, ν, due to loss of immunity after recovery and as a result of the natural death rate, μ. These

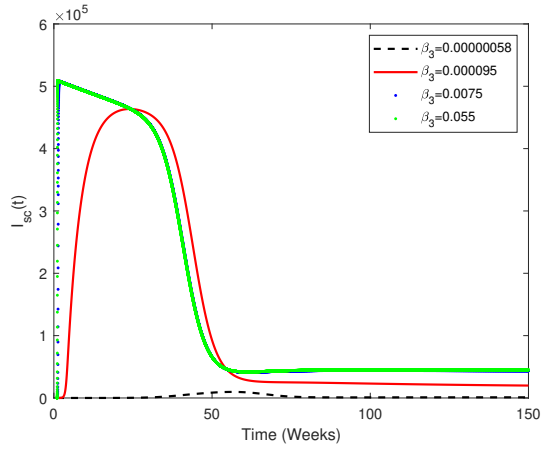

(a)

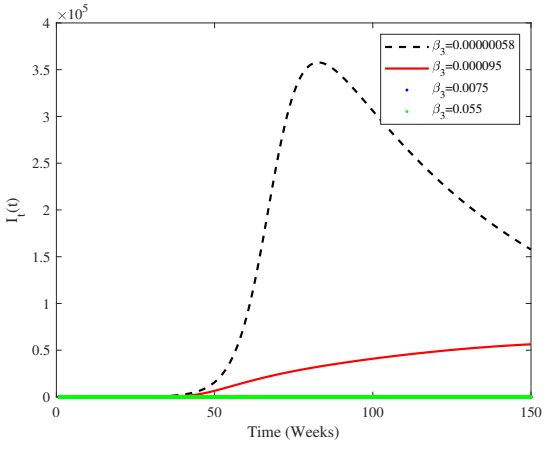

(b)

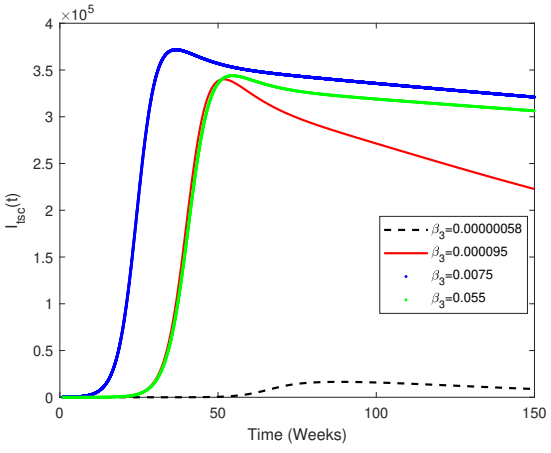

(c)

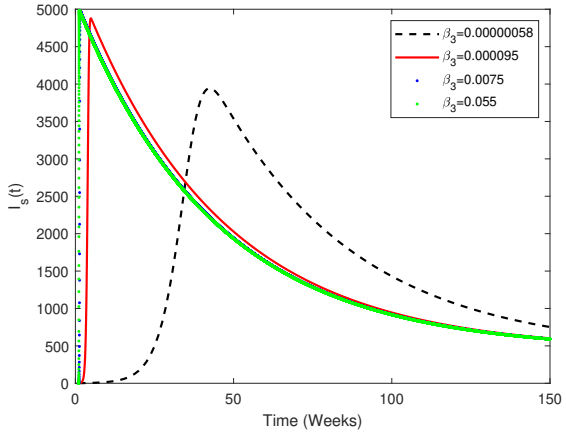

(d)

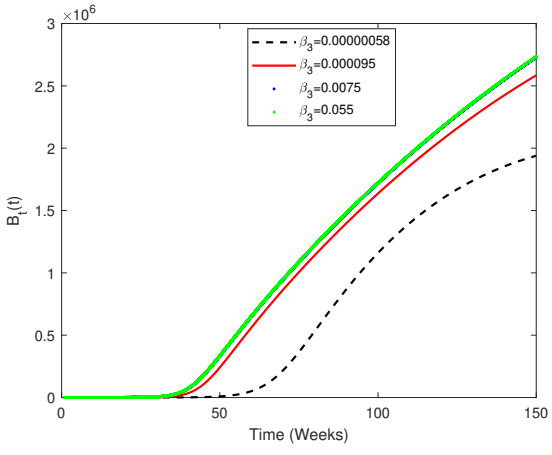

(e)

Figure 10: Plots showing the varying impact of schistosomiasis effective transmission rate from snail-to-human population, β_3: (a) Impact on $I_{sc}(t)$, (b) Impact on $I_t(t)$, (c) Impact on $I_{tsc}(t)$, (d) Impact on $I_s(t)$ and (e) Impact on $B_t(t)$.

dynamics give

$$\frac{dR_t}{dt} = pI_t - (\nu + \mu)R_t.$$

The number of individuals in the co-infected population rises at the rate θ due to screening and treatment of co-infected individ-

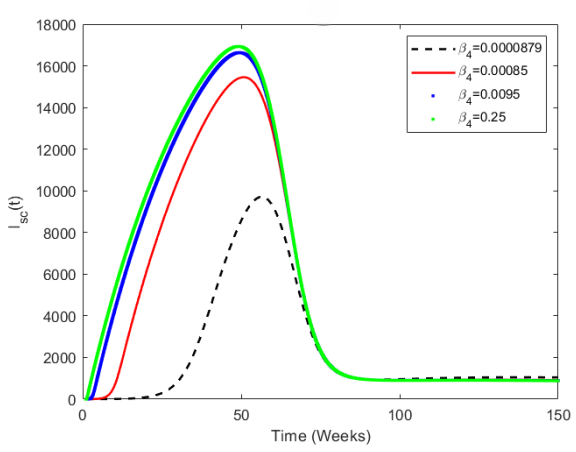

(a)

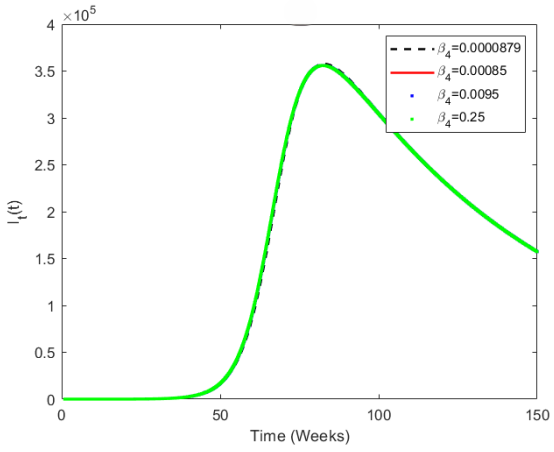

(b)

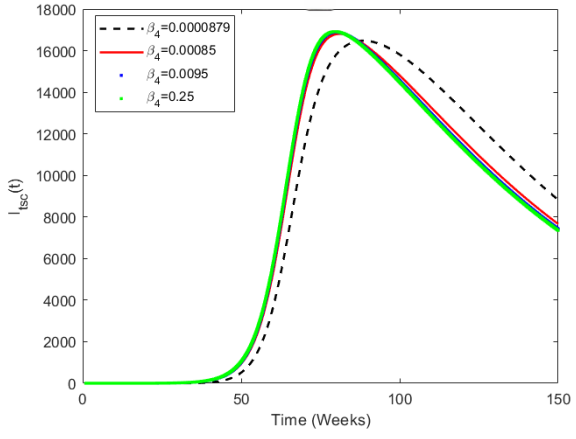

(c)

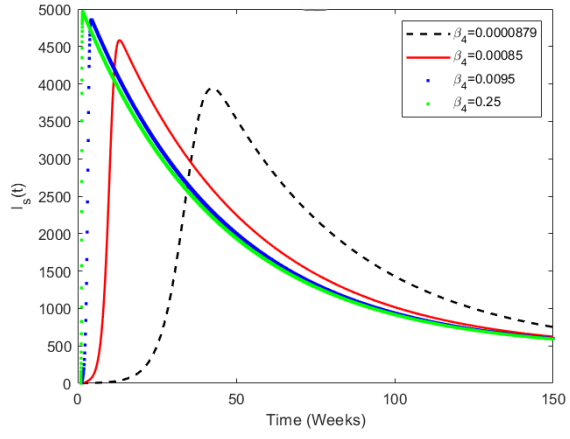

(d)

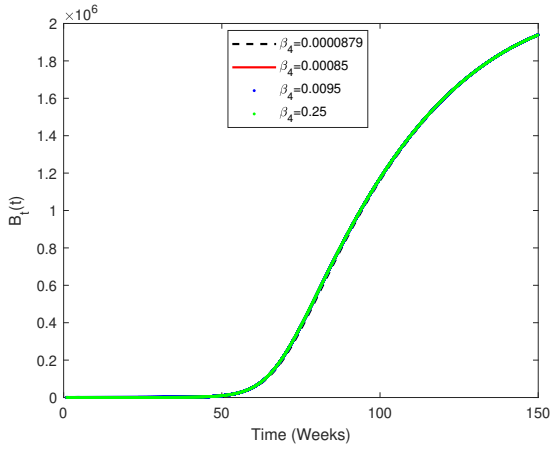

(e)

Figure 11: Plots showing the varying impact of schistosomiasis effective transmission rate from human-to-snail population, β_4: (a) Impact on $I_{sc}(t)$, (b) Impact on $I_t(t)$, (c) Impact on $I_{tsc}(t)$, (d) Impact on $I_s(t)$ and (e) Impact on $B_t(t)$.

uals. It declines due to loss of immunity at a rate, ϕ and natural death rate, μ. This yields

$$\frac{dR_{tsc}}{dt} = \theta I_{tsc} - (\mu + \phi)R_{tsc}.$$

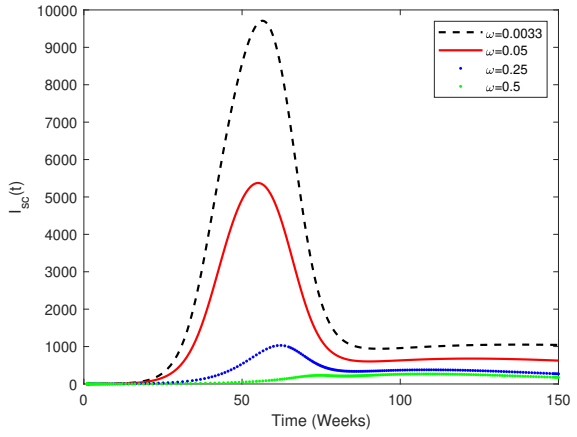

(a)

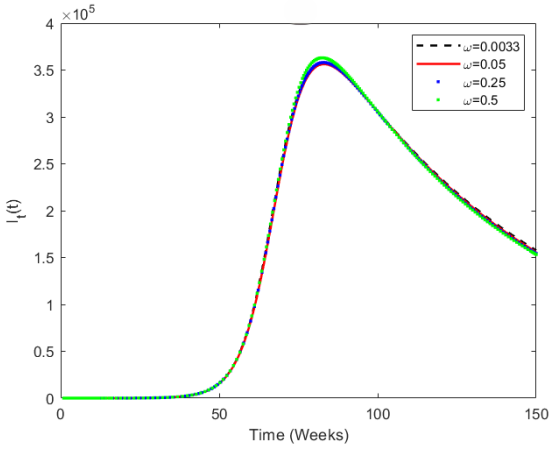

(b)

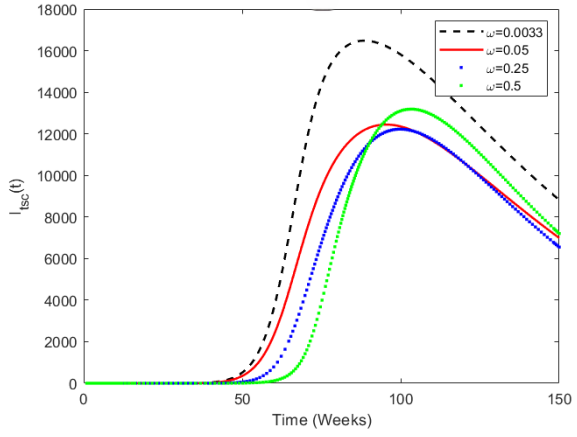

(c)

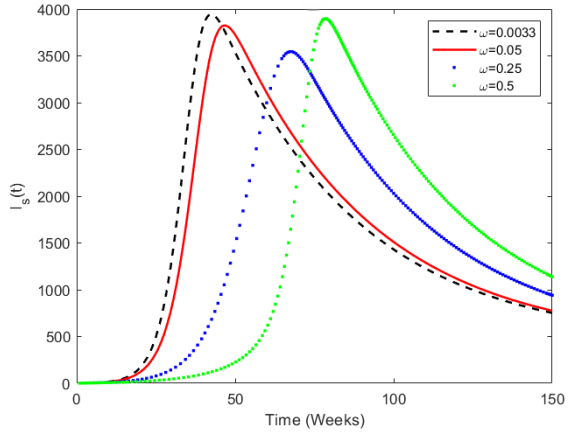

(d)

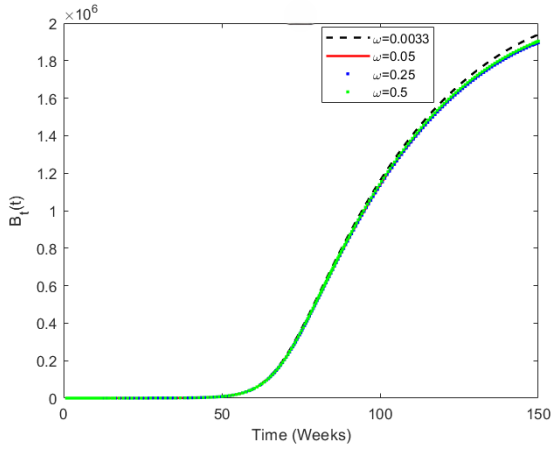

(e)

Figure 12: Plots showing the varying impact of recovery rate due to screening and treatment for schistosomiasis only infected humans, ω: (a) Impact on $I_{sc}(t)$, (b) Impact on $I_t(t)$, (c) Impact on $I_{tsc}(t)$, (d) Impact on $I_s(t)$ and (e) Impact on $B_t(t)$.

The snail population increases through recruitment birth rate, Λ_s. It reduces due to interaction with miracidia from infected humans at a rate, λ_4 and as a result of the natural death

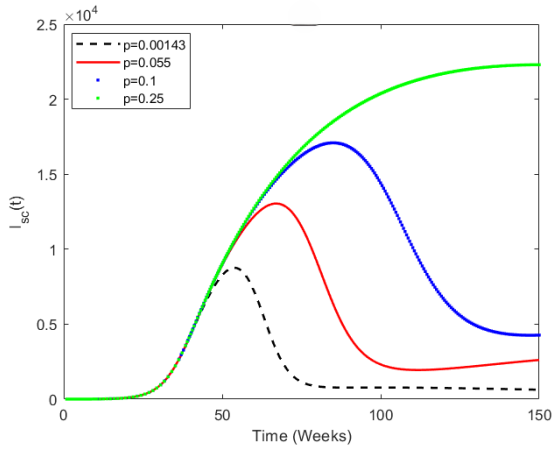

(a)

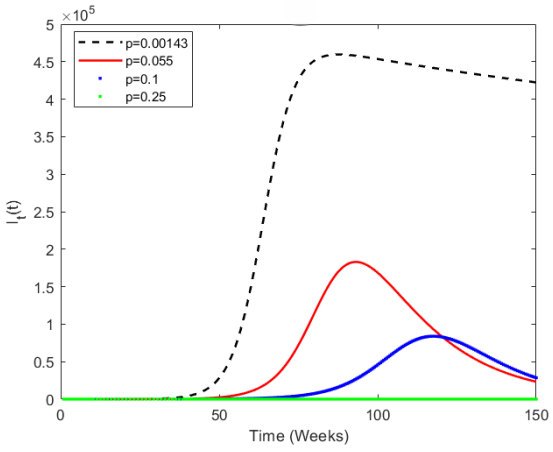

(b)

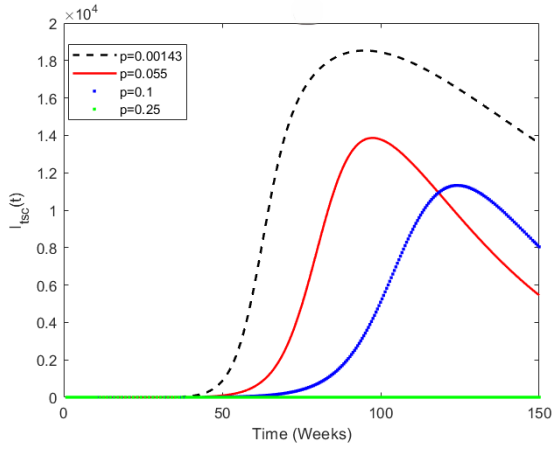

(c)

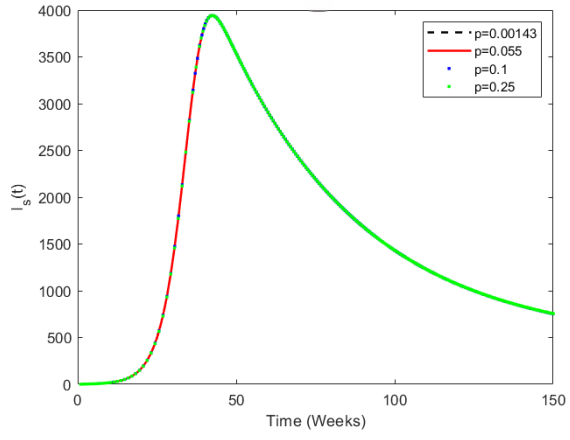

(d)

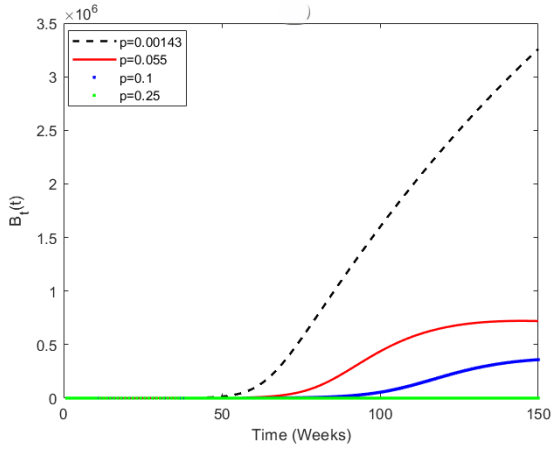

(e)

Figure 13: Plots showing the varying impact of recovery rate due to screening and treatment for typhoid fever only infected humans, p: (a) Impact on $I_{sc}(t)$, (b) Impact on $I_t(t)$, (c) Impact on $I_{tsc}(t)$, (d) Impact on $I_s(t)$ and (e) Impact on $B_t(t)$.

rate, μ_s. This gives

$$\frac{dS_s}{dt} = \Lambda_s - \lambda_3 S_s - \mu_s S_s,$$

where $\lambda_3 = \beta_4(I_{sc} + I_{tsc})$ with β_4 as the effective transmission rate from infected humans to snail via miracidia from shedding

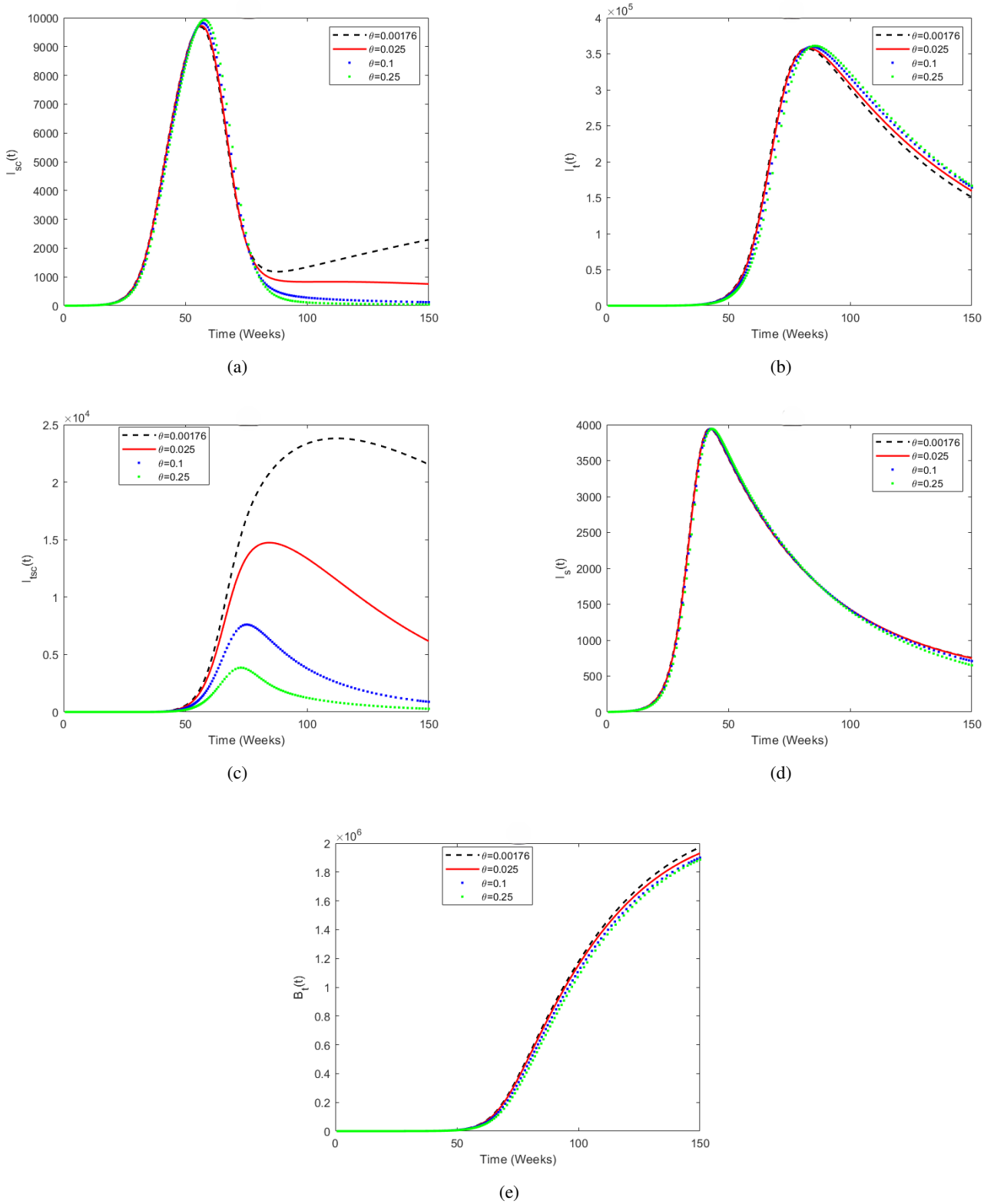

Figure 14: Plots showing the varying impact of recovery rate due to screening and treatment for co-infected infected humans, θ: (a) Impact on $I_{sc}(t)$, (b) Impact on $I_t(t)$, (c) Impact on $I_{tsc}(t)$, (d) Impact on $I_s(t)$ and (e) Impact on $B_t(t)$.

of eggs of schistosomiasis infected individuals.

The snail infected population rises due to susceptible snails infected at a rate, λ_3, and reduces at a natural and disease-induced death rates, μ_s and d, respectively, and this gives

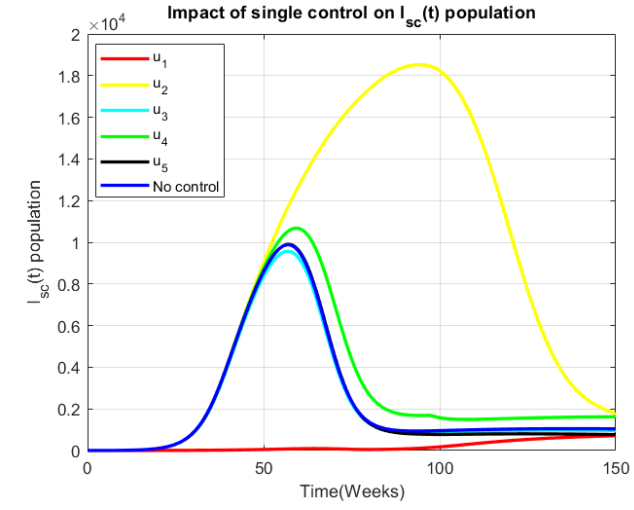

(a)

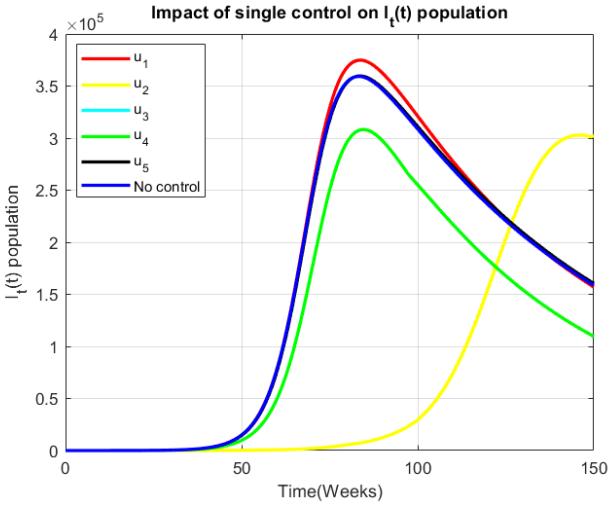

(b)

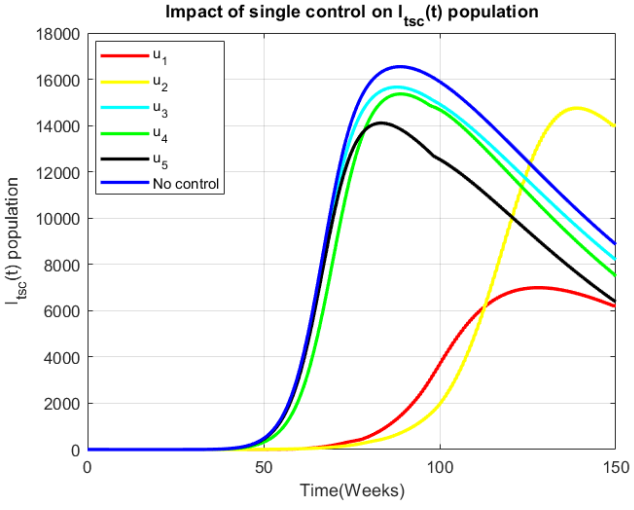

(c)

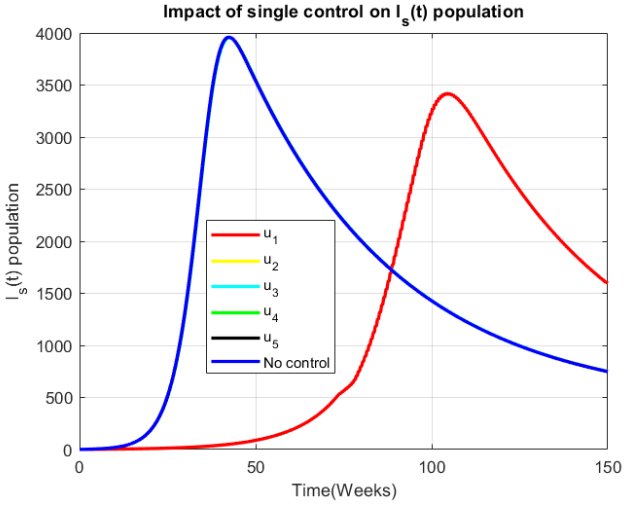

(d)

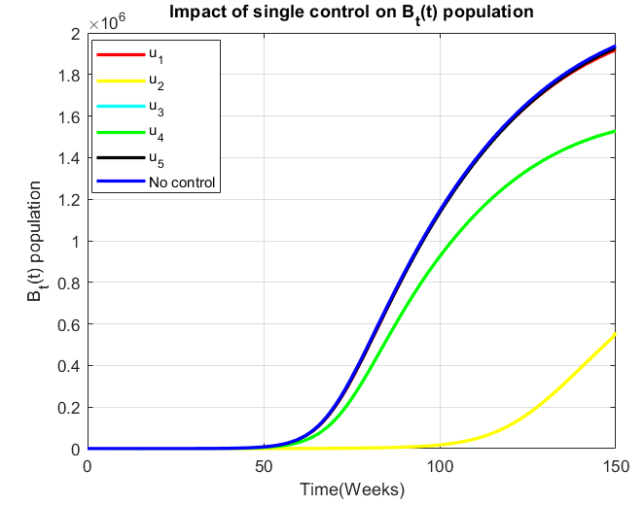

(e)

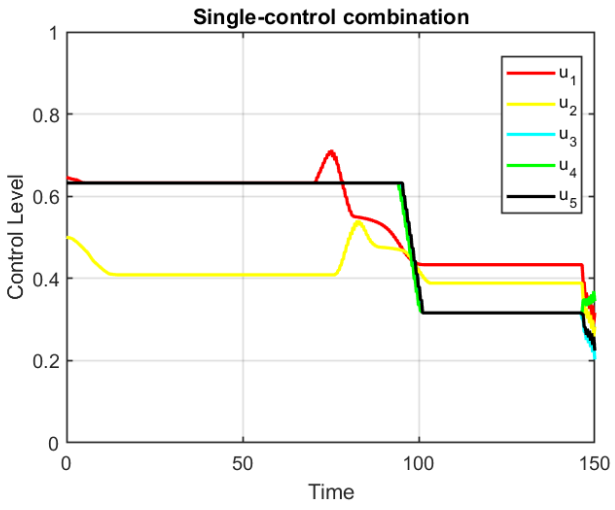

(f)

Figure 15: Numerical simulations of single control application on (a) $I_{sc}(t)$ population, (b) $I_t(t)$ population, (c) $I_{tsc}(t)$ population, (d) $I_s(t)$ population, (e) $B_t(t)$ population and (f) Control profile.

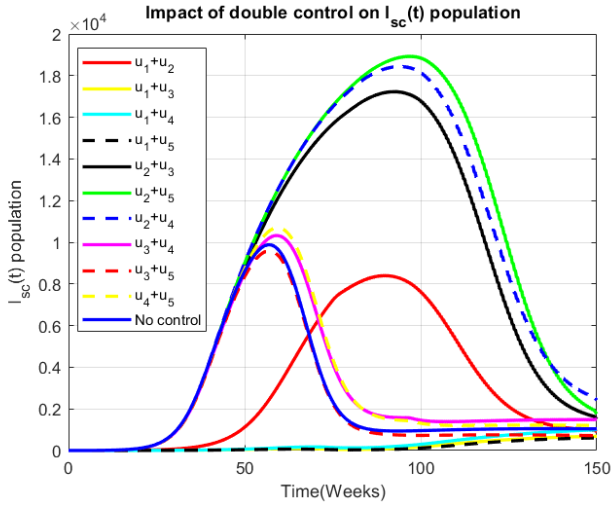

(a)

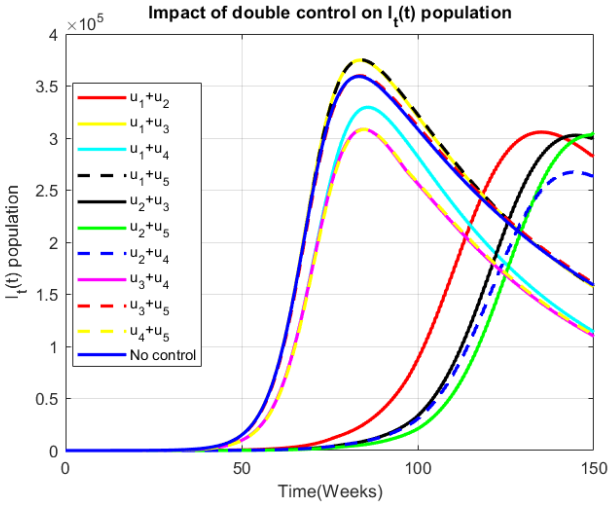

(b)

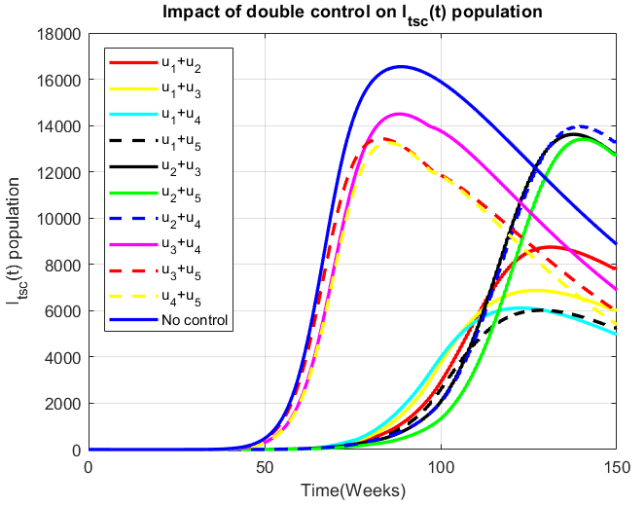

(c)

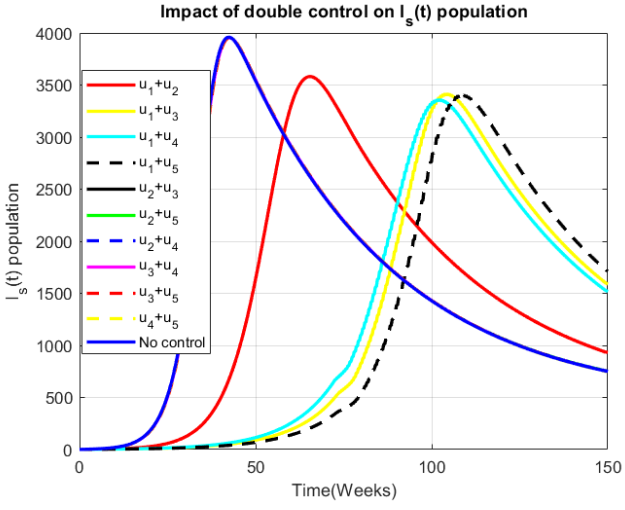

(d)

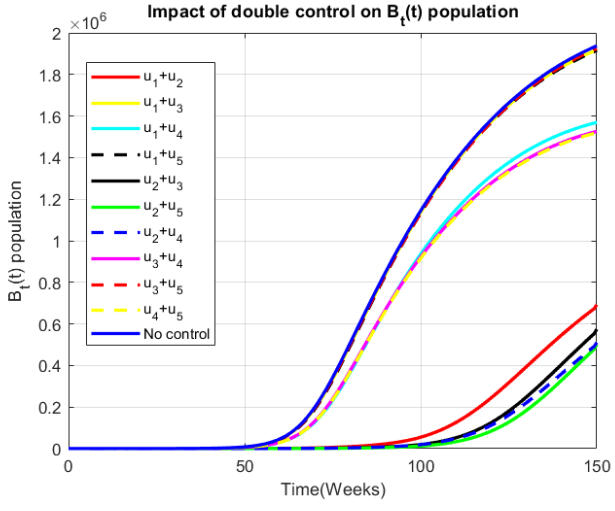

(e)

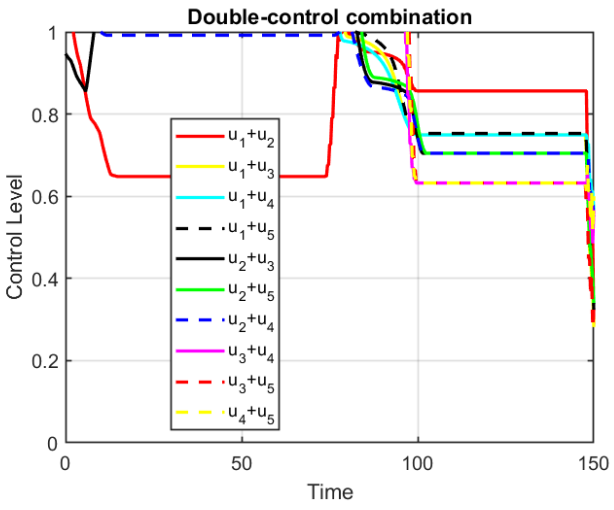

(f)

Figure 16: Numerical simulations of double control application on (a) $I_{sc}(t)$ population, (b) $I_t(t)$ population, (c) $I_{tsc}(t)$ population, (d) $I_s(t)$ population, (e) $B_t(t)$ population and (f) Control profile.

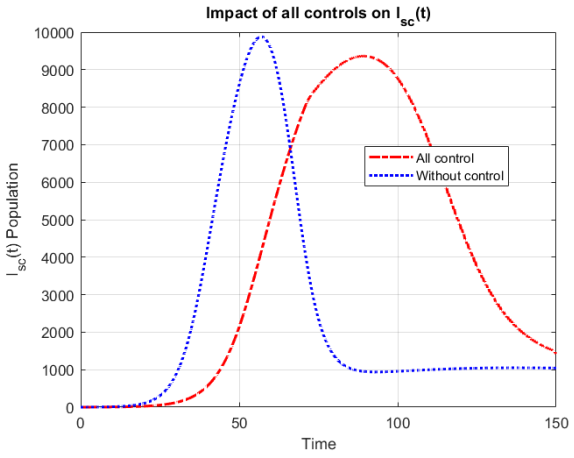

(a)

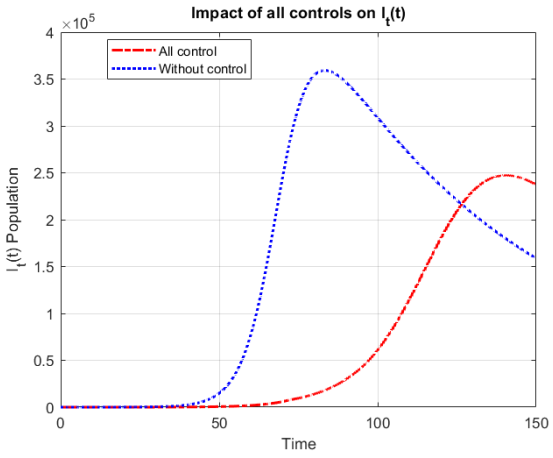

(b)

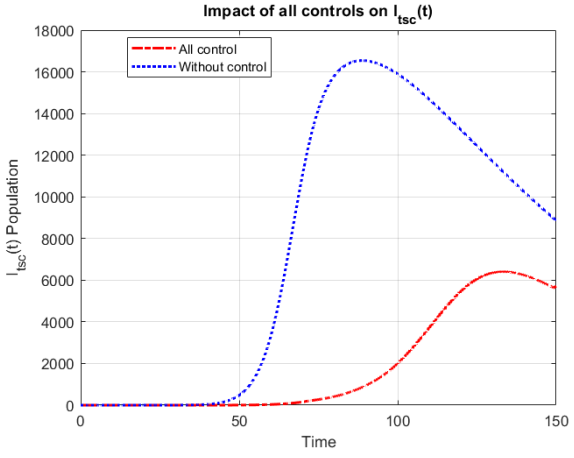

(c)

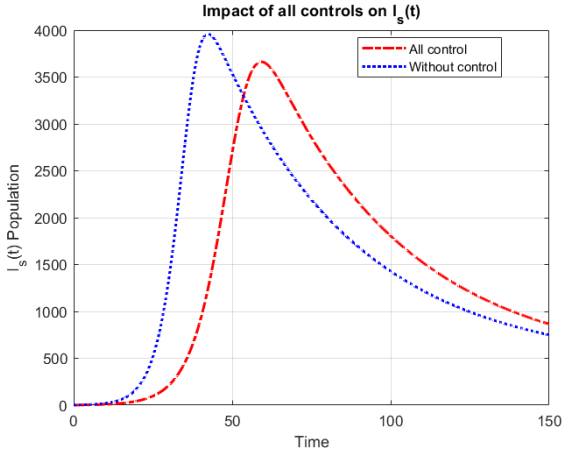

(d)

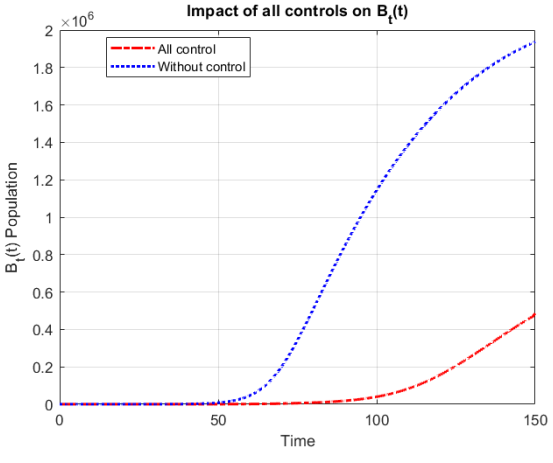

(e)

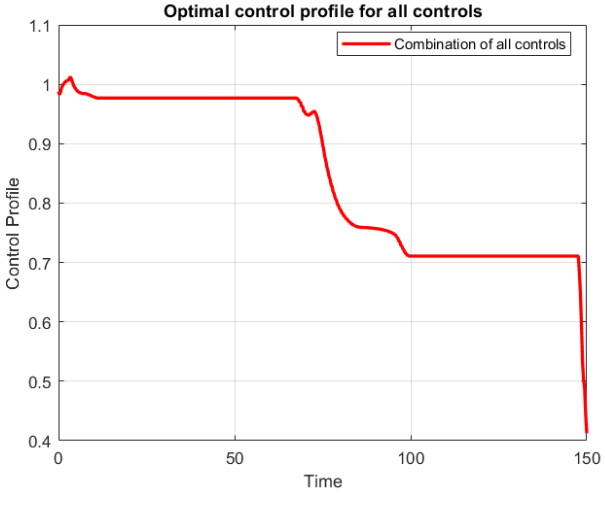

(f)

Figure 17: Numerical simulations of all the control application on (a) $I_{sc}(t)$ population, (b) $I_t(t)$ population, (c) $I_{tsc}(t)$ population, (d) $I_s(t)$ population, (e) $B_t(t)$ population and (f) Control profile.

yields:

$$\frac{dI_s}{dt} = \lambda_3 S_s - (\mu_s + d)I_s.$$

The bacteria concentration in the environment increases due to shedding from typhoid fever only infected individuals and co-infected individuals at the rates γ_1 and γ_2, respectively. The pathogen reduces in the environment due to natural decay at a rate, μ_B. The equation for this dynamics is given as

$$\frac{dB_t}{dt} = \gamma_1 I_t + \gamma_2 I_{tsc} - \mu_B B_t.$$

The flow of interaction and transition dynamics of the co-infection between the compartments is illustrated in Figure 1 and the description of all the parameters is given in Table 2.
The following assumptions are made in the formulation of the model;

- all human populations are homogeneous;
- there is disease-related death in all infected and infectious human classes [1],
- there is a disease-related death for the infected snail,
- snails recruitment rate is by birth,
- rather than modelling the transmission of the Schistosoma parasite from cercariae to humans, the approach directly utilises infected snails that shed cercariae into freshwater. Similarly, instead of modelling snail infection by miracidia, infected humans who release miracidia into freshwater are directly considered, as adopted by Ref.[10].
- reinfection is possible in both diseases after recovery [3, 6]
- both direct and indirect modes of transmission are considered in typhoid fever.

Using Figure 1 and the parameters in Table 1, we derive the system for the typhoid fever and schistosomiasis infection as follows:

$$\left.\begin{aligned}
\frac{dS_h}{dt} &= \Lambda + \phi R_{tsc} + \kappa R_{sc} + \nu R_t - \rho\lambda_2 S_h - (1-\rho)\lambda_1 S_h - \mu S_h,\\
\frac{dI_{sc}}{dt} &= \rho\lambda_2 S_h + \epsilon I_{tsc} - \lambda_1 I_{sc} - (\mu + \delta_1 + \omega)I_{sc},\\
\frac{dI_t}{dt} &= (1-\rho)\lambda_1 S_h + \xi I_{tsc} - \lambda_2 I_t - (\mu + \delta_2 + p)I_t,\\
\frac{dI_{tsc}}{dt} &= \lambda_1 I_{sc} + \lambda_2 I_t - (\mu + \delta_3 + \epsilon + \xi + \theta)I_{tsc},\\
\frac{dR_{sc}}{dt} &= \omega I_{sc} - (\kappa + \mu)R_{sc},\\
\frac{dR_t}{dt} &= pI_t - (\nu + \mu)R_t,\\
\frac{dR_{tsc}}{dt} &= \theta I_{tsc} - (\mu + \phi)R_{tsc},\\
\frac{dS_s}{dt} &= \Lambda_s - \lambda_3 S_s - \mu_s S_s,\\
\frac{dI_s}{dt} &= \lambda_3 S_s - (\mu_s + d)I_s,\\
\frac{dB_t}{dt} &= \gamma_1 I_t + \gamma_2 I_{tsc} - \mu_B B_t.
\end{aligned}\right\} \quad (1)$$

with non-negative initial conditions, $S_h(0) > 0$, $I_{sc}(0) > 0$, $I_t(0) > 0$, $I_{tsc}(0) > 0$, $R_{sc}(0) \geq 0$, $R_t(0) \geq 0$, $R_{tsc}(0) \geq 0$, $S_s(0) > 0$, $I_s(0) > 0$, $B_t(0) > 0$.
Adopting the concept of Okosun and Smith [10], the underlisted forces of infection are applied

$$\left.\begin{aligned}
\lambda_1 &= \underbrace{\beta_1(I_t + I_{tsc}) + +}_{\text{Human-to-human}} \underbrace{\frac{\beta_2 B_t}{K + B_t}}_{\text{Environment-to-human}},\\
\lambda_2 &= \underbrace{\beta_3 I_s}_{\text{Snail-to-human via shedding of cercariae in freshwater}},\\
\lambda_3 &= \underbrace{\beta_4(I_{sc} + I_{tsc})}_{\text{Human-to-snail via release of miracidia in freshwater}}.
\end{aligned}\right\} \quad (2)$$

3. Qualitative analysis of the schistosomiasis–typhoid fever model

In this section, we examine the essential properties of the model equation (1) by considering the schistosomiasis-typhoid fever model and its basic reproduction number, respectively.

3.0.1. Invariant region of the schistosomiasis-typhoid fever model

Here, we established the invariant region of the system of equations (1) such that the region at which the system is bounded is obtained for further analysis.

Considering all the human compartments, and the snail compartments of (1), we have

$$\left.\begin{aligned}
\frac{dN_h}{dt} &= \Lambda - \delta_1 I_{sc} - \delta_2 I_t - \delta_3 I_{tsc} - \mu N_h \leq \Lambda - \mu N_h,\\
\frac{dN_s}{dt} &= \Lambda_s - dI_s - \mu_s N_s \leq \Lambda_s - \mu_s N_s,
\end{aligned}\right\} \quad (3)$$

with initial conditions, $N_h(0) = N_{h_0}$, $N_s(0) = N_{s_0}$, and $B_t(0) = B_{t_0}$. We state the following theorem:

Theorem 3.1. All feasible solutions of the model are uniformly bounded in the set

$$\Pi_{\text{all}} = \Pi_h \times \Pi_s \times \Pi_{B_t},$$

where

$$\begin{aligned}
\Pi_h &= \left\{(S_h(t), I_{sc}(t), I_t(t), I_{tsc}(t), R_{sc}, R_t, R_{tsc}(t)) \in \mathfrak{R}_+^7 : \right.\\
&\qquad \left. 0 \leq N_h(t) \leq \frac{\Lambda}{\mu}\right\},\\
\Pi_s &= \left\{(S_s(t), I_s(t)) \in \mathfrak{R}_+^2 : 0 \leq N_s(t) \leq \frac{\Lambda_s}{\mu_s}\right\},\\
\Pi_{B_t} &= \left\{B_t \in \mathfrak{R}_+ : 0 \leq B_t \leq \Pi_{B_t} \in \left(\frac{\Lambda(\gamma_1 + \gamma_2)}{\mu\mu_B}\right)\right\}.
\end{aligned}$$

These are subsets for the human population, snail population, and bacteria population, respectively.

Proof 3.1. Using the approach of integrating factors to Equation (3) as applied by Ref. [50], we obtain

$$0 \le N_h(t) \le \frac{\Lambda}{\mu} + \left[N_{h_0} - \frac{\Lambda}{\mu}\right] e^{-\mu t},$$
$$0 \le N_s(t) \le \frac{\Lambda_s}{\mu_s} + \left[N_{s_0} - \frac{\Lambda_s}{\mu_s}\right] e^{-\mu_s t},$$

which satisfies $0 \le N_h(t) \le \frac{\Lambda}{\mu}$ and $0 \le N_s(t) \le \frac{\Lambda_s}{\mu_s}$ as $t \to \infty$, respectively. This means that the feasible solutions of the human and non-human mammals populations are in the region, $\Pi_h = \left\{\left((S_h(t), I_{sc}(t), I_t(t), I_{tsc}(t), R_{sc}, R_t, R_{tsc}(t)\right) \in \mathfrak{R}_+^7 : N_h(t) \le \frac{\Lambda}{\mu}\right\}$, $\Pi_s = \left\{\left(S_s(t), I_s(t)\right) \in \mathfrak{R}_+^2 : N_s(t) \le \frac{\Lambda_s}{\mu_s}\right\}$. Since $N_h(t) \le \frac{\Lambda}{\mu}$ and $N_s(t) \le \frac{\Lambda_s}{\mu_s}$, it means that $I_t(t) \le N_h(t) \le \frac{\Lambda}{\mu}$, and $I_{tsc}(t) \le N_h(t) \le \frac{\Lambda}{\mu}$, respectively. Therefore, the last equation of the model (1) can be written as

$$\frac{dB_t}{dt} \le \left(\frac{\Lambda}{\mu}(\gamma_1 + \gamma_2)\right) - \mu_B B_t, \tag{4}$$

solving Equation (4) yields

$$B_t \le \left(\frac{\Lambda}{\mu\mu_B}(\gamma_1 + \gamma_2)\right) + \left[B_{t_0} - \frac{\Lambda}{\mu\mu_B}(\gamma_1 + \gamma_2)\right] e^{-\mu_B t}. \tag{5}$$

As $t \to \infty$ in Equation (5), $0 \le B_t \le \frac{\Lambda}{\mu\mu_B}(\gamma_1 + \gamma_2)$. Therefore, the bacteria population has feasible solution that enters the region $\Pi_{B_t} = \left\{B_t \in \mathfrak{R}_+ : B_t \le \frac{\Lambda}{\mu\mu_B}(\gamma_1 + \gamma_2)\right\}$. Thus, the feasible region for the schistosomiasis-typhoid fever model (1) is $\Pi_{all} = \Pi_h \times \Pi_s \times \Pi_{B_t}$.

Based on the non-negative parameters and initial conditions for the system of model equations (1), we conclude the solutions are also non-negative. Hence, the dynamics of the schistosomiasis-typhoid fever model in (1) are analyzed within the region $\Pi_{all} = \Pi_h \times \Pi_s \times \Pi_{B_t}$. Hence, the model (1) is well-posed mathematically and has biological meaning, implying that the schistosomiasis-typhoid fever model is suitable for further analysis.

3.1. Analysis of schistosomiasis sub-model

Here, we analyse the schistosomiasis sub-model, and this is obtained by setting $I_t = I_{tsc} = R_t = R_{tsc} = B_t = 0$ in system (1) as adopted by Ref. [51].

$$\left.\begin{aligned}
\frac{dS_h}{dt} &= \Lambda + \kappa R_{sc} - \rho\beta_3 I_s S_h - \mu S_h,\\
\frac{dI_{sc}}{dt} &= \rho\beta_3 I_s S_h - (\mu + \delta_1 + \omega) I_{sc},\\
\frac{dR_{sc}}{dt} &= \omega I_{sc} - (\kappa + \mu) R_{sc},\\
\frac{dS_s}{dt} &= \Lambda_s - \beta_4 I_{sc} S_s - \mu_s S_s,\\
\frac{dI_s}{dt} &= \beta_4 I_{sc} S_s - (\mu_s + d) I_s,
\end{aligned}\right\} \tag{6}$$

3.1.1. Stability of schistosomiasis-free equilibrium (SchFE) and basic reproduction number, R_0

The schistosomiasis-free equilibrium (SchFE) of the sub-model of the system of equations (6) is obtained when $I_{sc} = R_{sc} = I_s = 0$. Thus, the SchFE of the sub-model (6), denoted by E_0^{Sch} is given by

$$E_0^{Sch} = (S_{h0}, I_{sc0}, R_{sc0}, S_{s0}, I_{s0}) = \left(\frac{\Lambda}{\mu}, 0, 0, \frac{\Lambda_s}{\mu_s}, 0\right).$$

Using the concept of Den Driessche and Watmough [52] for the computation of the R_0, such that the basic reproduction number, R_0^{Sch} of the schistosomiasis sub-model is the spectral radius (maximum eigenvalue) of the next generation matrix FV^{-1} computed at the E_0^S, where $F = \frac{\partial \mathcal{F}_i E_0^S}{\partial x_i}$ and $V = \frac{\partial \mathcal{V}_i E_0^{Sch}}{\partial x_i}$, means the transmission and transition matrices evaluated at E_0^{Sch}. For clarity sake, $\mathcal{F}_i$ stands for new infections in compartment i, and $\mathcal{V}_i$ represents transfer of infections between compartments, i. Let

$$q_1 = (\mu + \delta_1 + \omega), \quad q_4 = (\kappa + \mu), \quad q_7 = (\mu_s + d). \tag{7}$$

Then, we derived

$$F = \begin{pmatrix} 0 & \rho\beta_3 S_{h0} \\ \rho\beta_4 S_{s0} & 0 \end{pmatrix}, \; V = \begin{pmatrix} q_1 & 0 \\ 0 & q_7 \end{pmatrix},$$

$$V^{-1} = \begin{pmatrix} {q_1}^{-1} & 0 \\ 0 & {q_7}^{-1} \end{pmatrix}.$$

So, $R_0^S = \rho(FV^{-1})$ with ρ as the spectral radius of FV^{-1} is given as

$$R_0^{Sch} = \frac{\sqrt{q_1 q_7 S_{s0} S_{s0} \beta_3 \beta_4 \rho}}{q_1 q_7}.$$

With the definition in (7), we have the basic reproduction number of the schistosomiasis sub-model as

$$R_0^{Sch} = \sqrt{\frac{(\mu + \delta_1 + \omega)(\mu_s + d)\Lambda_s \Lambda \beta_3 \beta_4 \rho}{\mu\mu_s(\mu + \delta_1 + \omega)^2(\mu_s + d)^2}},$$

R_0^{Sch} denotes the contributions to the schistosomiasis basic reproduction number from two primary pathways: (1) transmission from infected humans to the snail population, characterized by the recruitment rate Λ_s and natural death rate μ_s, via the release of eggs that hatch into miracidia in freshwater at the effective transmission rate β_4; and (2) transmission from infected snails to the proportion ρ of the susceptible human population, with recruitment rate Λ and natural death rate μ, at the effective transmission rate β_3. We address the DFE stability of system (6) since the next-generation approach is employed for the derivation of R_0^{Sch}.

Theorem 3.2. E_0^S is locally asymptomatically stable if $R_0^{Sch} < 1$ and unstable if $R_0^{Sch} > 1$.

Proof 3.2. Theorem 3.2 implies that the schistosomiasis infection can be eliminated over time if $R_0^S < 1$, and this will be

carried out using the linearisation method by obtaining the Jacobian matrix, $J(E_0^S)$ of the system of equations (6), given as follow:

$$J(E_0^S) = \begin{pmatrix} -\mu & 0 & \kappa & 0 & -\rho\beta_3 S_{h0} \\ 0 & -q_1 & 0 & 0 & \rho\beta_3 S_{h0} \\ 0 & \omega & -q_4 & 0 & 0 \\ 0 & -\beta_4 S_{s0} & 0 & -\mu_s & 0 \\ 0 & \beta_4 S_{s0} & 0 & 0 & -q_7 \end{pmatrix}.$$

Using the inspection method in linear algebra as used by [53], we have the following eigenvalues, $-\mu, -\mu_s$, and $-q_4$, with the remaining eigenvalues obtained from the sub-matrix $J_2(E_0^{Sch})$ below

$$J_2(E_0^{Sch}) = \begin{bmatrix} -q_1 & \rho\beta_3 S_{h0} \\ \beta_4 S_{s0} & -q_7 \end{bmatrix}.$$

Solving for the eigenvalues of the sub-Jacobian matrix, $J_2(E_0^{Sch})$, we have the characteristic equation

$$\lambda^2 + H_1\lambda + H_2 = 0, \tag{8}$$

where

$$\begin{aligned} H_1 &= (q_1 + q_7), \\ H_2 &= q_1 q_7 (1 - R_0^{2\text{Sch}}). \end{aligned}$$

Adopting the concept presented by Heffernan *et al.* [54], which states that a system of equations is locally asymptotically stable if and only if all the coefficients of the characteristic equation of the Jacobian matrix of the system are all positive. Therefore, it is evident that the system of equations (6) of the schistosomiasis sub-model is locally asymptotically stable, since $H_1, H_2 > 0$ provided $R_0^{\text{Sch}} < 1$. This is consistent with the Routh-Hurwitz stability criterion of order 2, as all coefficients of the characteristic equation and the constant are positive when $R_0^{\text{Sch}} < 1$.

3.1.2. *Existence of endemic equilibrium state of schistosomiasis sub-model*

The endemic equilibrium state, E^e, is a state in which schistosomiasis persists within the population over time. From the second, third, fourth and fifth equations of system (6), respectively, we have

$$S_h^e = \frac{q_1 I_{sc}^e}{\rho\beta_3 I_s^e}, R_{sc}^e = \frac{\omega I_{sc}}{q_4}, S_s^e = \frac{\Lambda_s}{(\beta_4 I_{sc} + \mu_s)}, I_s^e = \frac{\beta_4 I_{sc} S_s^e}{q_7},$$

Substituting S_s^e into I_s^e, we have $I_s^e = \frac{\Lambda_s \beta_4 I_{sc}}{q_7(\beta_4 I_{sc} + \mu_s)}$ and upon substituting S_h^e, R_{sc}^e, I_s^e into the first equation of system (6), we get

$$I_{sc}^e = \frac{q_1 q_4 q_7 \mu\mu_s (R_0^{2\text{Sch}} - 1) - q_1 q_4 \rho\beta_3\beta_4\Lambda_s}{\mu q_1 q_4 q_7 \beta_4 - \kappa\omega\rho\beta_3\beta_4\Lambda_s}.$$

Hence, S_h^e, R_{sc}^e, S_s^e, and I_s^e are obtained by substituting I_{sc}^e.

3.1.3. *Existence of bifurcation analysis of the schistosomiasis sub-model*

A critical point, known as a bifurcation, is being examined to determine how certain factors affect the spread of schistosomiasis disease, particularly when the reproduction number, R_0, equals 1. Whenever a backward bifurcation occurs, schistosomiasis can persist in a diverse set of steady states even when $R_0 < 1$, making forecasting/predicting and controlling the disease, more complicated. The centre manifold theorem by Castillo-Chavez and Song [55] will be explored to carry out the bifurcation analysis on the system of equations (6) with

$$a = \sum_{k,i,j=1}^{n} z_k w_i w_j \frac{\partial^2 f_k(E^0)}{\partial x_i \partial x_j} \text{ and } b = \sum_{k,i=1}^{n} z_k w_i \frac{\partial^2 f_k(E^0)}{\partial x_i \partial \beta_3},$$

as bifurcation coefficients and β_3 as the bifurcation parameter such that $R_0^{\text{Sch}} = 1$ as employed by Okosun *et al.* [10] if and only if

$$\beta_3 = \beta_3^* = \frac{\mu\mu_s(\mu + \delta_1 + \omega)(\mu_s + d)}{\rho\beta_4\Lambda_s\Lambda}.$$

Then, we transformed the state variables such that $S_h = x_1, I_{sc} = x_2, R_{sc} = x_3, S_s = x_4, I_s = x_5$. Adopting vector notation $\vec{x} = (x_1, x_2, x_3.x_4.x_5)^T$, schistosomiasis sub-model (6) can be written in the form $\vec{x}' = F(\vec{x})$, such that $F = (f_1, f_2, f_3, f_4, f_5)^T$, written below as

$$\left.\begin{aligned} \frac{dx_1}{dt} &= \Lambda + \kappa x_5 - \rho\beta_3 x_5 x_1 - \mu x_1 = f_1, \\ \frac{dx_2}{dt} &= \rho\beta_3 x_5 x_1 - q_1 x_2 = f_2, \\ \frac{dx_3}{dt} &= \omega x_x - q_4 x_5 = f_3, \\ \frac{dx_4}{dt} &= \Lambda_s - \beta_4 x_2 x_8 - \mu_s x_8 = f_4, \\ \frac{dx_5}{dt} &= \beta_4 x_2 x_8 - (\mu_s + d) x_9 = f_5, \end{aligned}\right\} \tag{9}$$

with non-negative initial conditions. This technique requires that the Jacobian of the system (9) at the disease-free equilibrium, denoted by $J(E_0)$, have a simple zero eigenvalue and all other eigenvalues negative at $R_0^{Sch} = 1$. Hence, the right and left eigenvectors w and z corresponding to a simple zero eigenvalue of $J(E_0)$ are obtained respectively using $J(E_0) \cdot w = 0$ and $J^T(E_0) \cdot z = 0$. They are given as:

$$\begin{aligned} w_1 = \frac{(\omega\kappa q_7 - \rho\beta_3\beta_4 S_{h0} q_4) w_2}{\mu q_4 q_7}, w_3 = \frac{\omega w_2}{q_4}, \\ w_4 = \frac{-\beta_4 S_{s0} w_2}{\mu_s}, w_5 = \frac{\beta_4 S_{s0} w_2}{q_7}, \ w_2 = w_2 > 0, \end{aligned} \tag{10}$$

$$z_1 = z_3 = z_4 = 0, z_2 = z_2 > 0,$$

$$z_5 = \frac{\rho\beta_3 S_{h0} z_2}{q_7}, \tag{11}$$

with $w.z = 1$, $\vec{w} = (w_1, w_2, w_3, w_4, w_5)^T$ and $\vec{z} = (z_1, z_2, z_3, z_4, z_5)^T$.

Also, the non-zero second order derivatives of x_1, x_2, x_3, x_4, x_5 at disease-free equilibrium yield

$$\frac{\partial^2 f_2(E^0)}{\partial x_1 \partial x_5} = \rho\beta_3, \quad \frac{\partial^2 f_5(E^0)}{\partial x_4 \partial x_2} = \beta_4, \tag{12}$$

and

$$z_2 w_2 \frac{\partial^2 f_2(E^0)}{\partial x_5 \partial \beta_3} = z_2 w_5 \rho S_h^0. \tag{13}$$

Hence, employing the non-zero second-order partial derivatives of equation (12) and equation (13), with $w.z = 1$, we get

$$a = w_2^2 z_2 \left(\left[\frac{(\omega\kappa q_7 - \rho\beta_3\beta_4 S_{h0} q_4)\beta_4 S_{s0}\rho\beta_3}{\mu q_4 q_7^2} \right] - \frac{\beta_4 S_{s0}\rho\beta_3 S_{h0}\beta_4}{q_7\mu_s} \right),$$

and

$$b = z_2 w_2 \left[\frac{\rho\beta_4 S_{h0} S_{s0}}{q_7} \right] > 0, \tag{14}$$

with definition of q_1, q_4, q_7 in (7).

Figure 2 shows that the schistosomiasis sub-model exhibits forward bifurcation. This indicates that the disease-free state is likely globally stable, supporting disease elimination and a low risk of persistent transmission below the threshold. If the reproduction number exceeds 1, the endemic equilibrium persists, resulting in ongoing disease transmission. In summary, the endemic equilibrium is globally asymptotically stable when the reproduction number is greater than 1, while the disease-free equilibrium is globally asymptotically stable when the reproduction number is less than 1, as noted by Ref. [55].

3.2. Analysis of typhoid fever sub-model

Here, we analyse the typhoid fever sub-model, and this is obtained by setting $I_{sc} = I_{tsc} = R_{sc} = R_{tsc} = S_s = I_s = 0$ in the system of equations (1). So, we have

$$\left.\begin{aligned} \frac{dS_h}{dt} &= \Lambda + \nu R_t - (1-\rho)\left[\beta_1 I_t + \frac{\beta_2 B_t}{K + B_t}\right] S_h - \mu S_h, \\ \frac{dI_t}{dt} &= (1-\rho)\left[\beta_1 I_t + \frac{\beta_2 B_t}{K + B_t}\right] S_h - (\mu + \delta_2 + p) I_t, \\ \frac{dR_t}{dt} &= pI_t - (\nu + \mu) R_t, \\ \frac{dB_t}{dt} &= \gamma_1 I_t - \mu_B B_t. \end{aligned}\right\} \tag{15}$$

3.2.1. Stability of typhoid fever-free equilibrium (TfFE) and basic reproduction number, R_0^{Tf}

The typhoid fever-free equilibrium (TfFE) of the sub-model of the system of equations (15) is obtained when $I_t == R_t = B_t = 0$. Thus, the TfFE of the sub-model (15), denoted by E_0^{Tf} is given by

$$E_0^{Tf} = (S_{h0}, I_{t0}, R_{t0}, B_{t0}) = \left(\frac{\Lambda}{\mu}, 0, 0, 0\right).$$

Using the concept of Den Driessche and Watmough [52] for the computation of the reproduction number. we let

$$q_2 = (\mu + \delta_2 + p), \quad q_5 = (\nu + \mu), A = (1 - \rho). \tag{16}$$

Then, we derived

$$F = \begin{pmatrix} A\beta_1 S_{h0} & \frac{A\beta_2 S_{h0}}{K} \\ 0 & 0 \end{pmatrix}, \; V = \begin{pmatrix} q_2 & 0 \\ -\gamma_1 & \mu_B \end{pmatrix},$$

$$V^{-1} = \begin{pmatrix} {q_2}^{-1} & 0 \\ \frac{\gamma_1}{q_2\mu_B} & {\mu_B}^{-1} \end{pmatrix}.$$

So, $R_0^{Tf} = \rho(FV^{-1})$ with ρ as the spectral radius of FV^{-1} is given as

$$R_0^{Tf} = \frac{AS_{h0}(K\beta_1\mu_B + \beta_2\gamma_1)}{Kq_2\mu_B}.$$

With the definition in (16), we have the basic reproduction number of the typhoid sub-model as

$$R_0^{Tf} = \frac{(1-\rho)S_{h0}(K\beta_1\mu_B + \beta_2\gamma_1)}{K(\mu + \delta_2 + p)\mu_B},$$

and this can be written as $R_0^{\mathrm{Tf}} = R_{HH}^{\mathrm{Tf}} + R_{EH}^{\mathrm{Tf}}$, such that

$$\left.\begin{aligned} R_{HH}^{\mathrm{Tf}} &= \frac{\Lambda(1-\rho)\beta_1}{\mu(\mu + \delta_2 + p)}, \\ R_{EH}^{\mathrm{Tf}} &= \frac{\Lambda(1-\rho)\beta_2\gamma_1}{K\mu(\mu + \delta_2 + p)\mu_B}, \end{aligned}\right\} \tag{17}$$

where R_{HH}^{Tf} is the basic reproduction number of typhoid fever from human-to-human and R_{EH}^{Tf} is the basic reproduction number of typhoid fever from environment-to-human. R_0^{Tf} denotes the basic reproduction number for typhoid fever, incorporating contributions from both human-to-human transmission, represented by the proportion $(1-\rho)$ of the susceptible human population, with recruitment rate Λ and natural death rate μ, and the contribution from environment to proportion $(1-\rho)$ of human with recruitment rate Λ and natural death rate, μ at the transmission at rate β_2, mediated by the shedding rate γ_1 from infected individuals. R_{HH}^{Tf} refers to the human-to-human transmission component of R_0^{Tf}, whereas R_{EH}^{Tf} refers to the environment-to-human transmission component.

We address the DFE stability of system (15) since the next-generation approach is employed for the derivation of R_0^{Tf}.

Theorem 3.3. E_0^{Tf} is locally asymptomatically stable if $R_0^{Tf} < 1$ and unstable if $R_0^{Tf} > 1$.

Proof 3.3. Theorem 3.3 implies that the typhoid fever infection can be eliminated over time if $R_0^{Tf} < 1$, and this will be carried out using the linearisation method by obtaining the Jacobian matrix, $J(E_0^{Tf})$ of the system of equations (15), given as follow:

$$J(E_0^{Tf}) = \begin{pmatrix} -\mu & -A\beta_1 S_{h0} & \nu & \frac{-\rho\beta_3 S_{h0}}{K} \\ 0 & A\beta_1 S_{h0} - q_2 & 0 & \frac{\rho\beta_3 S_{h0}}{K} \\ 0 & p & -q_5 & 0 \\ 0 & \gamma_1 & 0 & -\mu_B \end{pmatrix}.$$

Using the inspection method in linear algebra as used by [53], we have the following eigenvalues, $-\mu$, and $-q_5$, with the remaining eigenvalues obtained from the sub-matrix $J_2(E_0^{Tf})$ below

$$J_2(E_0^{Tf}) = \begin{bmatrix} A\beta_1 S_{h0} - q_2 & \frac{A\beta_2 S_{h0}}{K} \\ \gamma_1 & -\mu_B \end{bmatrix}.$$

Solving for the eigenvalues of the sub-Jacobian matrix, $J_2(E_0^{Tf})$, we have the characteristic equation

$$\lambda^2 + H_1^*\lambda + H_2^* = 0, \tag{18}$$

where

$$\begin{aligned} H_1^* &= q_2(1 - R_{HH}^{\mathrm{Tf}}) + \mu_B, \\ H_2^* &= q_2\mu_B K(1 - R_0^{\mathrm{Tf}}). \end{aligned}$$

Adopting the concept presented by Heffernan *et al.* [54], which states that a system of equations is locally asymptotically stable if and only if all the coefficients of the characteristic equation of the Jacobian matrix of the system are all positive. Therefore, it is evident that the system of equations (15) of the typhoid fever sub-model is locally asymptotically stable, since $H_1^*, H_2^* > 0$ provided $R_{HH}^{\mathrm{Tf}} < 1$ and $R_0^{\mathrm{Tf}} < 1$. This also aligns with the Routh-Hurwitz stability criterion of order 2, since all the coefficient of the characteristic equation and the constant are positive, provided $R_0^{\mathrm{Tf}} < 1$.

3.2.2. *Existence of endemic equilibrium state of typhoid fever sub-model*

The endemic equilibrium state, E^*, is a state in which typhoid fever persists within the population over time. From the third, and the last equations of system (15), respectively, we have

$$R_t^e = \frac{pI_t}{q_5}, B_t^e = \frac{\gamma_1 I_t}{\mu_B},$$

Substituting B_t^e into $\left[\beta_1 I_t + \frac{\beta_2 B_t}{K+B_t}\right]$, we have $\left[\beta_1 I_t + \frac{\beta_2 B_t}{K+B_t}\right] = \frac{\beta_1\mu_B K I_t + \beta_1\gamma_1 I_t^2 + \beta_2\gamma_1 I_t}{\mu_B K + \gamma_1 I_t}$. Therefore, from the second equation of system (15), we have

$$S_h^e = \frac{q_2(\mu_B K + \gamma_1 I_i)}{A[\beta_1\mu_B K + \beta_1\gamma_1 I_t + \beta_2\gamma_1]}.$$

Hence, solving the first equation of the system (15) by substituting, Hence, S_h^e, R_{sc}^e, S_s^e, and I_s^e are obtained by substituting R_t^e, S_h^e and B_t^e, we have

$$A_1 I_t^2 + A_2 I_t + A_3 = 0,$$

where

$$\begin{aligned} A_1 &= A\gamma_1\beta_1(q_2q_5 - \nu p), \\ A_2 &= \Lambda A\beta_1\gamma_1 q_5 + \nu pA\beta_1\mu_B K + \nu pA\beta_2\gamma_1 \\ &\quad - q_2q_5A\beta_1\mu_B K - q_2q_5A\beta_2\gamma_1 - \mu q_2q_5\gamma_1, \\ A_3 &= \mu q_2q_5\mu_B K(1 - R_0^{\mathrm{Tf}}), \end{aligned}$$

with $q_2q_5 - \nu p > 0$ making $A_1 > 0$. $A_3 > 0$ if $R_0^{\mathrm{Tf}} < 1$ and $A_3 < 0$ if $R_0^{\mathrm{Tf}} > 1$. So, we have a unique positive endemic equilibrium when $R_0^{\mathrm{Tf}} > 1$ given as:

$$I_t^* = \frac{-A_2 + \sqrt{A_2^2 - -4A_1A_3}}{2A_1} > 0, \text{ if } R_0^{Tf} > 1.$$

3.2.3. *Bifurcation analysis of the typhoid fever sub-model*

Here, we also employed centre manifold theorem by Castillo-Chavez and Song [55] to carry out the bifurcation analysis on the system of equations (15) with

$$a = \sum_{k,i,j=1}^{n} z_k w_i w_j \frac{\partial^2 f_k(E^0)}{\partial x_i \partial x_j} \text{ and } b = \sum_{k,i=1}^{n} z_k w_i \frac{\partial^2 f_k(E^0)}{\partial x_i \partial \beta_1},$$

as bifurcation coefficients and β_1 as the bifurcation parameter such that $R_0^{\mathrm{Tf}} = 1$, if and only if

$$\beta_1 = \beta_1^* = \frac{\mu K(\mu + \delta_2 + p)\mu_B - (1-\rho)\Lambda\beta_2\gamma_1}{(1-\rho)\Lambda K\mu_B}.$$

Then, we transformed the state variables such that $S_h = x_1, I_t = x_2, R_t = x_3, B_t = x_4$. Adopting vector notation $\vec{x} = (x_1, x_2, x_3.x_4)^T$, typhoid fever sub-model (15) can be written in the form $\vec{x}' = F(\vec{x})$, such that $F = (f_1, f_2, f_3, f_4)^T$, written below as

$$\left.\begin{aligned} \frac{dx_1}{dt} &= \Lambda + \nu x_3 - (1-\rho)\left[\beta_1 x_2 + \frac{\beta_2 x_4}{K + x_4}\right]x_1 \\ &\quad - \mu x_1 = f_1, \\ \frac{dx_2}{dt} &= (1-\rho)\left[\beta_1 x_2 + \frac{\beta_2 x_4}{K + x_4}\right]x_1 - q_2 x_2 = f_2, \\ \frac{dx_3}{dt} &= px_2 - q_5 x_3 = f_3, \\ \frac{dx_4}{dt} &= \gamma_1 x_2 - \mu_B x_4 = f_4, \end{aligned}\right\} \tag{19}$$

with non-negative initial conditions.

Using the Jacobian matrix in Theorem 3.3, we have the right and left eigenvectors w and z at $R_0^{\mathrm{Tf}} = 1$ given as

$$\begin{aligned} w_1 &= -\frac{(A\beta_1 S_{h0} q_5 K\mu_B + \nu pK\mu_B + q_5 A\beta_2\gamma_1 S_{h0})w_2}{K\mu_B q_5}, \\ w_3 &= \frac{pw_2}{q_5}, w_4 = \frac{\gamma_1 w_2}{\mu_B}, \ w_2 = w_2 > 0, \end{aligned} \tag{20}$$

$$z_1 = z_3 = 0, z_2 = z_2 > 0,$$

$$z_4 = \frac{A\beta_2 S_{h0} z_2}{\mu_B K}, \tag{21}$$

with $w.z = 1$, $\vec{w} = (w_1, w_2, w_3, w_4)^T$ and $\vec{z} = (z_1, z_2, z_3, z_4)^T$. Also, the non-zero second order derivatives of x_1, x_2, x_3, x_4 at disease-free equilibrium yield

$$\frac{\partial^2 f_2(E^0)}{\partial x_1 \partial x_2} = A\beta_1, \ \frac{\partial^2 f_5(E^0)}{\partial x_1 \partial x_4} = \frac{A\beta_2}{K}, \tag{22}$$

and

$$z_2 w_2 \frac{\partial^2 f_2(E^0)}{\partial x_2 \partial \beta_1} = z_2 w_2 A S_h^0. \tag{23}$$

Hence, employing the non-zero second-order partial derivatives of equation (21) and equation (23), with $w.z = 1$, we get

$$a = -w_2^2 z_2 \frac{(A\beta_1 S_{h0} q_5 K\mu_B + \nu p K\mu_B + q_5 A\beta_2\gamma_1 S_{h0})}{K\mu_B q_5} \times \left(A\beta_1 + \frac{\gamma_1 A\beta_2}{K\mu_B}\right) < 0,$$

and

$$b = z_2 w_2 A S_{h0} > 0, \tag{24}$$

with definition of A, q_2, q_5 in (16).

The typhoid fever sub-model exhibits forward bifurcation as shown in Figure 3. This indicates that the disease-free state can be globally stable, supporting disease elimination and minimising persistent transmission when the reproduction number is below 1. If the reproduction number exceeds 1, the endemic equilibrium persists, resulting in ongoing disease transmission. In summary, according to Ref. [55], the endemic equilibrium is globally asymptotically stable when the reproduction number is greater than 1, while the disease-free equilibrium is globally asymptotically stable when the reproduction number is less than 1.

3.3. Further analysis of the full co-infection model

3.3.1. Stability of schistosomiasis-typhoid fever-free equilibrium (STFFE) and basic reproduction number, $R_0^{Sch\text{-}Tf}$

The schistosomiasis-typhoid fever-free equilibrium (STFFE) of the system of equations (1) is established when

$$I_{sc} = I_t = I_{tsc} = R_{sc} = R_t = R_{tsc} = I_s = B_t = 0.$$

Thus, the STFFE of the model (1), denoted by E_0^{ST} is

$$\begin{aligned} E_0^{\text{Sch-Tf}} &= (S_h, I_{sc}, I_t, I_{tsc}, R_{sc}, R_t, R_{tsc}, S_s, I_s, B_t) \\ &= \left(\frac{\Lambda}{\mu}, 0, 0, 0, 0, 0, 0, \frac{\Lambda_s}{\mu_s}, 0, 0\right). \end{aligned}$$

Applying the concept of Den Driessche and Watmough [52] for the computation of the $R_0^{\text{Sch-Tf}}$, such that the basic reproduction number, $R_0^{\text{Sch-Tf}}$ for the full model is the spectral radius (maximum eigenvalue) of the next generation matrix FV^{-1} computed at the E_0, we have $F = \frac{\partial \mathcal{F}_i E_0}{\partial x_i}$ and $V = \frac{\partial \mathcal{V}_i E_0}{\partial x_i}$. For clarity sake, $\mathcal{F}_i$ stands for new infections in compartment i, and $\mathcal{V}_i$ represents transfer of infections between compartments, i. Let

$$\begin{aligned} &q_1 = (\mu + \delta_1 + \omega), \quad q_2 = (\mu + \delta_2 + p), \\ &q_3 = (\mu + \delta_3 + \epsilon + \xi + \theta), q_4 = (\kappa + \mu), q_5 = (\nu + \mu), \\ &q_6 = (\mu + \phi), q_7 = (\mu_s + d), A = (1 - \rho). \end{aligned} \tag{25}$$

Then, we derived

$$F = \begin{pmatrix} 0 & 0 & 0 & \rho\beta_3 S_{h0} & 0 \\ 0 & A\beta_1 S_{h0} & A\beta_1 S_{h0} & 0 & \frac{A\beta_2 S_{h0}}{K} \\ 0 & 0 & 0 & 0 & 0 \\ \beta_4 S_{s0} & 0 & \beta_4 S_{s0} & 0 & 0 \\ 0 & 0 & 0 & 0 & 0 \end{pmatrix},$$

$$V = \begin{pmatrix} q_1 & 0 & -\epsilon & 0 & 0 \\ 0 & q_2 & -\xi & 0 & 0 \\ 0 & 0 & q_3 & 0 & 0 \\ 0 & 0 & 0 & q_7 & 0 \\ 0 & -\gamma_1 & -\gamma_2 & 0 & \mu_B \end{pmatrix},$$

$$V^{-1} = \begin{pmatrix} {q_1}^{-1} & 0 & \frac{\epsilon}{q_3 q_1} & 0 & 0 \\ 0 & {q_2}^{-1} & \frac{\xi}{q_2 q_3} & 0 & 0 \\ 0 & 0 & {q_3}^{-1} & 0 & 0 \\ 0 & 0 & 0 & {q_7}^{-1} & 0 \\ 0 & \frac{\gamma_1}{q_2\mu_B} & \frac{\xi\gamma_1 + q_2\gamma_2}{q_2 f_3 \mu_B} & 0 & {\mu_B}^{-1} \end{pmatrix}.$$

Upon obtaining the spectral radius of FV^{-1}, we have

$$R_0^{\text{Sch}} = \frac{\sqrt{q_1 q_7 \beta_4 S_{s0} \rho \beta_3 S_{h0}}}{q_1 q_7},$$

and

$$R_0^{\text{Tf}} = \frac{S_{ho}(1-\rho)\left(K\beta_1\mu_B + \beta_2\gamma_1\right)}{Kq_2\mu_B},$$

such that

$$R_0 = R_0^{\text{Sch-Tf}} = max\left(R_0^{\text{Sch}}, R_0^{\text{Tf}}\right).$$

such that

$$R_0^{\text{Sch}} = \sqrt{\frac{(\mu + \delta_1 + \omega)(\mu_s + d)\beta_4 \Lambda_s \rho \beta_3 \Lambda}{\mu\mu_s(\mu + \delta_1 + \omega)^2(\mu_s + d)^2}}.$$

$$R_0^{\text{Tf}} = \frac{\Lambda(1-\rho)\left(K\beta_1\mu_B + \beta_2\gamma_1\right)}{K\mu(\mu + \delta_2 + p)\mu_B}.$$

We address the DFE stability of system (1) since the next-generation approach is employed for the computation of $R_0^{\text{Sch-Tf}}$.

Theorem 3.4. *E_0 is locally asymptomatically stable if $R_0^{\text{Sch-Tf}} < 1$ and unstable if $R_0^{\text{Sch-Tf}} > 1$.*

Proof 3.4. Theorem 3.4 implies that the schistosomiasis-typhoid fever co-infection can be eliminated over time if $R_0^{\text{Sch-Tf}} < 1$ and this will be carried out using the linearisation

method by obtaining the Jacobian matrix, $J(E_0)$ of the system of equations (1), given as follows;

$$\begin{pmatrix} -\mu & 0 & -g & -g & \kappa & \nu & \phi & 0 & -\rho\beta_3 S_{h0} & -\frac{(1-\rho)\beta_2 S_{h0}}{K} \\ 0 & -q_1 & \epsilon & 0 & 0 & 0 & 0 & 0 & \rho\beta_3 S_{h0} & 0 \\ 0 & 0 & g-q_2 & g+\xi & 0 & 0 & 0 & 0 & 0 & \frac{(1-\rho)\beta_2 S_{h0}}{K} \\ 0 & 0 & 0 & -q_3 & 0 & 0 & 0 & 0 & 0 & 0 \\ 0 & \omega & 0 & 0 & -q_4 & 0 & 0 & 0 & 0 & 0 \\ 0 & 0 & p & 0 & 0 & -q_5 & 0 & 0 & 0 & 0 \\ 0 & 0 & 0 & \theta & 0 & 0 & -q_6 & 0 & 0 & 0 \\ 0 & -\beta_4 S_{s0} & 0 & -\beta_4 S_{s0} & 0 & 0 & 0 & -\mu_s & 0 & 0 \\ 0 & \beta_4 S_{s0} & 0 & \beta_4 S_{s0} & 0 & 0 & 0 & 0 & -q_7 & 0 \\ 0 & 0 & \gamma_1 & \gamma_2 & 0 & 0 & 0 & 0 & 0 & -\mu_B \end{pmatrix},$$

where $g = (1-\rho)\beta_1 S_{h0}$. Using the inspection method as used by Ref. [53], we have the first five eigenvalues, $\lambda_1, ..., \lambda_6$ as $-\mu, -q_3, -q_4, -q_5, -q_6$ and $-\mu_s$, with definition of $A, q_1, ..., q_7$ in (25). The remaining four eigenvalues obtained from the sub-matrix $J_2(E_{02})$ below $J_2(E_{02}^{\text{Sch-Tf}}) =$

$$\begin{bmatrix} -q_1 & \epsilon & \rho\beta_3 S_{h0} & 0 \\ 0 & A\beta_1 S_{h0} - q_2 & 0 & \frac{A\beta_2 S_{h0}}{M} \\ \beta_4 S_{s0} & 0 & -q_7 & 0 \\ 0 & \gamma_1 & 0 & -\mu_B \end{bmatrix}.$$

Solving for the eigenvalues of the sub-Jacobian matrix, $J_2(E_{02}^{\text{Sch-Tf}})$, we have the characteristic equation

$$\lambda^4 + T_1\lambda^3 + T_2\lambda^2 + T_3\lambda + T_4 = 0, \tag{26}$$

where

$$\begin{aligned} T_1 &= (\mu_B + q_1 + q_7 + g_2(1 - R_{HH}^{\text{Tf}})), \\ T_2 &= \mu_B(q_1 + q_7) + q_1q_7(1 - R_0^{2\text{Sch}}) \\ &\quad +\mu_B q_2(1 - R_0^{\text{Tf}}) + q_1q_2(1 - R_{HH}^{\text{Tf}}) \\ &\quad +q_2q_7(1 - R_{EH}^{\text{Tf}}), \\ T_3 &= q_1q_2q_7(1 - R_0^{2\text{Sch}})(1 - R_{HH}^{\text{Tf}}) \\ &\quad +q_2\mu_B(q_1 + q_7)(1 - R_0^{\text{Tf}}) \\ &\quad +q_1q_7\mu_B(1 - R_0^{2\text{Sch}}), \\ T_4 &= q_1q_2q_7\mu_B(1 - R_0^{2\text{Sch}})(1 - R_0^{\text{Tf}}). \end{aligned}$$

Adopting the concept presented by Heffernan *et al.* [54], which states that a system of equations is locally asymptotically stable if and only if all the coefficients of the characteristic equation of the Jacobian matrix of the system are all positive. Therefore, it is evident that the system of equations (1) of the schistosomiasis-typhoid fever co-infection model is locally asymptotically stable, since $T_1, ...T_4 > 0$ provided $R_{HH}^{\text{Tf}} < 1$, $R_{EH}^{\text{Tf}} < 1, R_0^{\text{Tf}} < 1, R_0^{\text{Sch}} < 1$.

3.3.2. Global stability of the Sch-Tf-free equilibrium state

We state the following lemma to establish the global stability of the sub-model (1).

Lemma 3.1. The system of equations (1) exhibits a globally asymptotically stable disease-free equilibrium when $R_0^{\text{Sch-Tf}} < 1$, whereas the equilibrium becomes unstable if $R_0^{\text{Sch-Tf}} > 1$.

The following theorem demonstrates the global stability of the schistosomiasis-typhoid-free equilibrium point, E_0^{Sch-Tf}.

Theorem 3.5. The schistosomiasis-typhoid-free equilibrium of the system (1) is globally asymptotically stable when $R_0^{\text{Sch-Tf}} < 1$, and loses stability when $R_0^{\text{Sch-Tf}} > 1$.

Proof 3.5. As established in Castillo-Chavez *et al.* [56], assuming that the schistosomiasis-free equilibrium is globally asymptotically stable for $R_0^{\text{Sch-Tf}} < 1$, two additional conditions must be met to ensure its global asymptotic stability. These conditions are highlighted below.

i The function $F(X_1, 0)$ represents a globally asymptotically stable equilibrium for $\frac{dX_1}{dt}$.

ii Let $G(X_1, Y_1) = AY - G^*(X_1, Y_1)$, where $G(X_1, Y_1) \geq 0$ for all $X_1, Y_1 \in Q$. Here, $A = D_Y G(X^*, 0)$ denotes an $M-$matrix of infected classes and Ω represents the biologically feasible region of the model.

We introduce new variables and decompose the system (1) into subsystems. Let $X_1 = (S_h, S_s)$, connoting the populations of susceptible humans and non-human mammals, respectively. Additionally, define $Y_1 = (I_{sc}, I_t, I_{tsc}, I_s, B_t)$ to denote the infected compartments, such that $R_{sc} = R_t = R_{tsc} = 0$. Then, system in (1) is transformed as follows:

$$\left.\begin{aligned} \frac{dX_1}{dt} &= F(X_1, Y_1) \\ \frac{dY_1}{dt} &= G(X_1, Y_1) \end{aligned}\right\} \text{where} \quad X_1 \in \mathbb{R}_+^2, Y_1 \in \mathbb{R}_+^5.$$

Consequently, the two vector-valued functions are defined as follows.

$$\left.\begin{aligned} F(X_1, Y_1) &= \Big(\Lambda + \phi R_{tsc} + \kappa R_{sc} + \nu R_t - \rho\lambda_2 S_h \\ &\quad - (1-\rho)\lambda_1 S_h - \mu S_h, \\ &\quad \Lambda_s - \lambda_3 S_s - \mu_s S_s, \Big)^T \\ G(X_1, Y_1) &= \Big(\rho\lambda_2 S_h + \epsilon I_{tsc} - \lambda_1 I_{sc} \\ &\quad - (\mu + \delta_1 + \omega) I_{sc}, \\ &\quad (1-\rho)\lambda_1 S_h + \xi I_{tsc} - \lambda_2 I_t - (\mu + \delta_2 + p) I_t, \\ &\quad \lambda_1 I_{sc} + \lambda_2 I_t - (\mu + \delta_3 + \epsilon + \xi + \theta) I_{tsc}, \\ &\quad \lambda_3 S_s - (\mu_s + d) I_s, \\ &\quad \gamma_1 I_t + \gamma_2 I_{tsc} - \mu_B B_t \\ &\quad ,\Big)^T \end{aligned}\right\}$$

Here, T denotes the transpose. For convenience, we treat X_1 as equivalent to $(X_1, 0)$ and Y_1 with $(0, Y_1) \in \mathbb{R}_+^2 \times \mathbb{R}_+^5$. Hence the reduced system: $\frac{dX_1}{dt} = F(X_1, 0)$ is

$$\left.\begin{aligned} \frac{dS_h}{dt} &= \Big(\Lambda - \rho\lambda_2 S_h - (1-\rho)\lambda_1 S_h - \mu S_h, \\ \frac{dS_{ma}}{dt} &= \Lambda_s - \lambda_3 S_s - \mu_s S_s \Big). \end{aligned}\right\} \tag{27}$$

The Jacobian matrix corresponding to the subsystem (27) is obtained as

$J(x^*) = \begin{pmatrix} -\mu & 0 \\ 0 & -\mu_s \end{pmatrix}$, which has negative eigenvalues $-\mu$ and $-\mu_s$. This indicates that it is a global asymptotically stable equilibrium point for the reduced system $\frac{dX_1}{dt}, F(X_1, 0)$ as established by Castillo-Chavez *et al.* [56],

Condition two specifies that $G(X_1, Y_1) = AY - G^*(X_1, Y_1)$, where $G(X_1, Y_1) \geq 0$ for $X_1, Y_1 \in Q$, and $A = D_Y G(X^*, 0)$ is an $M - matrix$. For Clearly $G(X_1, Y_1)$ satisfies the condition that $G(X_1, 0) = 0$ and $G(X_1, Y_1) = A^* Y_1 - G^*(X_1, Y_1), G^*(X_1, Y_1) \geq 0$, where

$$A^* = D_Y G(X_1, 0) = \begin{pmatrix} -q_1 & 0 & \epsilon & \beta_3 S_h^0 & 0 \\ 0 & g - q_2 & g + \xi & 0 & \frac{\beta_2 S_h^0}{K} \\ 0 & 0 & -q_3 & 0 & 0 \\ \beta_4 S_s^0 & 0 & \beta_4 S_s^0 & -q_7 & 0 \\ 0 & \gamma_1 & \gamma_2 & 0 & -\mu_B \end{pmatrix}$$

and

$$G^*(X_1, Y_1) = \begin{pmatrix} \rho\beta_3 I_s \left(S_h^0 - S_h\right) \\ \beta_1(1-\rho)\left(S_h^0 - S_h\right)(I_t + I_{tsc}) \\ \quad + \frac{\beta_2(S_h^0 K + B_t(S_h^0 - S_h))}{K(K + B_t)} \\ 0 \\ \beta_4 \left(S_s^0 - S_s\right)(I_{sc+I_{tsc}}) \\ 0 \end{pmatrix}.$$

with definition of $q_1, ..., q_7$ in (25). Since the human population assumes a steady-state value,

$$\rho\beta_3 I_s \left(S_h^0 - S_h\right) \geq 0,$$
$$\beta_1(1-\rho)\left(S_h^0 - S_h\right)(I_t + I_{tsc}) + \frac{\beta_2(S_h^0 K + B_t(S_h^0 - S_h))}{K(K + B_t)} \geq 0,$$
$$\beta_4 \left(S_s^0 - S_s\right)(I_{sc+I_{tsc}}) \geq 0,$$

because $S_h^0 \geq S_h$ and $S_s^0 \geq S_s$. Hence, the system of the co-infection model is globally asymptotically stable since it satisfies the two conditions, implying that the schistosoma parasite and the bacterial diseases will ultimately vanish, regardless of the initial number of infected persons, provided that $R_0^{\text{Sch-Tf}} < 1$.

From an epidemiological angle, this implies that schistosomiasis-typhoid fever co-infection will be eliminated from the population in the absence of external interventions, provided that the conditions of the stability of the disease-free equilibrium are sustained.

3.3.3. *Impact of typhoid fever on schistosomiasis and vice versa*

To examine the effects of typhoid fever on schistosomiasis, we start by expressing R_0^{Sch} in terms of R_0^{Tf}. Therefore, we solve for the human natural death rate, μ, in R_0^{Tf}.

$$R_0^{\text{Tf}} = \frac{M}{K\mu(\mu + \delta_2 + p)\mu_B},$$

where $M = \Lambda(1-\rho)\Big((K\beta_1\mu_B + \beta_2\gamma_1\Big)$. So, $\mu^2 K\mu_B R_0^{\text{Tf}} + \mu H_1 R_0^{\text{Tf}} - M = 0$, where $H_1 = (K\delta_2\mu_B + Kp\mu_B)$. Using the quadratic formula, we have

$$\mu = \frac{-H_1 R_0^{\text{Tf}} + \sqrt{H_1^2 R_0^{2\text{Tf}} + 4MK\mu_B R_0^{\text{Tf}}}}{2K\mu_B R_0^{\text{Tf}}}. \tag{28}$$

Substituting (28) into

$$R_0^{2\text{Sch}} = \frac{\Lambda\beta_4\Lambda_s\rho\beta_3}{\mu\mu_s(\mu + \delta_1 + \omega)(\mu_s + d)},$$

we get

$$R_0^{2\text{Sch}} = \frac{A^* 2K\mu_B R_0^{\text{Tf}}}{\mu_s q_7\Big[W\Big(W + (\delta_1 + \omega)NR_0^{\text{Tf}}\Big)\Big]},$$

where
$W = (-H_1 R_0^{\text{Tf}} + \sqrt{H_1 R_0^{2\text{Tf}} + H_2 R_0^{\text{Tf}}})$, $A^* = \Lambda\beta_4\Lambda_s\rho\beta_3$, $H_2 = 4MK\mu_B$, and $N = 2K\mu_B, q_7 = (\mu_s + d)$.

Therefore,

$$\frac{\partial R_0^{2\text{Sch}}}{\partial R_0^{\text{Tf}}} = \frac{2A^* K\mu_B\Big[W\Big(W + (\delta_1 + \omega)NR_0^{\text{Tf}}\Big) - R_0^{\text{Tf}} G\Big]}{\mu_s q_7\Big[W\Big(W + (\delta_1 + \omega)NR_0^{\text{Tf}}\Big)\Big]^2}, \tag{29}$$

where
$G = \Bigg(W\Big(W + (\delta_1 + \omega)NR_0^{\text{Tf}}\Big) \times \Big[-H_1 + \frac{1}{2}\frac{2H_1^2 R_0^{\text{Tf}} + H_2}{\sqrt{H_1^2 R_0^{2\text{Tf}} + H_2 R_0^{\text{Tf}}}}\Big] + W \times \Big[(\delta_1 + \omega) + (-H_1 + \frac{1}{2}\frac{2H_1^2 R_0^{\text{Tf}} + H_2}{\sqrt{H_1^2 R_0^{2\text{Tf}} + H_2 R_0^{\text{Tf}}}})\Big]\Bigg)$.

The analysis indicates that when (29) is strictly positive, typhoid fever enhances schistosomiasis infection; thus, an increase in typhoid fever cases leads to a corresponding increase in schistosomiasis cases within the population. If (29) equals zero, typhoid fever cases have no significant effect on the transmission dynamics of schistosomiasis. Conversely, if (29) is less than zero, an increase in typhoid fever cases results in a reduction of schistosomiasis cases in the population.
Similarly, solving for μ from

$$R_0^{2\text{Sch}} = \frac{\Lambda\beta_4\Lambda_s\rho\beta_3}{\mu\mu_s(\mu + \delta_1 + \omega)(\mu_s + d)},$$

we have

$$\mu^2\mu_s q_7 R_0^{2\text{Sch}} + \mu A_1 R_0^{2\text{Sch}} - \beta_4\Lambda\rho\beta_3\Lambda_s = 0, \tag{30}$$

where $A_1 = (\mu_s\delta_1 q_2 + \mu_s\omega q_7)$. Using quadratic formula to solve (30), we have

$$\begin{aligned}\mu &= \frac{-A_1R_0^{2\mathrm{Sch}} + \sqrt{A_1^2R_0^{4\mathrm{Sch}} + BR_0^{2\mathrm{Sch}}}}{2\mu_s q_7 R_0^{2\mathrm{Sch}}} \\ &= \frac{-A_1R_0^{\mathrm{Sch}} + \sqrt{A_1^2R_0^{2\mathrm{Sch}} + B}}{2\mu_s q_7 R_0^{\mathrm{Sch}}},\end{aligned} \tag{31}$$

with $B = 4\beta_4\Lambda\rho\beta_3\Lambda_s\mu_s q_7$. Substituting μ in

$$R_0^{\mathrm{Tf}} = \frac{M}{K\mu(\mu + \delta_2 + p)\mu_B},$$

where $M = \Lambda(1-\rho)\Big((K\beta_1\mu_B + \beta_2\gamma_1\Big)$, then we have

$$R_0^{\mathrm{Tf}} = \frac{2M\rho\mu_s q_7 R_0^{\mathrm{Sch}}}{\mu_B K\Big[M^*\Big(M^* + (\delta_2 + p)2\mu_s q_7 R_0^{\mathrm{Sch}}\Big)\Big]},$$

where $M^* = (-A_1R_0^{\mathrm{Sch}} + \sqrt{A_1^2R_0^{2\mathrm{Sch}} + B})$.
Differentiating R_0^{Tf} with respect to R_0^{Sch}, we have

$$\frac{\partial R_0^{\mathrm{Tf}}}{\partial R_0^{\mathrm{Sch}}} = \frac{2M\rho\mu_s q_7\Big[M^*\Big(M^* + (\delta_2 + P)2\mu_s q_7 R_0^{\mathrm{Sch}}\Big) - R_0^{\mathrm{Sch}}T^*\Big]}{\mu_B K\Big[M^*\Big(M^* + (\delta_2 + p)2\mu_s q_7 R_0^{\mathrm{Sch}}\Big)\Big]^2}, \tag{32}$$

where

$$\begin{aligned}T^* = &\Big(M^*\Big(M^* + (\delta_2 + p)2\mu_s q_7 R_0^{\mathrm{Sch}}\Big) \\ &\times\Big[-A_1 + \frac{A_1^2R_0^{\mathrm{Sch}}}{\sqrt{H_1^2R_0^{2\mathrm{Sch}} + B}}\Big] \\ &+ M^* \times \Big[(\delta_2 + p)2\mu_s q_7 + (-A_1 + \frac{A_1^2R_0^{\mathrm{Sch}}}{\sqrt{A_1^2R_0^{2\mathrm{Sch}} + B}})\Big]\Big).\end{aligned}$$

The analysis reveals that when (32) is strictly positive, schistosomiasis enhances the transmission of typhoid fever; thus, an increase in schistosomiasis cases leads to a corresponding increase in typhoid fever cases within the population. If (32) equals zero, schistosomiasis cases have no significant effect on the transmission dynamics of typhoid fever. However, if (32) is less than zero, an increase in schistosomiasis cases results in a reduction of typhoid fever cases in the population.

3.4. Existence of endemic equilibrium state and bifurcation analysis

3.4.1. Existence of endemic equilibrium state (EE)

Here, we established the endemic equilibrium state (EE) of the co-infection model (1). This corresponds to a state in which infections persist in the population, and the environmental reservoirs are also contaminated. So, the EE is denoted by

$$E^e = (S_h^e, I_{sc}^e, I_t^e, I_{tsc}^e, R_{sc}^e, R_t^e, R_{tsc}^e, S_s^e, I_s^e, B_t^e),$$

where all state variables are non-negative, and all infected classes are strictly positive. To obtain the E^e, we set the right-hand side of system (1) to zero and solve for the steady state. Due to the complexity of the model (1), we solved for E^e in terms of the infected state variables as adopted by Okongo *et al.* [57]. Using the definitions in (25) and obtaining B_t from the last equation of system (1) and then substitute into force of infection λ_1, and also obtaining I_s and further substitute into λ_2, we get the force of infection in term of I_{sc}, I_t, I_{tsc} as follow

$$\left.\begin{aligned}B_t^e &= \frac{\gamma_1 I_t^e + \gamma_2 I_{tsc}^e}{\mu_B}, \\ \lambda_1^e &= \beta_1(I_t^e + I_{tsc}^e) + \frac{\beta_2(\gamma_1 I_t^e + \gamma_2 I_{tsc}^e)}{K\mu_B + \gamma_1 I_t^e + \gamma_2 I_{tsc}^e}, \\ \lambda_2^e &= \beta_3 I_s^e = \frac{\beta_3\beta_4(I_{sc}^e + I_{tsc}^e)\Lambda_s}{q_7[\beta_4(I_{sc}^e + I_{tsc}^e) + \mu_s]}, \\ \lambda_3^e &= \beta_4(I_{sc}^e + I_{tsc}^e).\end{aligned}\right\} \tag{33}$$

Substituting (33) appropriately into the first, second, third, fourth, fifth, sixth, seventh, eighth and ninth equations of system (1), respectively, we have the following results

$$\left.\begin{aligned}S_h^e &= \frac{\Lambda + \phi R_{tsc}^e + \kappa R_{sc}^e + \nu R_t^e}{\rho\lambda_2^e + (1-\rho)\lambda_1^e + \mu}, \\ I_{sc}^e &= \frac{\rho\lambda_2^e S_h^e + \epsilon I_{tsc}^e}{\lambda_1^e + q_1}, \\ I_t^e &= \frac{(1-\rho)\lambda_1^e S_h^e + \xi I_{tsc}^e}{\lambda_2^e + q_2}, \\ I_{tsc}^e &= \frac{\lambda_1^e I_{sc}^e + \lambda_2^e I_t^e}{q_3}, \\ R_{sc}^e &= \frac{\omega I_{sc}^e}{q_4}, \\ R_t^e &= \frac{pI_t^e}{q_5}, \\ R_{tsc}^e &= \frac{\theta I_{tsc}^e}{q_6}, \\ S_s^e &= \frac{\Lambda_s}{\lambda_3^e + \mu_s}, \\ I_s^e &= \frac{\Lambda_s S_s^e}{q_7[\lambda_3^e + \mu_s]}.\end{aligned}\right\} \tag{34}$$

$$\begin{aligned}E^e = \Bigg(&\frac{\Lambda + \phi R_{tsc}^e + \kappa R_{sc}^e + \nu R_t^e}{\rho\lambda_2^e + (1-\rho)\lambda_1^e + \mu}, \frac{\rho\lambda_2^e S_h^e + \epsilon I_{tsc}^e}{\lambda_1^e + q_1}, \\ &\frac{(1-\rho)\lambda_1^e S_h^e + \xi I_{tsc}^e}{\lambda_2^e + q_2}, \frac{\lambda_1^e I_{sc}^e + \lambda_2^e I_t^e}{q_3}, \frac{\omega I_{sc}^e}{q_4}, \\ &\frac{pI_t^e}{q_5}, \frac{\theta I_{tsc}^e}{q_6}, \frac{\Lambda_s}{\lambda_3^e + \mu_s}, \frac{\Lambda_s S_s^e}{q_7[\lambda_3^e + \mu_s]}, \frac{\gamma_1 I_t^e + \gamma_2 I_{tsc}^e}{\mu_B}\Bigg).\end{aligned}$$

Here, S_h^e is determined by (34), using $R_{sc}^e, R_t^e, R_{tsc}^e$ and $I_{sc}^e, I_t^e, I_{tsc}^e$ as defined. Hence, (34) is the endemic equilibrium, E^e, which exists for $\lambda_1^e, \lambda_2^e, \lambda_3^e > 0$. The forces of infection are expressed in terms of $I_{sc}^e, I_t^e, I_{tsc}^e$, as specified in (33).

3.4.2. Existence of bifurcation analysis

In this subsection, centre manifold theorem by Castillo-Chavez and Song [55] will be explored to carry out the bifurcation analysis on the co-infection model (1) with

$$a = \sum_{k,i,j=1}^{n} z_k w_i w_j \frac{\partial^2 f_k(E^0)}{\partial x_i \partial x_j} \text{ and } b = \sum_{k,i=1}^{n} z_k w_i \frac{\partial^2 f_k(E^0)}{\partial x_i \partial \rho},$$

as bifurcation coefficients and ρ as the bifurcation parameter such that $R_0^{\text{Sch}} = 1$ and $R_0^{\text{Tf}} = 1$, as employed by Ref. [10, 51] if and only if

$$\rho = \rho^* = \frac{\mu\mu_s(\mu + \delta_1 + \omega)(\mu_s + d)}{\beta_3\beta_4\Lambda_s\Lambda},$$

and

$$\rho = \rho^* = \frac{K\beta_1\mu_B + \beta_2\gamma_1 - K\mu\mu_B(\mu + \delta_2 + p)}{K\beta_1\mu_B + \beta_2\gamma_1}.$$

Then, we transformed the state variables such that $S_h = x_1, I_{sc} = x_2, I_t - x_3, I_{tsc} = x_4, R_{sc} = x_5, R_t = x_6, R_{tsc} = x_7, S_s = x_8, I_s = x_9, B_t = x_{10}$. Adopting vector notation $\vec{x} = (x_1, x_2, x_3.x_4.x_5.x_6, x_7, x_8, x_9, x_{10})^T$, schistosomiasis-typhoid fever co-infection model (1) can be written in the form $\vec{x}' = F(\vec{x})$, such that $F = (f_1, f_2, f_3, f_4, f_5, f_6, f_7, f_8, f_9, f_{10})^T$, written below as

$$\left.\begin{aligned}
\frac{dx_1}{dt} &= \Lambda + \phi x_7 + \kappa x_5 + \nu x_6 - \rho\lambda_2 x_1 - (1-\rho)\lambda_1 x_1 \\
&\quad - \mu x_1 = f_1, \\
\frac{dx_2}{dt} &= \rho\lambda_2 x_1 + \epsilon x_4 - \lambda_1 x_2 - (\mu + \delta_1 + \omega)x_2 = f_2, \\
\frac{dx_3}{dt} &= (1-\rho)\lambda_1 x_1 + \xi x_4 - \lambda_2 x_3 - (\mu + \delta_2 + p)x_3 = f_3, \\
\frac{dx_4}{dt} &= \lambda_1 x_2 + \lambda_2 x_3 - (\mu + \delta_3 + \epsilon + \xi + \theta)x_4 = f_4, \\
\frac{dx_5}{dt} &= \omega x_2 - (\kappa + \mu)x_5 = f_5, \\
\frac{dx_6}{dt} &= p x_3 - (\nu + \mu)x_6 = f_6, \\
\frac{dx_7}{dt} &= \theta x_4 - (\mu + \phi)x_7 = f_7, \\
\frac{dx_8}{dt} &= \Lambda_s - \lambda_3 x_8 - \mu_s x_8 = f_8, \\
\frac{dx_9}{dt} &= \lambda_3 x_8 - (\mu_s + d)x_9 = f_9, \\
\frac{dx_{10}}{dt} &= \gamma_1 x_3 + \gamma_2 x_4 - \mu_B x_{10} = f_{10},
\end{aligned}\right\} \tag{35}$$

with non-negative initial conditions, where

$$\left.\begin{aligned}
\lambda_1 &= \underbrace{\beta_1(x_3 + x_4)}_{\text{Human-to-human}} + \underbrace{\frac{\beta_2 x_{10}}{K + x_{10}}}_{\text{Environment-to-human}}, \\
\lambda_2 &= \underbrace{\beta_3 x_9}_{\text{Snail-to-human via shedding of cercariae in freshwater}}, \\
\lambda_3 &= \underbrace{\beta_4(x_2 + x_4)}_{\text{Human-to-snail via release of miracidia in freshwater}}.
\end{aligned}\right\} \tag{36}$$

This technique requires that the Jacobian of the system (35) have a simple zero eigenvalue and other eigenvalues negative at $R_0^{\text{Sch}} = 1$ and $R_0^{\text{Tf}} = 1$, denoted by $J(E_0)$. Hence, using the Jacobian matrix in (3.4) , we have the right and left eigenvectors w and z at $R_0^{\text{Sch}} = 1$ and $R_0^{\text{Tf}} = 1$, given as:

$$\begin{aligned}
w_1 &= \left[\frac{\nu p}{\mu q_5} + \frac{\epsilon q_7 \beta_4 S_s^0}{\mu q_7 (q_1 q_7 - p\beta_3\beta_4 S_h^0 S_s^0)} - \frac{(1-\rho)\beta_1 S_h^0}{\mu} \right. \\
&\quad \left. - \frac{K\omega\epsilon q_7}{\mu q_4 (q_1 q_7 - p\beta_3\beta_4 S_h^0 S_s^0)} - \frac{(1-\rho)\beta_2 S_h^0 \gamma_1}{\mu\mu_B K}\right] w_3, \\
w_2 &= \frac{-\epsilon q_7 w_3}{(q_1 q_7 - p\beta_3\beta_4 S_h^0 S_s^0)}, \\
w_5 &= \frac{-\epsilon\omega q_7 w_3}{(q_1 q_7 - p\beta_3\beta_4 S_h^0 S_s^0) q_4}, \quad w_6 = \frac{p w_3}{q_5}, \\
w_8 &= \frac{\epsilon q_7 \beta_4 S_s^0 w_3}{\mu_s (q_1 q_7 - p\beta_3\beta_4 S_h^0 S_s^0)}, \\
w_9 &= \frac{-\epsilon q_7 \beta_4 S_s^0 w_3}{q_7 (q_1 q_7 - p\beta_3\beta_4 S_h^0 S_s^0)}, \quad w_{10} = \frac{\gamma_1 w_3}{\mu_B}, \\
w_4 &= w_7 = 0, \quad w_3 = w_3 > 0,
\end{aligned} \tag{37}$$

with definition of $q_1, .., q_7$ in (25) and

$$\begin{aligned}
z_2 &= -Q_1 z_3, z_4 = Q_2 z_3, z_8 = Q_3 z_3, z_9 = -\frac{p\beta_3 S_s^0 Q_1 z_3}{q_7}, \\
z_{10} &= \frac{(1-\rho)\beta_2 S_h^0 z_3}{K\mu_B}, z_1 = z_5 = z_6 = z_7 = 0, z_3 = z_3 > 0,
\end{aligned}$$

where

$$\begin{aligned}
Q_1 &= \frac{\left[K\mu_B[(1-\rho)\beta_1 S_h^0 - q_2] + \gamma_1(1-\rho)\beta_2 S_h^0\right]}{\epsilon K\mu_B}, \\
Q_2 &= \frac{D}{q_3 K\mu_B}, \\
Q_3 &= \frac{Q_1 q_1 q_2 - \beta_4\beta_3 S_s^2 p Q_1}{q_2\beta_4 S_s^0},
\end{aligned} \tag{38}$$

with $\mathbf{w.z} = 1$, where $D = \left[q_7 K\mu_B[(1-\rho)\beta_1 S_h^0 - q_2] - [\beta_4 S_s^0 Q_3 K q_7 \mu_B + \beta_4 S_s^0 p\beta_3 Q_1 K\mu_B] + \gamma_2(1-\rho)\beta_2 S_h^0\right]$

$$\vec{w} = (w_1, w_2, w_3, w_4, w_5, w_6, w_7, w_8, w_9, w_{10})^T$$

and

$$\vec{z} = (z_1, z_2, z_3, z_4, z_5, z_6, z_7, z_8, z_9, z_{10})^T.$$

Also, the non-zero second order derivatives of $x_1, x_2, x_3.x_4.x_5.x_6, x_7, x_8, x_9, x_{10}$ at E_{02}^{Sch-Tf} yield

$$\begin{aligned}
\frac{\partial^2 f_2(E_{02}^{Sch-Tf})}{\partial x_1 \partial x_9} &= \rho\beta_3, \quad \frac{\partial^2 f_2(E_{02}^{Sch-Tf})}{\partial x_2 \partial x_3} = -\beta_1, \\
\frac{\partial^2 f_2(E_{02}^{Sch-Tf})}{\partial x_2 \partial x_{10}} &= -\frac{\beta_2}{K}\beta_1, \quad \frac{\partial^2 f_3(E_{02}^{Sch-Tf})}{\partial x_1 \partial x_3} = (1-\rho)\beta_1,
\end{aligned}$$

$$\begin{aligned}
&\frac{\partial^2 f_3(E_{02}^{Sch-Tf})}{\partial x_1 \partial x_{10}} = (1-\rho)\frac{\beta_2}{K}, \quad \frac{\partial^2 f_3(E_{02}^{Sch-Tf})}{\partial x_2 \partial x_9} = -\beta_3,\\
&\frac{\partial^2 f_4(E_{02}^{Sch-Tf})}{\partial x_2 \partial x_3} = \beta_1, \quad \frac{\partial^2 f_4(E_{02}^{Sch-Tf})}{\partial x_2 \partial x_{10}} = \frac{\beta_2}{K},\\
&\frac{\partial^2 f_4(E_{02}^{Sch-Tf})}{\partial x_2 \partial x_{10}} = \beta_3, \quad \frac{\partial^2 f_8(E_{02}^{Sch-Tf})}{\partial x_8 \partial x_2} = -\beta_4,\\
&\frac{\partial^2 f_9(E_{02}^{Sch-Tf})}{\partial x_8 \partial x_2} = \beta_4,
\end{aligned} \tag{39}$$

and

$$\begin{aligned}
z_2 w_9 \frac{\partial^2 f_2(E_{02}^{Sch-Tf})}{\partial x_9 \partial \rho} &= z_2 w_9 \beta_3 S_h^0,\\
z_3 w_3 \frac{\partial^2 f_3(E_{02}^{Sch-Tf})}{\partial x_3 \partial \rho} &= -z_3 w_3 \beta_1 S_h^0,\\
z_3 w_{10} \frac{\partial^2 f_3(E_{02}^{Sch-Tf})}{\partial x_{10} \partial \rho} &= -z_3 w_{10} \frac{\beta_1 S_h^0}{K}.
\end{aligned} \tag{40}$$

Hence, employing the non-zero second-order partial derivatives of equation (39) and equation (40), with $\mathbf{w.z} = 1$, we have

$$\begin{aligned}
a = w_3^2 z_3 \Bigg(& Q_1 \Bigg[\frac{\nu p}{\mu q_5} + \frac{\epsilon q_7 \beta_4 S_s^0}{\mu q_7 (q_1 q_7 - p\beta_3\beta_4 S_h^0 S_s^0)} \\
& - \frac{(1-\rho)\beta_1 S_h^0}{\mu} - \frac{K\omega\epsilon q_7}{\mu q_4 (q_1 q_7 - p\beta_3\beta_4 S_h^0 S_s^0)} \\
& - \frac{(1-\rho)\beta_2 S_h^0 \gamma_1}{\mu\mu_B K} \Bigg] \frac{\epsilon q_7 \beta_4 S_s^0}{q_7 (q_1 q_7 - p\beta_3\beta_4 S_h^0 S_s^0)} \rho\beta_3 \\
& - \frac{Q_1 \epsilon q_7 \beta_1}{(q_1 q_7 - p\beta_3\beta_4 S_h^0 S_s^0)} - \frac{Q_1 \epsilon q_7}{(q_1 q_7 - p\beta_3\beta_4 S_h^0 S_s^0)} \frac{\gamma_1}{\mu_B} \frac{\beta_2\beta_1}{K} \\
& + \Bigg[\frac{\nu p}{\mu q_5} + \frac{\epsilon q_7 \beta_4 S_s^0}{\mu q_7 (q_1 q_7 - p\beta_3\beta_4 S_h^0 S_s^0)} - \frac{(1-\rho)\beta_1 S_h^0}{\mu} \\
& - \frac{K\omega\epsilon q_7}{\mu q_4 (q_1 q_7 - p\beta_3\beta_4 S_h^0 S_s^0)} - \frac{(1-\rho)\beta_2 S_h^0 \gamma_1}{\mu\mu_B K} \Bigg] (1-\rho)\beta_1 \\
& + \Bigg[\frac{\nu p}{\mu q_5} + \frac{\epsilon q_7 \beta_4 S_s^0}{\mu q_7 (q_1 q_7 - p\beta_3\beta_4 S_h^0 S_s^0)} - \frac{(1-\rho)\beta_1 S_h^0}{\mu} \\
& - \frac{K\omega\epsilon q_7}{\mu q_4 (q_1 q_7 - p\beta_3\beta_4 S_h^0 S_s^0)} - \frac{(1-\rho)\beta_2 S_h^0 \gamma_1}{\mu\mu_B K} \Bigg] \frac{\gamma_1}{\mu_B} \frac{(1-\rho)\beta_2}{K} \\
& - \frac{\epsilon q_7}{(q_1 q_7 - p\beta_3\beta_4 S_h^0 S_s^0)} \frac{\epsilon q_7 \beta_4 \beta_3 S_s^0}{q_7 (q_1 q_7 - p\beta_3\beta_4 S_h^0 S_s^0)} \\
& - \frac{Q_2 \epsilon q_7 \beta_1}{(q_1 q_7 - p\beta_3\beta_4 S_h^0 S_s^0)} - \frac{Q_2 \epsilon q_7}{(q_1 q_7 - p\beta_3\beta_4 S_h^0 S_s^0)} \frac{\gamma_1}{\mu_B} \frac{\beta_2}{K} \\
& - \frac{Q_2 \epsilon q_7 \beta_4 \beta_3 S_s^0}{q_7 (q_1 q_7 - p\beta_3\beta_4 S_h^0 S_s^0)} \\
& + \frac{Q_3 \epsilon q_7 \beta_4 S_s^0}{\mu_s (q_1 q_7 - p\beta_3\beta_4 S_h^0 S_s^0)} \frac{\epsilon q_7 \beta_4}{(q_1 q_7 - p\beta_3\beta_4 S_h^0 S_s^0)} \\
& - \frac{p\beta_3 S_s^0 Q_1}{q_7} \frac{\epsilon q_7 \beta_4 S_s^0}{\mu_s (q_1 q_7 - p\beta_3\beta_4 S_h^0 S_s^0)} \frac{\epsilon q_7}{(q_1 q_7 - p\beta_3\beta_4 S_h^0 S_s^0)} \beta_4 \Bigg),
\end{aligned}$$

and

$$\begin{aligned}
b = z_3 w_3 \Bigg[& Q_1 \frac{\epsilon q_7 \beta_4 S_s^0}{q_7 (q_1 q_7 - p\beta_3\beta_4 S_h^0 S_s^0)} \beta_3 S_h^0 - \beta_1 S_h^0 \\
& - \frac{\gamma_1}{\mu_B} \frac{\beta_1 S_h^0}{K} \Bigg],
\end{aligned} \tag{41}$$

with definition of $q_1, ..., q_7$ in (25).

According to Ref. [55] as applied by Ref. [10], whenever the coefficient b is positive, we have the following lemma;

Lemma 3.2. Suppose $b > 0$, then we have the following:

- The co-infection system of equations (35) will undergo a backward bifurcation if the coefficient a is positive.
- The co-infection system of equations (35) will undergo forward bifurcation if the coefficient a is negative.

Remark. In the first scenario, the schistosomiasis-typhoid-free state (E_{02}^{Sch-Tf}) is locally asymptotically stable but not globally stable. This suggests that the disease may persist in the population even if the reproduction number is less than one, so stability at this equilibrium may not be sufficient for disease elimination. In the second scenario, the E_{02}^{Sch-Tf} is globally stable, indicating that the disease can be eradicated and the risk of persistent transmission is low. When the reproduction number exceeds one, the endemic equilibrium remains stable, and the disease persists in the population. In summary, the endemic equilibrium is globally asymptotically stable when the reproduction number is greater than one, while the disease-free equilibrium is globally asymptotically stable when the reproduction number is less than one.

However, based on the bifurcation analyses of the sub-models, which show forward bifurcation, it can be deduced that the co-infection exhibits forward bifurcation, as established by Sayooj *et al.* [51].

4. Numerical simulation

The co-infection of schistosomiasis and typhoid fever is prevalent in most African countries, including Nigeria and, by extension, Benue State, because both diseases are waterborne [4]. Each of these diseases, as a single entity or a co-infection, has been a public health challenge; hence, the need for proper attention and effective control measures. Therefore, when conducting numerical simulations of the co-infection of the dual diseases, it is pertinent to estimate model parameter values that reflect real conditions, even in the absence of real data. This will help simulate results that are valuable in the Nigerian context, specifically in the context of this study, Makurdi, Benue State.

4.1. Parameter estimation

In this subsection, we estimated the model parameter values to conduct a numerical analysis of the dynamics of

schistosomiasis-typhoid fever co-infection for effective forecasting and prediction. Our parameter values are estimated in weeks using the demographic data of Makurdi, Benue State, Nigeria. According to Ref. [15, 58], the population of Makurdi, (S_h^0) and the life expectancy of human in Makurdi is 509,000 and ≈ 56 years, respectively.

Therefore, since human natural death rate, $\mu = \frac{1}{\text{Life expectancy}}$, then, $\mu = \frac{1}{56\times52} = 0.000343$ per week. Also, since, $S_h^0 = \frac{\Lambda}{\mu}$, then, the human recruitment rate, $\Lambda = 509000 \times 0.000343 \approx 175$ per week. In addition, we assumed a population of 5000 snails in the area under consideration, and, according to Ref. [16], snails can live up to 10 years. Hence, the natural death rate for snails, $\mu_s = \frac{1}{10\times52} = 0.00192$ per week. Therefore, the snail recruitment rate, $\Lambda_s = 5000 \times 0.00192 \approx 10$. We estimated the value of θ to be equivalent to the sum of ω ana p, which equals 0.0176 per weeks.Also, we estimated the value of the disease-induced death rate for co-infected population, δ_3 as the sum of δ_1 and δ_2, with assumption that individuals co-infected with the two diseases are most likely to die faster due to the grave effect of the dual diseases in the body system, hence, $\delta_3 = 0.000846$. Details of the other parameter values are stated in Table 2 Also, we assumed the following initial conditions for the state variables for simulations $I_{sc0} = 1$, $I_{t0} = 1$, $I_{tsc0} = 1$, $R_{sc0} = 0$, $R_{t0} = 0$, $R_{tsc0} = 0$, $I_{s0} = 1$, $B_t = 500$, and after deduction of the infected compartment(s) from S_{h0} and S_{s0}, then $S_{h0} = 508997$, and $S_{s0} = 4999$.

4.2. Baseline plots

In the subsection, we performed numerical simulations on each of the equations of the system (1) using the parameter values in Table 2 with initial conditions $(S_h, I_{sc}, I_t, I_{tsc}, R_{sc}, R_t, R_{tsc}, S_s, I_s, B_t) = (508997, 1, 1, 1, 0, 0, 0, 4999, 1, 500)$, this is to examine the dynamics of the co-infection of schistosomiasis-typhoid fever in the population.

Figure 4a in Figure 4 presents the dynamics of each human class in model (1). The susceptible human population (S_h) declines steadily from approximately 509,000 at week 1 to 2,725 at week 100, and further to 2,091 at week 150, primarily due to schistosomiasis and typhoid fever infections. The population infected only with schistosomiasis (I_{sc}) rises to about 8,780 at week 50, then decreases to 1,780 by week 150, likely reflecting the effects of screening and treatment. Individuals infected only with typhoid fever (I_t) increase rapidly, peaking at 357,670 at week 80, before declining to 157,654 at week 150, reflecting recovery from screening and treatment. These trends indicate that typhoid fever spreads more rapidly and is more prevalent than schistosomiasis. The co-infected population (I_{tsc}) increases from week 60, reaching a peak of 16,481 at week 88, then decreases to 8,820 at week 150, which may also reflect recovery following screening and treatment. This illustrates the dynamics of the human population in the co-infection model.

The R_{sc}, R_t, and R_{tsc} values in 4a illustrate the recovery patterns for populations infected with only schistosomiasis, only typhoid fever, or both diseases. The sharp increase in the typhoid fever recovery rate may indicate greater disease awareness and more frequent screening and treatment compared to schistosomiasis. Figure 4b in Figure 4 presents the trends of susceptible and infected snail populations in system (1). The infected snail population I_s increases rapidly, while the susceptible snail population S_s declines. Figure 4c in Figure 4 shows a sharp increase in environmental bacteria concentration.

4.3. Sensitivity analysis

Here, a global sensitivity analysis was conducted to identify and examine the influence of some parameters on the co-dynamics of schistosomiasis-typhoid fever transmission. Based on this, we employed the partial rank correlation coefficient (PRCC) with the Latin Hypercube Sampling (LHS) technique, with 1000 runs Ref. [59], which has been adopted by several authors, such as Refs. [9, 47], for nonlinear deterministic models such as this study. This technique is applied to analyse the influence of several parameters on the schistosomiasis-typhoid fever reproduction number, R_0, as shown in Figure 7. For clarity sake, it is imperative to note that those parameters with positive sign or on the positive side, increase the reproduction number as they increase and by extension, increase schistosomiasis-typhoid fever co-infection in society while those with negative sign or on the negative side, reduce the R_0, as they increase and by extension, reduce the co-infection dynamics of the diseases in the population.

In addition, the parameters with PRCCs ≥ 0.5 are the most significant in influencing the co-infection dynamics; those with PRCCs < 0.5 can also influence the spread of the co-infection dynamics and cannot be underestimated, as explained in Refs. [34, 59]. Here, we computed the sensitivity analysis on the sub-models reproduction numbers as well as when combined, as seen in Figures 5, 6 and 7

As shown in Figure 5, the parameters Λ (human recruitment rate), Λ_s (snail recruitment rate), β_3 (schistosomiasis transmission rate from infected snails to humans), ρ (proportion moving from susceptible to R_{sc} due to schistosomiasis), and β_4 (contact rate from infected humans to snails) have the strongest positive correlation with only schistosomiasis reproduction number, R_0^{Sch}. An increase in these parameters leads to a higher R_0^{Sch}, which in turn raises schistosomiasis infection rates in the population. There is a strong negative relationship with ω (the progression rate from I_{sc} to R_{sc} due to screening and treatment of individuals with schistosomiasis only), μ_s (the natural death rate of the snail population), and d (the disease-induced death rate for snails). Increasing these parameters reduces schistosomiasis infections in the population.

Figure 6 shows that Λ (human recruitment rate), Λ_s (snail recruitment rate), and β_1 (typhoid fever effective transmission rate from human to human) have the strongest positive correlation with the typhoid fever reproduction number R_0^{Tf}. Increases in these parameters raise R_0^{Tf} and lead to more typhoid fever infections. γ_1 (bacteria shedding rate from I_t) and β_2 (effective contact rate from environment to human) have moderate positive PRCC values and also contribute to the spread of typhoid fever. p (progression rate from I_t to R_t due to screening and treatment) and ρ (proportion moving from susceptible

to R_{sc} due to schistosomiasis) show a strong positive relationship with R_0^{Tf}; however, increasing these parameters results in the eradication of typhoid fever infections. δ_2 (disease-induced death rate due to typhoid fever), d (disease-induced death rate for snails), and μ_B (bacteria decay rate) have moderate negative PRCC values and contribute to reductions in R_0^{Tf}.

Figure 7 shows the sensitivity analysis of the co-infection reproduction number, R_0. The results are similar to those for the individual reproduction number. However, ρ (the proportion moving from susceptible to R_{sc} due to schistosomiasis) is a key determinant of co-infection dynamics. When ρ increases to 1, only schistosomiasis infection remains in the population. The parameters Λ (human recruitment rate), Λ_s (snail recruitment rate), β_1 (typhoid fever effective transmission rate from human to human), β_3 (schistosomiasis effective transmission rate from infected snails to humans via cercariae in freshwater), and β_4 (schistosomiasis effective contact rate from infected humans to snails via miracidia in freshwater) have the strongest positive correlation with R_0. Increases in these parameters raise R_0 and support the persistence of co-infection dynamics. γ_1 (bacteria shedding rate from I_t) and β_2 (typhoid fever effective contact rate from environment to human) show moderate positive PRCC values. While their correlation with R_0 is weaker, they may still contribute to the spread of co-infection and should not be ignored.

On the other hand, parameters p (progression rate from I_t to R_t due to screening and treatment of infected individuals with typhoid fever only), ω (progression rate from I_sc to R_{sc} due to screening and treatment of infected individuals with schistosomiasis only), μ_s (natural death rate for snail population), and ρ (proportion of progression from S_h to I_{sc})—demonstrated strong negative PRCC values. This indicates that increases in these parameters correspond to decreases in R_0, thereby reducing the transmission of schistosomiasis-typhoid fever co-infection within the population. Also, δ_1 (disease-induced death rate due to schistosomiasis only), δ_2 (disease-induced death rate due to typhoid fever only), d (disease-induced death rate for snail) and μ_B (bacteria decay rate) demonstrated moderate negative PRCC values, which also contribute to reductions in R_0 and, consequently, the spread of co-infection. In summary, these parameters are inversely related to the co-infection reproduction number R_0 and, more broadly, their increase alleviates the transmission dynamics of the schistosomiasis-typhoid fever co-infection.

4.4. *Impact of varying parameters β_1, β_2, β_3, β_4, ω, p, and θ, on the transmission dynamics of the co-infection model*

Numerical simulations were performed to investigate the effects of varying parameters β_1, β_2, β_3, β_4, ω, p, and θ on the transmission dynamics of the co-infection model, as illustrated in the following figures.

Figure 8 illustrates how changes in the human-to-human transmission rate of typhoid fever, β_1, affect several populations: individuals infected only with schistosomiasis (I_{sc}), only with typhoid fever (I_t), co-infected humans (I_{tsc}), infected snails (I_s), and environmental bacteria concentration (B_t). As shown in sub-Figure 8a, increasing β_1 reduces the number of individuals susceptible to schistosomiasis, resulting in fewer cases of schistosomiasis-only infection. Conversely, as β_1 decreases, the population infected only with schistosomiasis increases. Sub-Figure 8b shows that higher β_1 values lead to more typhoid fever cases, peaking at the highest β_1. Similarly, as β_1 increases, both the co-infected human population (8c) and the infected snail population (8d) rise. Regarding environmental bacteria concentration (8e), higher β_1 results in increased bacteria levels, since more infected individuals shed bacteria into the environment. Therefore, for effective control of typhoid fever in the population, human-to-human transmission rate of typhoid fever, β_1, must be maintained below 0.0000007.

Similarly, Figure 9 shows the effect of the environment-to-human typhoid fever transmission rate. β_2 affects each class in Figure 9 (9a, 9b, 9c, 9d, and 9e) similarly. This pattern is consistent with the observed impact of β_1.

Figure 10 illustrates how changes in the schistosomiasis transmission rate from snails to humans, β_3, affect each subpopulation. As β_3 decreases, the number of individuals infected only with schistosomiasis also decreases, as shown in sub-Figure 10a. Conversely, a lower β_3 increases the number of individuals infected only with typhoid fever, since more people remain susceptible to typhoid, as seen in sub-Figure 10b. An increase in β_3 leads to higher numbers of co-infected individuals, infected snails, and greater pathogen concentration in the environment, because individuals already infected with typhoid continue to shed bacteria, as shown in 10c, 10d, and 10e. To effectively control schistosomiasis in the population, the schistosomiasis transmission rate from snails to humans, β_3, must not exceed 0.00000058.

Figure 11 shows that increasing the schistosomiasis effective transmission rate from humans to snails (β_4) leads to higher populations of individuals infected only with schistosomiasis, co-infected individuals, and infected snails, as illustrated in sub-Figures 11a, 11c, and 11d. This parameter does not affect the population infected only with typhoid fever or the environmental pathogen concentration, as shown in sub-Figures 11b and 11e.

Figure 12 presents the simulation results for the impact of the recovery rate due to screening and treatment for schistosomiasis-only infected humans, ω, on the I_{sc}, I_t, I_{tsc}, I_s, and B_t compartments. Increasing ω sharply reduces the number of individuals infected only with schistosomiasis (sub-figure 12a), and significantly decreases both the co-infected population and the infected snail population (sub-figures 12c and 12d). This must be sustained above 50%. There is no significant effect on the population infected only with typhoid fever or on environmental bacterial concentration, as shown in sub-figures 12b and 12e.

Figure 13 illustrates the effect of the recovery rate from screening and treatment for typhoid fever, p, on the I_{sc}, I_t, I_{tsc}, I_s, and B_t populations. As more individuals infected only with typhoid fever are screened, treated, and recover, the populations of those infected solely with typhoid fever, co-infected humans, and environmental bacteria decrease, as shown in sub-figures 13b, 13c, and 13e, which must be maintained not lower

that 25%. However, sub-figure 13a shows that as p increases, the population infected only with schistosomiasis rises. This occurs because increased recovery from typhoid fever reduces the number of individuals susceptible to typhoid fever and increases those susceptible to schistosomiasis. The recovery rate for typhoid fever in humans does not affect the snail-infected population, as demonstrated in 13d.

The simulation results in Figure 14 show that increasing the recovery rate due to screening and treatment for co-infected humans, θ, significantly reduces the co-infected population, as seen in sub-figure 14c. This rate also affects the schistosomiasis-only infected population, particularly between weeks 97 and 150, as shown in sub-figure 14a. There is a slight impact on the typhoid fever-only infected population and bacteria concentration, as indicated in sub-figures 14b and 14e. The effect on the snail-infected population is negligible, as seen in sub-figure 14d.

In summary, it is essential to implement comprehensive preventive measures, including promoting hygiene, maintaining environmental sanitation, raising public awareness, treating water, and vaccinating against typhoid fever. These actions help prevent the spread of typhoid fever and schistosomiasis among at-risk populations. Infected individuals and snails should receive appropriate treatment or control measures, whether for single or co-infections, as recommended by Refs. [1, 5, 6, 62].

5. Optimal-control analysis and numerical simulations

5.1. Optimal control analysis

In this subsection, we employed the concept of Pontryagin's Maximum Principle (PMP) with a forward-backward sweep technique to determine the necessary conditions for optimal control of the schistosomiasis-typhoid fever co-infection. We introduced five (5) time-dependent controls into model (1) to determine the optimal strategy for controlling the disease. Thus, the optimal control model version formulated is given as follows;

$$
\begin{aligned}
\frac{dS_h}{dt} &= \Lambda + \phi R_{tsc} + \kappa R_{sc} + \nu R_t - \rho\beta_3(1-u_1(t))I_sS_h \\
&\quad - (1-\rho)\Big(\beta_1(1-u_2(t))(I_t+I_{tsc}) + \frac{\beta_2(1-u_2(t))B_t}{K+B_t}\Big)S_h \\
&\quad - \mu S_h, \\
\frac{dI_{sc}}{dt} &= \rho\beta_3(1-u_1(t))I_sS_h + (1+u_4(t))\epsilon I_{tsc} \\
&\quad - \Big(\beta_1(1-u_2(t))(I_t+I_{tsc}) + \frac{\beta_2(1-u_2(t))B_t}{K+B_t}\Big)I_{sc} \\
&\quad - (\mu+\delta_1+(1+u_3(t))\omega)I_{sc}, \\
\frac{dI_t}{dt} &= (1-\rho)\Big(\beta_1(1-u_2(t))(I_t+I_{tsc}) + \frac{\beta_2(1-u_2(t))B_t}{K+B_t}\Big)S_h \\
&\quad + (1+u_3(t))\xi I_{tsc} \\
&\quad - \beta_3(1-u_1(t))I_sI_t - (\mu+\delta_2+p(1+u_4(t)))I_t, \\
\frac{dI_{tsc}}{dt} &= \Big(\beta_1(1-u_2(t))(I_t+I_{tsc}) + \frac{\beta_2(1-u_2(t))B_t}{K+B_t}\Big)I_{sc} \\
&\quad + \beta_3(1-u_1(t))I_sI_t \\
&\quad - (\mu+\delta_3+(1+u_4(t))\epsilon + (1+u_3(t))\xi + (1+u_5(t))\theta)I_{tsc}, \\
\frac{dR_{sc}}{dt} &= \omega(1+u_3(t))I_{sc} - (\kappa+\mu)R_{sc}, \\
\frac{dR_t}{dt} &= p(1+u_4(t))I_t - (\nu+\mu)R_t, \\
\frac{dR_{tsc}}{dt} &= (1+u_5(t))\theta I_{tsc} - (\mu+\phi)R_{tsc}, \\
\frac{dS_s}{dt} &= \Lambda_s - \beta_4(1-u_1(t))(I_{sc}+I_{tsc})S_s - \mu_sS_s, \\
\frac{dI_s}{dt} &= \beta_4(1-u_1(t))(I_{sc}+I_{tsc})S_s - (\mu_s+d)I_s, \\
\frac{dB_t}{dt} &= \gamma_1(1-u_2(t))I_t + \gamma_2(1-u_2(t))I_{tsc} - \mu_B(1+u_2(t))B_t,
\end{aligned}
\tag{42}
$$

with initial conditions of the system (1) and

- $u_1(t)$ is the intensified effort to prevent schistosomiasis infections spread,
- $u_2(t)$ is the intensified effort to prevent typhoid fever infections from spreading,
- $u_3(t)$ is the effective screening and treatment control for humans infected with schistosomiasis,
- $u_4(t)$ is the effective screening and treatment control for humans infected with typhoid fever,
- $u_5(t)$ is the effective screening and treatment control for humans infected with co-infections.

The choice of control interventions is consistent with the literature on infectious disease control, such as Refs. [10, 36, 41]. It is noteworthy to mention that our control problem entails a situation in which the number of schistosomiasis-infected individuals, typhoid fever infected individuals, co-infected individuals and the cost of applying screening and treatments controls $u_3(t), u_4(t),$ and $u_5(t)$ are minimised, while the preventive controls u_1 and u_2 are being maximised, hence, the reason controls u_1 and u_2 are having negative in the objective function (43) because of the forward-backward scheme technique as used by Ref. [10]. The objective function to be minimised is given as

$$
\begin{aligned}
\Pi(u_1(t),u_2(t),u_3(t),u_4(t),u_5(t)) &= \int_0^{t_f}\Big(B_1I_{sc} + B_2I_t + B_3I_{tsc} \\
&\quad + B_4I_s + B_5B_t - \frac{1}{2}a_1u_1^2 - \frac{1}{2}a_2u_2^2 + \frac{1}{2}\sum_{i=3}^{5}a_iu_i^2(t)\Big)dt,
\end{aligned}
\tag{43}
$$

where the coefficient associated with the infected state variables, B_1, B_2, B_3, B_4, B_5, and the control weight coefficients, a_1, a_2, a_3, a_4, a_5, are assumed positive. The quadratic form of the control variables, $\sum_{i=1}^{5} a_iu_i^2(t)$ in (43), is due to the nonlinearity of the cost of controls as used in the literature on optimal control of infectious diseases [9, 47]. The objective functional goal is to minimise the number of infected humans and infected snails, the concentration of bacteria in the environment, and

the cost of implementing them. Thus, the optimal controls, $u_1^*(t), u_2^*(t), u_3^*(t), u_4^*(t), u_5^*(t)$ is seek such that

$$\begin{aligned}\Pi\left(u_1^*(t), u_2^*(t), u_3^*(t), u_4^*(t), u_5^*(t)\right) = \\ \min_{\Phi_1} \Pi\left(u_1(t), u_2(t), u_3(t), u_5(t), u_4(t)\right),\end{aligned} \tag{44}$$

where

$$\begin{aligned}\Phi_1 = \Big\{u_i(t), i = 1, 2, 3, 4, 5 \text{ are measurable with} \\ u_i(t) \in [0, 1], \text{ for } 0 \le t \le t_f\Big\}.\end{aligned} \tag{45}$$

The state and the control variables of equations (43) and (44) are non-negative, as established in Subsection (3.1) and the condition in Equation (44); this implies that the set Φ_1 is closed, convex and exists. The optimal control exists by applying Corollary 4.1 of Pages 68–69 in [60] as implemented in [36].

Obtaining the Hamiltonian and optimality system by applying the Pontryagin maximum principle (PMP) [61] to the optimal control problem. PMP transforms Equations (42) and (43) into a problem of minimizing pointwise Hamiltonian, M, that is presented as;

$$\begin{aligned}M\left(S_h, I_{sc}, I_t, I_{tsc}, R_{sc}, R_t, R_{tsc}, S_s, I_s, B_t\right) = \\ L(I_{sc}, I_t, I_{tsc}, I_s, B_t, u_1(t), u_2(t), u_3(t), u_4(t), u_5(t)) \\ +\lambda_1\frac{dS_h}{dt} + \lambda_2\frac{dI_{sc}}{dt} + \lambda_3\frac{dI_t}{dt} + \lambda_4\frac{dI_{tsc}}{dt} + \lambda_5\frac{dR_{sc}}{dt} \\ +\lambda_6\frac{dR_t}{dt} + \lambda_7\frac{dR_{tsc}}{dt} + \lambda_8\frac{dS_s}{dt} + \lambda_9\frac{dI_s}{dt} + \lambda_{10}\frac{dB_t}{dt}\end{aligned} \tag{46}$$

where $\lambda_1, \lambda_2, \lambda_3, \lambda_4, \lambda_5, \lambda_6, \lambda_7, \lambda_8, \lambda_9, \lambda_{10}$ are the adjoint variables for the respective state variables. Using a similar approach in [28, 36], we state the following optimality theorem;

Theorem 5.1. With the optimal control $u_1^*(t), u_2^*(t), u_3^*(t), u_4^*(t), u_5^*(t)$ and solutions $S_h, I_{sc}, I_t, I_{tsc}, R_{sc}, R_t, R_{tsc}, S_s, I_s, B_t$ that minimizes $\Pi(u_1(t), u_2(t), u_3(t), u_4(t), u_5(t))$ over Φ_1, there exist non-trivial adjoint functions λ_i, for $i = 1, ..., 10$ that satisfies;

$$\begin{aligned}\frac{d\lambda_1}{dt} &= (\lambda_1 - \lambda_2)\rho\beta_3(1 - u_1(t)) \\ &\quad + (\lambda_1 - \lambda_3)(1 - \rho) \times \left(\beta_1(1 - u_2(t))(I_t + I_{tsc}) \right. \\ &\quad \left. + \frac{\beta_2(1 - u_2(t))B_t}{K + B_t}\right) + \lambda_1\mu, \\ \frac{d\lambda_2}{dt} &= -B_1 + (\lambda_2 - \lambda_4)\left(\beta_1(1 - u_2(t))(I_t + I_{tsc}) \right. \\ &\quad \left. + \frac{\beta_2(1 - u_2(t))B_t}{K + B_t}\right) \\ &\quad + (\lambda_2 - \lambda_5)\omega(1 + u_3(t)) + (\lambda_8 - \lambda_9)\beta_4(1 - u_1(t))S_s \\ &\quad + \lambda_2(\mu + \delta_1), \\ \frac{d\lambda_3}{dt} &= -B_2 + (\lambda_1 - \lambda_2)(1 - \rho)\beta_1(1 - u_2(t))S_h + (\lambda_2 - \lambda_4) \\ &\quad \times\beta_1(1 - u_2(t))I_{sc} + (\lambda_3 - \lambda_4)\beta_3(1 - u_1(t))I_s \\ &\quad + (\lambda_3 - \lambda_6)p(1 + u_4(t)) + \lambda_3(\mu + \delta_2) - \lambda_{10}\gamma_1(1 - u_2(t)), \\ \frac{d\lambda_4}{dt} &= -B_3 + (\lambda_1 - \lambda_3)(1 - \rho)\beta_1(1 - u_2(t))S_h + (\lambda_2 - \lambda_4) \\ &\quad \times\beta_1(1 - u_2(t))I_{sc} + (\lambda_8 - \lambda_9)\beta_4(1 - u_1(t))S_s + (\lambda_4 - \lambda_2) \\ &\quad \epsilon(1 + u_4(t)) + (\lambda_3 - \lambda_4)\xi(1 + u_3(t)) + (\lambda_4 - \lambda_7)\theta(1 + u_5(t)) \\ &\quad + \lambda_4(\mu + \delta_3) - \lambda_{10}\gamma_2(1 - u_2(t)), \\ \frac{d\lambda_5}{dt} &= (\lambda_5 - \lambda_1)\kappa + \lambda_5\mu, \\ \frac{d\lambda_6}{dt} &= (\lambda_6 - \lambda_1)\nu + \lambda_6\mu, \\ \frac{d\lambda_7}{dt} &= (\lambda_7 - \lambda_1)\phi + \lambda_7\mu, \\ \frac{d\lambda_8}{dt} &= (\lambda_8 - \lambda_9)\beta_4(1 - u_1(t))(I_{sc} + I_{tsc}) + \lambda_8\mu_s, \\ \frac{d\lambda_9}{dt} &= -B_4 + (\lambda_1 - \lambda_2)\rho\beta_3(1 - u_1(t))S_h + (\lambda_3 - \lambda_4)\beta_3 \\ &\quad (1 - u_1(t))I_t + \lambda_9(\mu_s + d), \\ \frac{d\lambda_{10}}{dt} &= -B_5 + (\lambda_1 - \lambda_3)(1 - \rho)\frac{\beta_2(1 - u_2(t))S_h}{(K + B_t)^2} \\ &\quad + (\lambda_2 - \lambda_4)\frac{\beta_2(1 - u_2(t))I_{sc}}{(K + B_t)^2} + \lambda_{10}\mu_B(1 + u_2(t)),\end{aligned} \tag{47}$$

with the transversality condition $\lambda_i(t_f) = 0, i = 1, ..., 10$ and the controls $u_1^*(t), u_2^*(t), u_3^*(t), u_4^*(t), u_5^*(t)$ that satisfies the optimality condition;

$$\begin{aligned}u_1^* &= max\left\{0, min\left(1, \frac{J_1}{a_1}\right)\right\}, \\ u_2^* &= max\left\{0, min\left(1, \frac{J_2}{a_2}\right)\right\}, \\ u_3^* &= max\left\{0, min\left(1, \frac{(\lambda_4 - \lambda_3)\xi I_{tsc} + (\lambda_2 - \lambda_5)\omega I_{sc}}{a_3}\right)\right\}, \\ u_4^* &= max\left\{0, min\left(1, \frac{(\lambda_4 - \lambda_2)\epsilon I_{tsc} + (\lambda_3 - \lambda_6)pI_t}{a_4}\right)\right\}, \\ u_5^* &= max\left\{0, min\left(1, \frac{(\lambda_4 - \lambda_7)\theta I_{tsc}}{a_5}\right)\right\},\end{aligned} \tag{48}$$

where $J_1 = (\lambda_1 - \lambda_2)\beta_3\rho I_s S_h + (\lambda_8 - \lambda_9)\beta_4(I_{sc} + I_{tsc})S_s + (\lambda_3 - \lambda_4)\beta_3 I_s I_t$, $J_2 = (\lambda_1 - \lambda_3)(1 - \rho)QS_h + (\lambda_2 - \lambda_4)QI_{sc} - \lambda_{10}\gamma_1 I_t - \lambda_{10}\gamma_2 I_{tsc} - \lambda_{10}\mu_B B_t$, and $Q = \left[\beta_1(I_t + I_{tsc}) + \frac{\beta_2 B_t}{K + B_t}\right]$.

Proof 5.1. Using PMP, the adjoint system (47) is obtained by differentiating equation (12) with respect to their corresponding state variables, $S_h, I_{sc}, I_t, I_{tsc}, R_{sc}, R_t, R_{tsc}, S_s, I_s, B_t$, that is obtained by evaluating the optimal control functions $u_1(t), u_2(t), u_3(t), u_4(t), u_5(t)$ and after then apply negative to the differentials. The optimality condition equation (14) is obtained by solving for the controls, $u_1^*(t), u_2^*(t), u_3^*(t), u_4^*(t), u_5^*(t)$ at the respective steady states

$$\frac{\partial M}{\partial u_1} = \frac{\partial M}{\partial u_2} = \frac{\partial M}{\partial u_3} = \frac{\partial M}{\partial u_4} = \frac{\partial M}{\partial u_5} = 0$$

on the interior of the control set. Thus, the optimality system is

given by equations (47) and (48) substituted into (42), and this completes the proof.

5.2. Numerical simulations results and discussion of the optimal control model results

Numerical simulations of the optimality system, used to determine optimal control solutions, were performed using the Fourth-order Runge-Kutta method implemented in MATLAB R2024a. The simulations utilised the parameter values presented in Table 2 and the initial conditions specified in the parameter estimation section. The following weight constants were applied: $B_1 = 1, B_2 = 2, B_3 = 1, B_4 = 1, B_5 = 1,$ and $a_1 = 95\times10^3, a_2 = 100\times10^3, a_3 = 30\times10^3, a_4 = 400, a_5 = 50\times10^3$. Three categories of simulations were considered here: the application of a single control category, the application of a double-combined control category, and the application of all combined control categories. The presentation was restricted to single, double (pairwise) and full-combination categories in this study because of the avoidance of redundancy and excessive proliferation of simulation scenarios and due to the fact that economic and epidemiological effects of triple and quadruplet categories are greatly intermediate between those of the corresponding pairwise-control and full strategies, and so, do not initiate qualitatively new insights and portend the tenet of reality.

5.2.1. Application of the single-control category

In this category, a single control is applied at a time, with all others set to zero. For example, application of u_1 (intensified effort to prevent the spread of schistosomiasis infections) implies $u_1 \neq 0, u_2 = u_3 = u_4 = u_5 = 0$; application of u_2 (intensified effort to prevent the spread of typhoid fever infections) implies $u_2 \neq 0, u_1 = u_3 = u_4 = u_5 = 0$, application of u_3 (effective screening and treatment control for humans infected with schistosomiasis) implies $u_3 \neq 0, u_1 = u_2 = u_4 = u_5 = 0$, application of u_4 (effective screening and treatment control for humans infected with typhoid fever) implies $u_4 \neq 0, u_1 = u_2 = u_3 = u_5 = 0$, and application of u_5 (effective screening and treatment control for humans infected with co-infections) implies $u_5 \neq 0, u_1 = u_2 = u_3 = u_4 = 0$ as illustrated in Figure 15.

5.2.2. Application of the double-control category

In this category, two controls are applied simultaneously while the remaining controls are set to zero. For example, application of $u_1 + u_2$ (intensified effort to prevent the spread of schistosomiasis infections and intensified effort to prevent the spread of typhoid fever infections) implies $u_1 + u_2 \neq 0, u_3 = u_4 = u_5 = 0$, implementation of $u_1 + u_3$ (intensified effort to prevent the spread of schistosomiasis infections and effective screening and treatment control for humans infected with schistosomiasis) implies $u_1 + u_3 \neq 0, u_2 = u_4 = u_5 = 0$, implementation of $u_1 + u_4$ (intensified effort to prevent the spread of schistosomiasis infections and effective screening and treatment control for humans infected with typhoid fever) implies $u_1 + u_4 \neq 0, u_2 = u_3 = u_5 = 0$, implementation of $u_1 + u_5$ (intensified effort to prevent the spread of schistosomiasis infections and effective screening and treatment control for humans infected with co-infections) implies $u_1 + u_5 \neq 0, u_2 = u_3 = u_4 = 0$, implementation of $u_2 + u_3$ (intensified effort to prevent typhoid fever infections from spreading and effective screening and treatment control for humans infected with schistosomiasis) implies $u_2 + u_3 \neq 0, u_1 = u_4 = u_5 = 0$, implementation of $u_2 + u_4$ (intensified effort to prevent typhoid fever infections from spreading and effective screening and effective screening and treatment control for humans infected with typhoid fever) implies $u_2 + u_4 \neq 0, u_1 = u_3 = u_5 = 0$, implementation of $u_2 + u_5$ (intensified effort to prevent typhoid fever infections from spreading and effective screening and effective screening and treatment control for humans infected with co-infections) implies $u_2 + u_5 \neq 0, u_1 = u_4 = u_5 = 0$, implementation of $u_3 + u_5$ (effective screening and treatment control for humans infected with schistosomiasis and effective screening and treatment control for humans infected with co-infections) implies $u_3 + u_5 \neq 0, u_1 = u_2 = u_5 = 0$, implementation of $u_3 + u_4$ (effective screening and treatment control for humans infected with schistosomiasis and effective screening and treatment control for humans infected with typhoid fever) implies $u_3 + u_4 \neq 0, u_1 = u_2 = u_5 = 0$ and implementation of $u_4 + u_5$ (effective screening and treatment control for humans infected with typhoid fever and effective screening and treatment control for humans infected with co-infections) implies $u_4 + u_5 \neq 0, u_1 = u_2 = u_3 = 0$ All pairwise combinations of the five controls were considered, yielding 10 possible combinations, as shown in the simulation results in Figure 16.

5.2.3. Application of the all-combined-control category

In this category, all five controls are applied simultaneously, such that $u_1+u_2+u_3+u_4+u_5 \neq 0$, as demonstrated in Figure 17.

5.2.4. Application of the single-control category

Figure 15 presents the effects of single control strategies on infected human, snail, and bacterial populations. Sub-figure 15a shows that u_1 (intensified effort to prevent schistosomiasis transmission) is the most effective single control for reducing the schistosomiasis-only infected population, as recommended by [4]. u_3 also has a notable, though lesser, effect. Sub-figure 15b indicates that u_2 (intensified effort to prevent typhoid fever transmission) is most effective for limiting the typhoid fever-only infected population, followed by u_4 (effective screening and treatment for typhoid fever), consistent with [7]. Sub-figure 15c demonstrates that u_2 is most effective at delaying the increase in the co-infected population, followed by u_1 and then u_3 (effective screening and treatment for schistosomiasis), in line with [2, 6]. For the snail-infected population, sub-figure 15d shows that u_1 is the most efficient and effective single control, while other controls have minimal impact, as confirmed by Refs. [1, 23]. Finally, sub-figure 15e demonstrates that u_2 is the most effective single control for reducing environmental bacteria concentration, followed by u_4, as recommended by Refs. [7, 23].

The control profile for the single-control category is shown in sub-figure 15f of 15. This profile outlines the recommended implementation levels for each control to achieve the desired out-

comes in the populations discussed above. Maintain u_1, u_3, u_4, and u_5 at a minimum of 60% before week 90, and keep u_1 at least at 40% before week 75.

5.2.5. Application of the double-control category

Figure 16 shows the effects of double combined-control interventions on the optimality function for infected human, snail, and bacterial populations. Sub-figure 16a indicates that $u_1 + u_3$ (intensified prevention of schistosomiasis spread and effective screening and treatment for schistosomiasis-infected humans) is the most effective for reducing the schistosomiasis-only infected population. The next most effective combinations are $u_1 + u_5$ (intensified prevention of schistosomiasis spread with treatment for co-infected humans) and $u_1 + u_4$ (intensified prevention of schistosomiasis spread and effective screening and treatment for typhoid fever-infected humans), consistent with Refs. [1, 4]. For the typhoid fever-only infected population, sub-figure 16b shows $u_2 + u_5$ (intensified prevention of typhoid fever spread and intensified prevention of schistosomiasis spread with treatment for co-infected humans) is most effective, followed by $u_2 + u_4$ and $u_2 + u_3$, corroborating Refs. [6, 22, 23]. For co-infected humans, sub-figure 16c demonstrates that $u_1 + u_5$ is most effective, followed by $u_2 + u_5$ and $u_1 + u_2$, as recommended by [3, 6]. For infected snails, sub-figure 16d shows $u_1 + u_5$ is most efficient, followed by $u_1 + u_3$ and $u_1 + u_4$ [4]. To reduce environmental bacteria concentration, $u_2 + u_5$ is most effective, followed by $u_2 + u_4$ and $u_2 + u_3$, as shown in sub-figure 16e [6, 23]. Control profiles for each intervention over 150 weeks are presented in sub-figure 16f.

5.2.6. Application of the all-combined-control category

Figure 17 presents the impact of applying all five controls simultaneously on infected human, snail, and bacteria populations, as determined by the optimality function. Sub-figure 17a shows that this strategy delays the peak of the schistosomiasis-only infected population to approximately week 90, with a maximum of 9300 cases, compared to 10000 at week 55 without control. Sub-figure 17b shows a similarly significant reduction in the typhoid fever-only infected population. The combined controls also substantially reduce the co-infected population, snail-infected population, and environmental bacterial concentration, as shown in sub-figures 17c, 17d, and 17e. Overall, applying all five controls is effective in managing the transmission dynamics of these diseases, both individually and as co-infections. The combined control profile is shown in 17f of Figure 17.

6. Conclusion and recommendations

In this research, we formulated a ten-compartment nonlinear ordinary differential equation (ODE) model to examine the co-infection dynamics of schistosomiasis and typhoid fever, based on the demographic setting of Makurdi, Benue State, Nigeria. We established the qualitative properties of the model, considering sub-models and the complete co-infection model. The basic reproduction numbers were computed and used to establish stability and bifurcation analyses. We further assessed the impact of schistosomiasis on typhoid fever and vice versa. We conducted a global sensitivity analysis (GSA) to assess the significance of model parameters influencing co-dynamics. Subsequently, an optimal control model version with five time-dependent control interventions, namely; the intensified effort to prevent schistosomiasis infections spread, the intensified effort to prevent typhoid fever infections spread, the effective screening and treatment control for humans infected with schistosomiasis, the effective screening and treatment control for humans infected with typhoid fever, and the effective screening and treatment control for humans infected with co-infections, is constructed and analysed using Pontryagin maximum principle (PMP) with forward-backward sweep method. Numerical simulations were conducted under three categories: single, pairwise (double), and full combination. Our findings revealed that, for effective control and eradication of these diseases, whether as single entities or co-infections, concurrent implementation of all controls is optimal when sufficient funding is available. However, in reality and in case of limited resources where the concurrent implementation of the five controls is not possible, the intensified effort to prevent schistosomiasis infections spread (u_1) is the most efficient single control for eradication of schistosomiasis only infections, snail infections, and intensified effort to prevent typhoid fever infections spread (u_2) is the best single control for eradication of typhoid fever only infection and bacteria concentration in the environment. For co-infection infections, u_2 followed by u_1 is the most effective and efficient single control intervention. For the double control category, combination of the intensified effort to prevent schistosomiasis infections spread (u_1) + effective screening and treatment control for humans infected with schistosomiasis (u_3) is the most effective double control for controlling schistosomiasis only infections, followed by $u_1 + u_5$, while $u_1 + u_5$ (the intensified effort to prevent schistosomiasis infections spread (u_1) + the effective screening and treatment control for humans infected with co-infections (u_5)) followed by $u_1 + u_3$ is the best double control for eradicating snail infections in the population. Also, for the eradication of typhoid fever, only the infection and bacterial concentration in the environment, $u_2 + u_5$, is the most effective double control; this may not be unrelated to the impact schistosomiasis has on the spread of typhoid fever, followed by $u_2 + u_4$. Meanwhile, the combination $u_1 + u_5$ is the best double control for reducing co-infections, followed by $u_2 + u_5$.

The results indicate that prevention-only interventions for both diseases are more effective than treatment-only interventions. However, implementing prevention and treatment strategies for both diseases is highly effective. In cases of co-infection with schistosomiasis and typhoid fever, the findings suggest that simultaneous implementation of control interventions for both diseases is recommended to achieve efficient and effective co-infection management. The limitations of this study include assumptions regarding certain parameter values and the lack of application of more detailed real-world data and cost-effectiveness analysis. These limitations will be addressed in future research.

Data availability

All data (parameter values) used in this study are cited in Table 2.

Declaration of competing interest

The authors declare that they have no known competing financial interests or personal relationships that could have appeared to influence the work reported in this manuscript.

Funding

International Mathematical Union (IMU) for the financial support as one of the beneficiaries of the Graduate Assistantships grant in Developing Countries, 2025.

Acknowledgment

The authors express their profound gratitude to the International Mathematical Union (IMU) for the financial support as one of the beneficiaries of the Graduate Assistantships grant in Developing Countries, 2025.

References

[1] World Health Organization, "Schistosomiasis", 2023. Available online: https://www.who.int/news-room/fact-sheets/detail/schistosomiasis.

[2] World Health Organization, Guideline on Control and Elimination of Human Schistosomiasis, World Health Organization, Geneva, Switzerland, 2022. Available online: https://www.who.int/publications/i/item/9789240041608.

[3] Centers for Disease Control and Prevention, "Schistosomiasis", 2024. Available online: https://www.cdc.gov/dpdx/schistosomiasis/index.html.

[4] A. Marege, M. Seid, B. Boke, S. Thomas, M. Arage, N. Mouze, T. Yohanes, M. Woldemariam & A. Manilal, "Prevalence of *Schistosoma mansoni–Salmonella* coinfection among patients in southern Ethiopia", New Microbes and New Infections **40** (2021) 100842. https://doi.org/10.1016/j.nmni.2021.100842.

[5] R. S. Barsoum, G. Esmat & T. El-Baz, "Human schistosomiasis: clinical perspective: review", Journal of Advanced Research **4** (2013) 433. https://doi.org/10.1016/j.jare.2013.01.005.

[6] World Health Organization, "Typhoid", 2023. Available online: https://www.who.int/news-room/fact-sheets/detail/typhoid.

[7] Centers for Disease Control and Prevention, "About typhoid fever and paratyphoid fever", 2024. Available online: https://www.cdc.gov/typhoid-fever/about/index.html.

[8] J. Bhandari, P. K. Thada, M. F. Hashmi & E. DeVos, "Typhoid fever", in StatPearls, StatPearls Publishing, Treasure Island, FL, 2026. Available online: https://www.ncbi.nlm.nih.gov/books/NBK557513/.

[9] K. A. Tijani, C. E. Madubueze & R. I. Gweryina, "Typhoid fever dynamical model with cost-effective optimal control", Journal of the Nigerian Society of Physical Sciences **5** (2023) 1579. https://doi.org/10.46481/jnsps.2023.1579.

[10] K. O. Okosun & R. Smith, "Optimal control analysis of malaria–schistosomiasis co-infection dynamics", Mathematical Biosciences and Engineering **14** (2017) 377. https://doi.org/10.3934/mbe.2017024.

[11] E. T. Chiyaka, G. Magombedze & L. Mutimbu, "Modelling within host parasite dynamics of schistosomiasis", Computational and Mathematical Methods in Medicine **11** (2010) 124376. https://onlinelibrary.wiley.com/doi/10.1080/17486701003614336.

[12] H. O. Nyaberi & J. S. M. Musaili, "Mathematical modeling of the impact of treatment on the dynamics of typhoid", Journal of the Egyptian Mathematical Society **29** (2021) 15. https://doi.org/10.1186/s42787-021-00125-8.

[13] M. Ghosh, P. Chandra, P. Sinha & J. B. Shukla, "Modelling the spread of bacterial infectious disease with environmental effect in a logistically growing human population", Nonlinear Analysis: Real World Applications **7** (2006) 341. https://doi.org/10.1016/j.nonrwa.2005.03.005.

[14] T. D. Mangal, S. Paterson & A. Fenton, "Predicting the impact of long-term temperature changes on the epidemiology and control of schistosomiasis: a mechanistic model", PLoS ONE **3** (2008) e1438. https://doi.org/10.1371/journal.pone.0001438.

[15] Macrotrends, "Nigeria life expectancy 1950–2025", 2025. Available online: https://www.macrotrends.net/global-metrics/countries/nga/nigeria/life-expectancy.

[16] I. J. Uloko & A. J. Michael, "Comparative studies of water leaf (*Talinnu triangulare*), pawpaw leaf (*Carica papaya*), Siam weed (*Chromolaena dorata*) and growers mash on the growth of African giant snail (*Achatina achatina*)", East African Scholars Journal of Agriculture and Life Sciences **2** (2019). https://doi.org/10.36349/easjals.2019.v02i07.004.

[17] J. M. Mutua, F. B. Wang & N. K. Vaidya, "Modeling malaria and typhoid fever co-infection dynamics", Mathematical Biosciences **264** (2015) 128. https://doi.org/10.1016/j.mbs.2015.03.014.

[18] C. DerSarkissian, "Typhoid fever (*Salmonella Typhi*)", 2024. Available online: https://www.webmd.com/a-to-z-guides/typhoid-fever.

[19] M. Kgosimore & G. Kelatlhegile, "Mathematical analysis of typhoid infection with treatment", Journal of Mathematical Science: Advances and Applications **40** (2016) 75. http://dx.doi.org/10.18642/jmsaa_7100121689.

[20] A. Hsiao, T. Toy, H. J. Seo & F. Marks, "Interaction between *Salmonella* and schistosomiasis: a review", PLoS Pathogens **12** (2016) e1005928. https://doi.org/10.1371/journal.ppat.1005928.

[21] A. A. F. Mahmoud, "Schistosomiasis", in Tropical Medicine: Science and Practice, A. A. F. Mahmoud (Ed.), Imperial College Press, London, UK, 2001. https://www.amazon.co.uk/Schistosomiasis-Tropical-Medicine-Science-Practice/dp/186094146X?asin=186094146X&revisionId=&format=4&depth=1.

[22] P. I. Eche & P. O. Adikwu, "Assessment of water and sanitation conditions in Benue South Senatorial District, Benue State, Nigeria", European Journal of Biology and Medical Science Research **13** (2025) 61. Available online: https://doi.org/10.37745/ejbmsr.2013.

[23] O. Maxwell, A. Oklo & A. Bernard, "Profile of water related diseases in Benue State, Nigeria", American Journal of Human Ecology **1** (2012) 87. https://scispace.com/pdf/profile-of-water-related-diseases-in-benue-state-nigeria-f4yk2ya6ru.pdf.

[24] V. U. Obisike, E. M. Victor, V. C. Uzoma & E. U. Amuta, "Urinary schistosomiasis in some Otukpo communities in Otukpo Local Government Area of Benue State Nigeria", Asian Journal of Medical Principles and Clinical Practice **4** (2021) 1. Available online: https://journalajmpcp.com/index.php/AJMPCP/article/view/66.

[25] H. O. Okpala, G. O. Nwobu, M. I. Agba & J. O. Akor, "Prevalence of schistosomiasis in Wurukum, Makurdi Local Government Area of Benue State, Nigeria", Journal of Medical Laboratory Sciences **12** (2005) 47. https://doi.org/10.4314/jmls.v12i2.35288.

[26] D. Yandev, V. N. Chigor & E. A. Eze, "Studies on biochemical characterization of *Salmonella* and mixed infection cases with schistosomiasis in Kwande LGA, Benue State, Nigeria", International Journal of Sciences: Basic and Applied Research **61** (2022) 1. https://www.gssrr.org/JournalOfBasicAndApplied/article/view/12870.

[27] G. Zaman, I. H. Jung, F. M. D. Torres & A. Zeb, "Mathematical modelling and control of infectious disease", Computational and Mathematical Methods in Medicine **2017** (2017) 7149154. https://doi.org/10.1155/2017/7149154.

[28] G. T. Tilahun, O. D. Makinde & D. Malonza, "Modelling and optimal control of typhoid fever disease with cost-effective strategies", Computational and Mathematical Methods in Medicine **2017** (2017) 2324518. https://doi.org/10.1155/2017/2324518.

[29] S. Musa, N. Bello & A. Umar, "Mathematical modelling of the transmission dynamics, control and vaccination of schistosomiasis with a variable population size", Bayero Journal of Pure and Applied Sciences **12** (2019) 70. https://doi.org/10.4314/bajopas.v12i1.10.

[30] W. Nur, Trisilowati, A. Suryanto & W. M. Kusumawinahyu, "Mathematical model of schistosomiasis with health education and molluscicide intervention", Journal of Physics: Conference Series **1821** (2021) 012033. https://doi.org/10.1088/1742-6596/1821/1/012033.

[31] E. Kanyi, A. S. Afolabi & N. O. Onyango, "Mathematical modeling and analysis of transmission dynamics and control of schistosomiasis", Journal of Applied Mathematics **2021** (2021) 6653796. https://doi.org/10.1155/2021/6653796.

[32] F. E. T. Nkuimeni & B. Tsanou, "Schistosomiasis mathematical model in a spatially heterogeneous environment", Results in Applied Mathematics **23** (2024) 100488. https://doi.org/10.1016/j.rinam.2024.100488.

[33] O. Robert & A. M. Baba, "Mathematical model for schistosomiasis transmission dynamics and optimal control in Uganda", International Journal of Science for Global Sustainability **11** (2025) 195. Available online: https://fugus-ijsgs.com.ng/index.php/ijsgs/article/view/802.

[34] K. A. Tijani, C. E. Madubueze & R. I. Gweryina, "Modelling typhoid fever transmission with treatment relapse response: optimal control and cost-effectiveness analysis", Mathematical Models and Computer Simulations **16** (2024) 457. https://doi.org/10.1134/S2070048224700169.

[35] K. S. Abdulai & S. Baba, "A mathematical model on the transmission dynamics of typhoid fever with treatment and booster vaccination", Frontiers in Applied Mathematics and Statistics **9** (2023) 1151270. https://doi.org/10.3389/fams.2023.1151270.

[36] O. F. Lawal, T. T. Yusuf & A. Abidemi, "On mathematical modelling of optimal control of typhoid fever with efficiency analysis", Journal of the Nigerian Society of Physical Sciences **6** (2024) 2057. https://doi.org/10.46481/jnsps.2024.2057.

[37] J. Nthiiri, O. Lawi, C. Akinyi, D. Oganga, W. Muriuki, M. Musyoka, P. Otieno & L. Koech, "Mathematical modelling of typhoid fever disease incorporating protection against infection", British Journal of Mathematics & Computer Science **14** (2016) 1. https://doi.org/10.9734/BJMCS/2016/23325.

[38] F. K. Alalhareth, M. H. Alharbi & M. A. Ibrahim, "Modeling typhoid fever dynamics: stability analysis and periodic solutions in epidemic model with partial susceptibility", Mathematics **11** (2023) 3713. https://doi.org/10.3390/math11173713.

[39] S. Nana-Kyere, J. K. K. Asamoah, J. D. Ankamah, E. Okyere, B. Seidu, D. Kwarteng, E. L. Ayetey & J. B. Odum, "Mathematical modeling and cost-effectiveness analysis of an $S_eE_eI_eR_e$ typhoid fever model", Journal of Mathematics **2025** (2025) 1212057. https://doi.org/10.1155/jom/1212057.

[40] S. Mushayabasa & C. P. Bhunu, "Modeling schistosomiasis and HIV/AIDS codynamics", Computational and Mathematical Methods in Medicine **2011** (2011) 846174. https://onlinelibrary.wiley.com/doi/10.1155/2011/846174.

[41] E. A. Bakare & R. C. Nwozo, "Mathematical analysis of malaria–schistosomiasis coinfection model", Epidemiology Research International **2016** (2016) 3854902. https://doi.org/10.1155/2016/3854902.

[42] E. Bonyah, K. O. Okosun, O. O. Okosun & L. Ossei, "Mathematical modeling of lymphatic filariasis–schistosomiasis co-infection dynamics: insight through public education", International Journal of Ecology & Development **33** (2018). https://www.researchgate.net/publication/325115297_Mathematical_modeling_of_Lymphatic_filariasis-schistosomiasis_co-infection_dynamicsInsight_through_public_education.

[43] I. I. Ako & R. U. Omoregie, "Sensitivity analysis of a mathematical model for tuberculosis–schistosomiasis model with vaccination and treatment", Earthline Journal of Mathematical Sciences **15** (2025) 849. https://doi.org/10.34198/ejms.15525.849872.

[44] L. Matsebula & F. Nyabadza, "Mathematical analysis of cholera–typhoid co-infection transmission dynamics", Frontiers in Applied Mathematics and Statistics **8** (2022) 892098. https://doi.org/10.3389/fams.2022.892098.

[45] D. S. Mgonja, A. Hugo, A. Hassan & O. D. Makinde, "Mathematical modeling and analysis of COVID-19 and typhoid fever co-dynamics with treatment", Scientific Reports **15** (2025) 33206. https://doi.org/10.1038/s41598-024-82955-x.

[46] M. S. Wameko, P. R. Koya & A. G. Wedajo, "Mathematical modeling of co-infections of hepatitis A viral disease and typhoid fever with optimal control strategies", International Journal of Nonlinear Analysis and Applications **13** (2022) 899. https://doi.org/10.22075/ijnaa.2022.21134.2237.

[47] K. A. Tijani & C. E. Madubueze, "Understanding the dynamics of ameobiasis using mathematical modelling approach: optimal control strategies and cost-effectiveness analysis", International Journal of Mathematical Sciences and Optimization: Theory and Applications **11** (2025) 138. https://ijmso.unilag.edu.ng/article/view/2908.

[48] A. A. Modebe, A. U. Nnachi, C. O. Ukaegbu, N. Tata, M. V. Agah, O. E. Udu-Ibiam & I. A. Nnachi, "Dual infections of Enteric Salmonella species with Schistosoma mansoni among Patients from Two Hospitals in Jos, Nigeria ", Journal of Applied & Environmental Microbiology **2**(4) (2014) 198. https://doi.org/10.12691/jaem-2-4-14.

[49] A. M. A. Mohamed & M. N. M. Hamad, "Relationship between intestinal schistosomiasis and enteric fever among Sudanese patients, New Halfa Town, Kassala State, Sudan", Journal of Microbiology & Experimentation **8** (2020) 109. https://doi.org/10.15406/jmen.2020.08.00293.

[50] C. E. Madubueze, R. I. Gweryina & K. A. Tijani, "A dynamic of typhoid fever model with optimal control analysis", Ratio Mathematica **41** (2021) 255. http://dx.doi.org/10.23755/rm.v41i0.657.

[51] A. J. Sayooj, R. Raja, B. T. Omede, R. P. Agarwal, J. Alzabut, J. Cao & V. E. Balas, "Mathematical modeling on co-infection: transmission dynamics of Zika virus and Dengue fever", Nonlinear Dynamics **111** (2023) 4879. https://doi.org/10.1007/s11071-022-08063-5.

[52] P. van den Driessche & J. Watmough, "Reproduction numbers and subthreshold endemic equilibria for compartmental models of disease transmission", Mathematical Biosciences **180** (2002) 29. https://www.sciencedirect.com/science/article/abs/pii/S0025556402001086.

[53] M. M. Lunga, Mathematical Models for the Coinfection Dynamics of Cholera and Typhoid, Ph.D. dissertation, University of Johannesburg, Johannesburg, South Africa, 2012. Available online: https://ujcontent.uj.ac.za/esploro/outputs/doctoral/Mathematical-models-for-the-coinfection-dynamics/9910470507691#file-0.

[54] J. M. Heffernan, R. J. Smith & L. M. Wahl, "Perspectives on the basic reproductive ratio", Journal of the Royal Society Interface **2** (2005) 281. https://doi.org/10.1098/rsif.2005.0042.

[55] C. Castillo-Chavez & B. Song, "Dynamical models of tuberculosis and their applications", Mathematical Biosciences and Engineering **1** (2004) 361. https://doi.org/10.3934/mbe.2004.1.361.

[56] C. Castillo-Chavez, Z. Feng & W. Huang, "On the computation of R_0 and its role on the global stability", in Mathematical Approaches for Emerging and Reemerging Infectious Diseases: An Introduction, C. Castillo-Chavez, S. Blower, P. van den Driessche, D. Kirschner & A. A. Yakubu (Eds.), Springer, New York, NY, USA, 2002, pp. 229–250. Available online: https://www.researchgate.net/profile/Carlos-Castillo-Chavez/publication/228915276_ON_THE_COMPUTATION_OF_R_AND_ITS_ROLE_ON_GLOBAL_STABILITY/links/0fcfd50a569d32c708000000/ON-THE-COMPUTATION-OF-R-AND-ITS-ROLE-ON-GLOBAL-STABILITY.pdf.

[57] W. Okongo, C. Muhumuza, N. S. Aguegboh, E. Bwambale & B. Diallo, "Mathematical modelling of the co-infection dynamics of soil-transmitted helminths and schistosomiasis with optimal control", Boundary Value Problems **2025** (2025) 160. https://doi.org/10.1186/s13661-025-02146-z.

[58] Macrotrends, "Makurdi, Nigeria metro area population 1950–2026", 2025. Available online: https://www.macrotrends.net/global-metrics/cities/23539/makurdi/population.

[59] S. M. Blower & H. Dowlatabadi, "Sensitivity and uncertainty analysis of complex models of disease transmission: an HIV model, as an example", International Statistical Review **62** (1994) 229. https://doi.org/10.2307/1403510.

[60] W. H. Fleming & R. W. Rishel, Deterministic and Stochastic Optimal Control, Springer, New York, NY, USA, 1975. https://doi.org/10.1007/978-1-4612-6380-7.

[61] L. S. Pontryagin, V. G. Boltyanskii, R. V. Gamkrelidze & E. F. Mishchenko, The Mathematical Theory of Optimal Processes, John Wiley & Sons, London, UK, 1962. https://doi.org/10.1002/zamm.19630431023.

[62] World Health Organization, Guidelines for Laboratory and Field Testing of Molluscicides for Control of Schistosomiasis, World Health Organization, Geneva, Switzerland, 2019. Available online: https://www.who.int/publications/i/item/9789241515405.